

DISCLAIMER:

This document does not meet the
current format guidelines of
the Graduate School at
The University of Texas at Austin.

It has been published for
informational use only.

Copyright
by
DUONG THAI NGUYEN
2016

**The Thesis Committee for Duong Thai Nguyen
Certifies that this is the approved version of the following thesis:**

**Production Mechanism of Diluent Injection in
Heavy oil and Bitumen**

**APPROVED BY
SUPERVISING COMMITTEE:**

Supervisor:

Quoc P. Nguyen

Larry W. Lake

Production Mechanism of Diluent Injection in Heavy oil and Bitumen

by

Duong Thai Nguyen, B.S.P.E

Thesis

Presented to the Faculty of the Graduate School of

The University of Texas at Austin

in Partial Fulfillment

of the Requirements

for the Degree of

Master of Science in Engineering

The University of Texas at Austin

December, 2016

Dedication

To my father and mother

Acknowledgements

I gratefully thank my supervisor Prof. Quoc P. Nguyen for his supports, and for sharing his knowledge with me.

I would also extend my thanks to Marco Verlaan, Orlando Castellanos-Diaz, and Johan van Dorp, whom they are from Shell Oil Company, for helping me look for different perspectives related to the solvent injection experiments.

Thank you to Prof. Larry W. Lake for his support and guidance during the low points in my journey.

Special thanks to Glen Baum, Gary Miscoe, and Daryl Nygaard for answering to all my lab emergency issues.

It is my honor and privilege to take courses with faculties member at PGE.

To all my friends and lab Assistants-Tyler Seay, Peter Lin, Samuel Lau, Andrew Lau, Jack Liu, Nicholas Osborn, and Yehuda Soewargo...without you, those three- days long experiments in this thesis would not exist.

To all my fellow researchers, thank you for all engaging hallway discussions.

I must express my very profound attitude to my family, and my girlfriend for providing me with unfailing support and encouragement throughout my years of study. This journey could not have been possible without them. Thank you.

Finally, I want to say thank you to all people have touched my life during this journey.

Abstract

Production Mechanism of Diluent Injection in Heavy oil and Bitumen

Duong Thai Nguyen, MSE

The University of Texas at Austin, 2016

Supervisor: Quoc P. Nguyen

The invention of horizontal and hydraulic fractured have shaped the oil and gas industry in such a way that engineers could never imagine. Thanks to the new technology, tight formation productions help the United States comes tantalizingly close to energy independent. After four decades, the U.S lifted the ban on crude oil export increased the competition in the energy market. However, tight formations productions require high capital investment, and high water consumption but its production declines fast. Scientist have been actively seeking for alternative resources for future supply. Heavy oil and bitumen is one of interesting alternative, as the resource can be all over the world, but the largest reserves are concentrated in Americas: Venezuela, and in Canada's Alberta Province.

The production of heavy oil and bitumen is an extremely energy-intensive activity with the associated high environmental impact. Most common methods for heavy oil and bitumen production are surface mining or heat injection. The heat lost associated with steam injection is a big concern, sometimes it can be as high as 90%.

To reduce heat loss, the use of solvent was employed. However, solvent processes with vertical wells could be much slower than the thermal process such as steam injection. Since the introduction of horizontal well and hydraulic fracture that helps increase the contact area between the solvent and oil, the investigation of solvent injection process has been widely revisited.

Solvent or diluent injection without understanding asphaltene behavior can cause permeability and porosity reduction. In this study, I have investigated the mass transfer mechanisms in diluent processes with focus on understanding how these mechanisms govern asphaltene precipitation, flocculation and transportation.

Table of Contents

List of Tables	x
List of Figures	xi
Chapter 1: Introduction.....	13
1.1 Background.....	13
1.2 Outline.....	17
PART 1: LIQUID DILUENT PROCESS	19
Chapter 2: The Effect of Diluent Rate on the Extraction of Bitumen	20
2.1 Introduction.....	20
2.2 Material and methods.....	21
2.2.1 Core Preparation	23
2.2.2 Solvent Injection	27
2.2.3 Asphaltene Analysis.....	29
2.2.4 Permeability and Porosity Reduction Measurement.....	30
2.3 Results.....	30
2.3.1 Base Case -2cc/min.....	30
2.3.2 Lower Injection Rate effect- 0.5 cc/min	35
2.3.3 High Injection Rate Effect	37
2.4 Discussion	42
2.4.1 Injection Rate	42
2.4.2 Asphaltene.....	45
2.5 Chapter summary	51
Chapter 3: The Effect of Temperature and Diluent Type	53
3.1 Introduction.....	53
3.2 Material and methods.....	53
3.2.1 Materials	54
3.2.2 Procedure	54
3.3 Results and discussion	59

3.3.1 Base Case	59
3.3.2 Effect of Temperature – DCM 50°C	62
3.3.3 Diluent type effect- Pentane 50°C	65
3.3.4 Asphaltenes Effect -Butane 25°C	71
3.3.5 Sub-critical injection rate and temperature effect	75
3.3.6 Residual Oil Summary	78
3.4 Chapter summary	80
PART 2: VAPOR DILUENT PROCESS	81
Chapter 4: Effects of Temperature and Injection Rates on Vapor Diluent Process	82
4.1 Introduction	82
4.2 Material and Methods	83
4.3 Results and Discussion	86
4.3.1 Base Case- N-Butane at 50°C, 3cc/min	86
4.3.2 Temperature Effect –Butane 80°C 3cc/min	91
4.3.3 Rate Effect on Mass Transfer	94
4.3.4 Asphaltene Effect-DCM 80°C 3 cc/min	96
4.4 Chapter summary	102
Chapter 5: Effects of Diluent Pressure on Vapor Process	104
5.1 Introduction	104
5.2 Materials and Methods	104
5.3 Results and Discussions	106
5.3.1 DCM-80°C 75% Vapor Pressure	107
5.3.2 DCM-80°C 50% Vapor Pressure	108
5.3.3 n-Butane-80°C 75% Vapor Pressure	109
5.3.4 n-Butane-80°C 50% Vapor Pressure	110
5.3.5 Discussion	111
5.4 Chapter summary	116
Chapter 6: Conclusion and Future Works	117
Bibliography	121

List of Tables

Table 2.1:	Properties of the Cores.....	24
Table 2.1:	Thermal expansion of oil during heating (25°C to 50°C).....	26
Table 2.3:	Experimental parameters	28
Table 2.4:	Permeability and porosity reductions after each experiment.	48
Table 3.1:	Thermodynamic Parameters of the liquids.	54
Table 3.2:	Experiment Grid of this experiment	56
Table 3.3:	Mass fraction of asphaltenes in Butane 25°C and Butane 50°C	73
Table 3.4:	The asphaltene analysis of sub-critical cases of butane.....	78
Table 4.1:	Cores properties for Chapter 4.....	83
Table 4.2:	Thermal expansion of oil during heating (25°C to 50°C).....	84
Table 4.3:	Experimental parameters for this chapter	85
Table 4.4:	Mass balance of Chapter 4 Experiments.....	102
Table 5.1:	Rock Properties from Chapter 5 experiment.	105
Table 5.2:	Experiment grid for Chapter 5 experiments.....	105
Table 5.3:	Experiment grid for Chapter 5 experiments.....	116
Table 6.1:	Experiment grid for future work.	120

List of Figures

Figure 1.1: Recent heavy oil recovery techniques.....	13
Figure 2.1: Schematic of experimental apparatus	22
Figure 2.2: Illustration of Core Preparation Process (not to scale)	25
Figure 2.3: Summary of Chapter 1 parameter with visual demonstration.	28
Figure 2.4: Results from the injection rate of 2 cc/min experiment.	32
Figure 2.5: Asphaltene deposited after core flooding	34
Figure 2.6: Results from the injection rate of 0.5 cc/min experiment.	35
Figure 2.7: Results from the injection rate of 4 cc/min experiment.	37
Figure 2.8: Results from the injection rate of 10 cc/min experiment.	39
Figure 2.9: Results from the injection rate of 6 cc/min experiment.	41
Figure 2.10: Produced rates of five experiments during stable condition.....	43
Figure 2.11: Recovery fraction of the five experiments at different times.	44
Figure 2.13: Effluent oils contain more of the small carbon number.....	46
Figure 2.14: Viscosity of heavy oil vs. asphaltene content.	47
Figure 3.1: Summary of Chapter 3 parameter with visual demonstration.	57
Figure 3.3: Experiment data for Base Case-DCM 25°C	60
Figure 3.4: Experiment data of DCM at 50°C	62
Figure 3.5: DCM and P.R. viscosity at 25 and 50°C	63
Figure 3.6: Experimental data from Pentane at 50°C	66
Figure 3.7: Viscosity of P.R and various of diluent	67
Figure 3.8: Driving force of P.R and various of diluent.....	68
Figure 3.9: Fracture of various diluent case after experiment.....	70
Figure 3.10: Experiment data of Butane at 25°C.....	72

Figure 3.11: Effluent analysis.....	74
Figure 3.12: Experimental data of Butane at 40°C injection at 2 cc/min	76
Figure 3.13: Viscosity of P.R and butane mixture at 50°C and 40°C.....	77
Figure 3.14: Summary of residual oil of all the experiment.....	79
Figure 4.1: Chapter 4 parameter with visual demonstration	86
Figure 4.2: Results from experiment of Butane at 50 °C- 3 cc/min	88
Figure 4.3: Schematic of penetration- film theory	89
Figure 4.4: Results from experiment of Butane at 80°C- 3cc/min	91
Figure 4.5: Viscosity of P.R bitumen and n-Butane.....	93
Figure 4.6 : Results from experiment of Butane at 80 °C- 1 cc/min.....	94
Figure 4.7: Results from experiment of Butane at 50 °C- 1 cc/min	96
Figure 4.8: No asphaltene deposited after core flooding as in liquid.....	97
Figure 4.9: Results from experiment of DCM at 80 °C- 3 cc/min	98
Figure 4.10: Mass of oil and mass of asphaltene of cores sample by sections...100	
Figure 5.1: Summary of Chapter 5 parameters with visual demonstration.	106
Figure 5.2: Results from experiment of DCM at 75%-80 °C.....	107
Figure 5.3: Results from experiment of DCM at 50%- 80 °C.....	109
Figure 5.4: Results from experiment of n-Butane at 75%- 80 °C	110
Figure 5.5: Results from experiment of n-Butane at 50%- 80 °C	111
Figure 5.6: Summary of Chapter 5 experiments recovery fractions.	113
Figure 5.7: Percent of vapor pressure plot vs. oil drainage rate	114
Figure 5.8: Mass balance analysis for pressure partition effect	115

Chapter 1: Introduction

1.1 BACKGROUND

The surge in demand for oil, and the sharp decline in the supply of conventional oil and gas have initiated greater attention for exploration and development of unconventional resources such as tight oil formations, heavy oil, and extra heavy oil reservoirs (Ali et al., 2002). For the scope of this thesis, only technologies regarding heavy oil development are discussed. Heavy oil is often defined by its resistance to flow at the reservoir condition, i.e.: viscosity (larger than 100 mPa.s). The word bitumen is often used interchangeably with heavy oil, yet, the term bitumen refers to a much higher spectrum of fluid viscosity, i.e.: viscosity larger than 10,000 mPa.s) (Briggs et al., 1988). As provided in Figure 1.1, heavy oil extraction techniques can be divided into three groups. The advantages and disadvantages of each group are introduced in the following paragraphs.

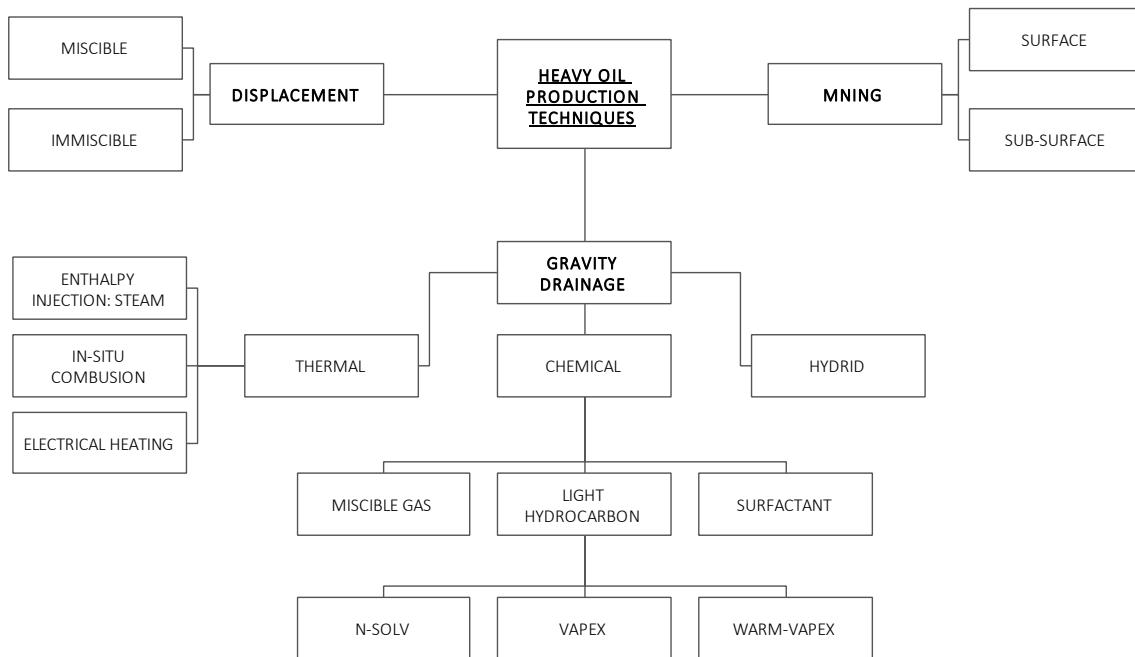


Figure 1.1: Recent heavy oil recovery techniques.

Heavy oil mining techniques have been used for thousands of years. Heavy oils were hand-dugged from shallow surface mines in the Middle East hundred years B.C (DeMirjian et al., 1978). However, large scale development of heavy oil mining only began to expand globally at the end of 20th century in the following regions: Pechelbronn Field in France, Higashiyama field in Japan, Weize Field in Germany, Yarega Field in USSR, and Athabasca Field in Canada (Lyman, 1984; Bellows, 1963). Surface mining technique can only be applied to reservoirs in which the ratio between the thickness of the bitumen bed and the overburden thickness falls within a range of 1:3.5 for large oil field and smaller for smaller mines in order to be considered economically feasible (Spragins et al., 1967). Furthermore, both mining and the processing of tar sands can cause a variety of environmental impacts including the release of greenhouse gas emissions, disturbance of mined land, disruptions on local wildlife, as well as air and water quality degradation. The development of commercial tar sand mining requires large amounts of water for processing; currently, tar sands extraction and processing require several barrels of water for each barrel of oil produced (BLM, 2014). Although sub-surface mining demonstrates technical viability, it is not an attractive option due to hazardous mining environments as well as the fact that the process is not economically feasible unless it is also thermal assisted (Lyman et al.,1984).

The concept of using heated miscible solvents to recover heavy oil and bitumen started in the early 1970s. Instead of water flooding the oil field, Ali and Snyder, in an isothermal experiment and Awang and Ali (1980), in a non-isothermal experiment, suggested the use of heated miscible fluid (naphtha) to displace the viscous oil in the laboratory. They found that the process of naphtha injection tended to be ineffective due gravity segregation and low swept efficiency (Ali et al., 1973). Although immiscible displacement may not have as many benefits when compared to miscible displacement,

which include the elimination of capillary hold up and viscous forces, people still study the effects of immiscible displacement in heavy oil recovery. The resulting increase in oil production when injecting low salinity water compared to high salinity formation water in an oil field has led Abass et al. (2013) to propose the technique of injecting low salinity water to displace viscous oil. This technique can also alter the wettability of the reservoir and detach surrounding clay particles. It is normally very difficult to combine chemicals in high thermal settings, such as those of heavy oils, since high temperatures negatively affect the chemical reaction process. However, theoretically, the effects of wettability alternation and viscosity reduction positively increase as the density of the oil increases. Therefore, injecting low salinity water would add a new mechanism into the process of thermal enhanced oil recovery. The results obtained from the laboratory using sand packs, extra heavy oil (1700 mPa.s at 65⁰C), and consolidated cores with heavy oil (700cp at 35⁰C) support up to a 25% increase in oil recovery and a much lower water cut. However, Rivet (2010) found that the increase in ultimate recovery was only observed in mix-wet rocks when injecting low salinity water, due to an improvement of the displacing stability.

Gravity drainage is the most reliable technique when it comes to extracting heavy oil. Engineers found the method to work with a variety of rocks, ranging from mix-wet to oil-wet reservoirs, where it is not possible to establish a differential pressure to push the oil during conventional displacement due to low mobility ratio, high fracture permeability, etc. (Boerrigter et al., 2007). However, due to the viscous nature of oil, it only drains when the viscosity of the oil is low enough, i.e. it requires extra force.

Injecting enthalpy, the most studied technique in heavy oil recovery process, both in field and in laboratories, compares to in-situ combustion and electrical heating. Although combustion is found to work better both theoretically and in lab scale settings, the performance of the fireflood method is proven to be ineffective in field. Due to the

difficulty in controlling the flood front by cause of air flow sensitivity, one of the most encountered problems in fire flooding is that it burns and destroys the production wells (Briggs et al., 1988). Because of high maintenance costs and low rates of return on electrical heating, it is only applicable in select reservoirs (Hascakir et al., 2008).

In areas, too deep for mining, oil is extracted using thermal injection methods such as Cyclic Steam Stimulation (CSS), and Steam Assisted Gravity Drainage (SAGD). Although Roger Butler's SAGD was patented back in 1969, the process has been revitalized by the implementation of horizontal wells. Since then, SAGD has become the method of choice in gravity drainage projects. The concept behind SAGD is to transfer the enthalpy from steam to the reservoir fluid in order to reduce the oil viscosity, and then use gravity in order to produce mobilized oil in a horizontal well. However, the production of the steam-based process largely ranges from 25% to 60% of the OOIP due to geological heterogeneity, reservoir thickness, heat lost, and gas cap/aquifer influences. Furthermore, a particular SAGD project consumes over 10 barrels of cold water to recover one barrel of oil (Gates et al., 2007). The more water it takes to recover the oil, the less economically feasible the project is due to its high-water supply cost, high-energy intensity, and large environmental footprint.

To overcome excess water usage and intense energy requirement due heat lost to the cap rock, solvent was utilized at its dew point temperature instead of steam. The mechanism behind the technique involves taking advantage of mass diffusion with out without latent heat to mobilize the viscous oil; however, it was concluded that due to the difference in orders of magnitude between molecular and thermal diffusivity, the viscosity reduction by the solvent would be much slower than steam processes (Das et al., 1998).

The main objective of this work is to investigate a low temperature production process for viscous fracture reservoirs. To achieve this purpose, the work is focused on a diluent injection strategy that combines the benefits of N-Solv, Vapor Extraction (VAPEX), and gas-oil gravity drainage (GOGD) to successfully produce viscous oil using low-temperature solvent injection.

1.2 OUTLINE

Chapter 2 provides the effect of diluent rate on the extraction of bitumen recovery in a fractured sand stone core. We conducted five experiments of liquid diluent at five different injection rates to identify the critical rate where the oil production no longer depends on the diluent rate. We examined how liquid diluent extracts the bitumen and upgrading bitumen in situ in order to gain understanding of the rate effect on asphaltene deposition.

Chapter 3 continues the investigation of temperature effect and diluent type on the production mechanisms of liquid diluent process and de-asphaltene process. Dichloromethane (DCM) was used as the diluent that does not precipitate asphaltenes when mixing with the bitumen. Using DCM helps isolate the effect of asphaltenes precipitation from the production mechanisms of liquid diluent extraction.

Chapter 4 starts a series of study on vapor-bitumen drainage process. By using the systematic method of isolating the effect of temperature, diluent rate, diluent type, and asphaltene precipitation as in the previous chapter, we establish the main mechanisms and influencing factors in the vapor diluent process .

Chapter 5 continues studying the importance of partition pressure on vapor process. A decrease in system pressure causes a decrease in vapor diluent solubility in bitumen.

Reducing the concentration of vapor in bitumen results in higher mixture viscosity that could ultimately decrease the drainage rate.

Chapter 6 highlight the experimental observations that could potential fuel more in-depth future studies of the liquid and vapor diluent processes.

PART 1: LIQUID DILUENT PROCESS

Chapter 2: The Effect of Diluent Rate on the Extraction of Bitumen

2.1 INTRODUCTION

Nenninger and Dunn introduced the concept of condensing solvent injection in 2008, in which operating conditions allow the injected solvent to condense at the cold oil interface. They proposed to elevate the temperature of the injected solvent, thus further reducing oil viscosity through both mass transfer (more effective in liquid phase compared to vapor phase) and thermal diffusion. On the other hand, Rankin et al. (2014) presented a low energy consumption solvent injection concept for fractured viscous oil reservoirs that combined liquid extraction observed in condensing solvent techniques with vapor solvent-assisted film drainage. When injecting warm vapor solvent into the reservoir, the solvent condenses when it contacts the cold oil and reservoir rock (liquid extraction). After the system reached the target operating temperature, the injected solvent remains in the vapor phase when it contacts the oil (solvent-enhanced film gravity drainage). The work in this paper focuses on the understanding of the production mechanism of bitumen in contact with liquid solvent under the isothermal condition.

Heavy oil naturally contains a significant amount of asphaltenes, which can cause problems in oil production, transportation, and processing. Asphaltene is soluble in carbon disulfide and insoluble in light alkanes such as n-pentane and n-heptane (McCain, 1999). When bitumen is in contact with solvent, the asphaltene deposition was observed. Inappropriate utilization of solvent in high asphaltic oil can destabilize asphaltene, which could potentially damage the oil production mechanism.

2.2 MATERIAL AND METHODS

An experimental setup with controllable temperature, pressure, and liquid injection rates was built to investigate the mechanisms of extraction during liquid diluent being injected into a bitumen saturated core with an artificial fracture. The experiments were carried out in three stages: core preparation, solvent injection, and the analysis of asphaltene content in the residual and produced oil. A two-foot long, two-inch diameter core holder (Figure. 2.1 (1)) was used. The long core was used to reduce the capillary effects during the gravity drainage process.

Core preparation and solvent injection was executed in an oven at an elevated temperature under confining pressures of 3.55 MPa axially and 6.99 MPa radially. The core holder (1) and oil accumulator (2) were then loaded inside the oven. An Omega temperature sensor was placed at 18" from the inlet to measure the temperature of the liquid entering the system. Pressure was monitored using two Rosemount absolute pressure transducers at the inlet and outlet. The temperature and pressure data was stored digitally by Lab View Instrument (8). The pressure of the system was controlled by an Equilibar backpressure regulator (BPR). The fluid pressure once it enters the system should be larger than the set dome pressure of BPR with some friction loss to be able to pass through. The BPR's dome pressure was held constant by a second BPR that released expanding dome gas during the heating of the system.

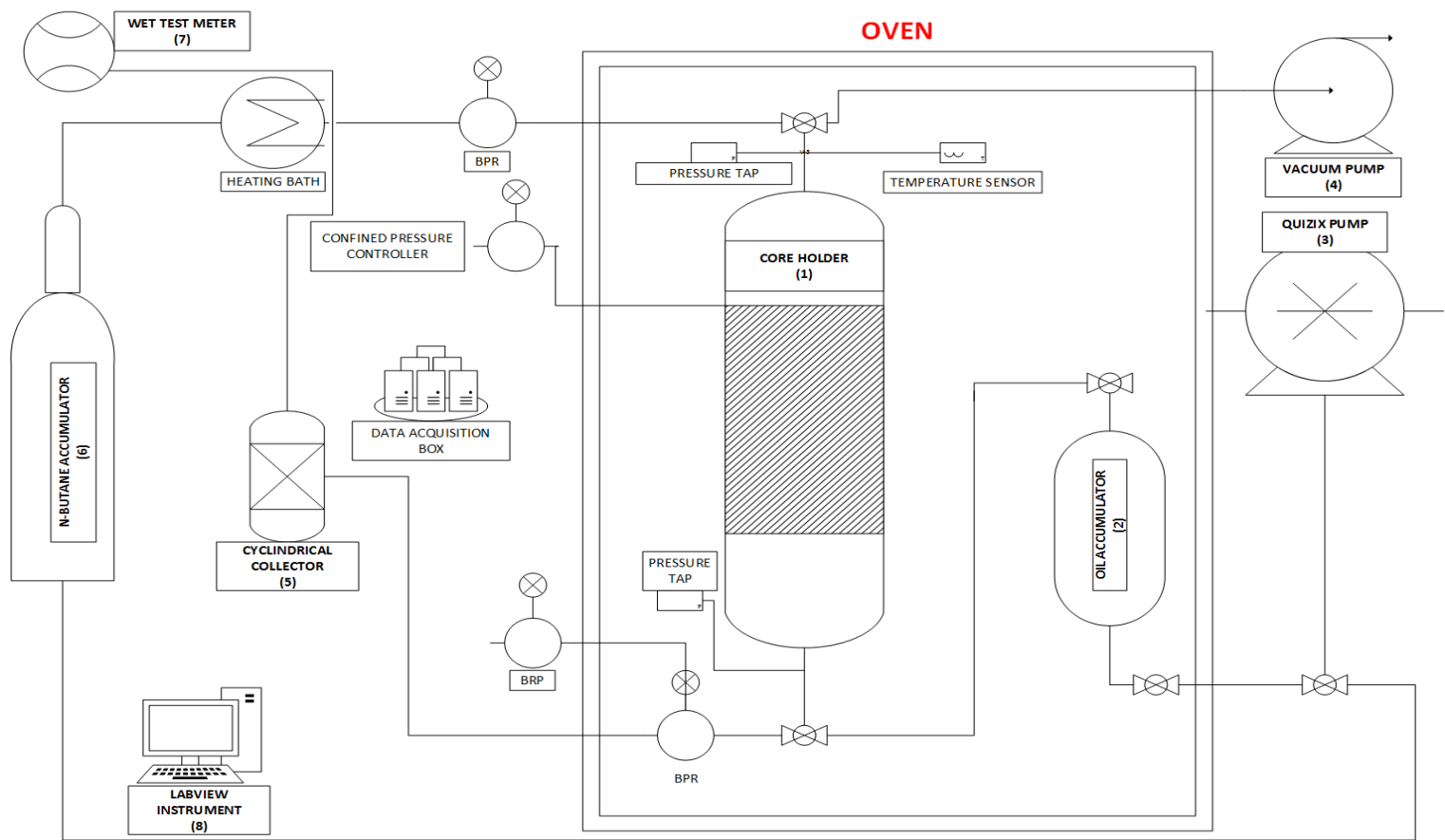


Figure 2.1: Schematic of experimental apparatus

The confining pressure of the system was also kept constant using the same process (confining pressure controller in Figure 2.1. The effluent gathered in a graduated one-liter glass collector (5). The oil was measured in the cylindrical collector (5), and gas exited through the top of the apparatus. After leaving the accumulator, the gas flowed through an Elster American wet test meter (7) and was vented to the fume hood. The wet test meter records the gas flow rate, which is stored digitally with Lab View. A description of each experimental stage is given in the following sections

2.2.1 Core Preparation

The first step in each experiment was core preparation. Idaho Gray sandstone was chosen because it is a highly permeable porous media. Once drilled, the cores were split axially to create an artificial fracture. The two halves were dried in an oven at 150 °C for 48 hours to remove all water. Exact dimensions of each core were measured to calculate bulk volume. To prepare for oil saturation, a rubber sheet was placed between the two halves to prevent early break through and to prevent oil from filling the gap, which would lead to inaccurate pore volume calculations. Temperature resistant tape was tightly wrapped around the two pieces to keep the two halves together. Finally, the core was covered with aluminum foil and held in place by heat shrink tubing.

The core was then loaded into the core holder, where the confining pressures were applied. The aforementioned steps are pictorially summarized in Figure 2.1 (a-d). To mobilize the bitumen (100000 cp. at 25 °C), saturation was carried out at a temperature of 50°C. While pulling a vacuum on the core, the core holder and oil accumulator were equilibrated to this temperature. The total volume of injection, minus the volume of effluent produced, minus the dead volume of the system, gives the value of each core pore

volume, and thus the porosity is as shown in Table 2.1. The axial split along the core affects the measurement of the permeability if obtained from the oil pressure drop during saturation. Permeability to brine was indirectly determined using representative plugs cut from each core's block. Auxiliary relationship was performed independently on each plug and provided in Table 2.1. After two pore volumes of oil were produced, the injection was stopped, and the system cooled to ambient temperatures

Case #	Porosity %	Pore Volume (cm³)	Brine Permeability (Darcy)
1	31	296.4	2.7
2	32	329.7	2.3
3	31	320.3	2.7
4	31	315.4	2.4
4	31	320.7	2.4

Table 2.1: Properties of the Cores

When the equipment cooled, the confining pressure was released. The oil-saturated core was removed. The external core wrappings and the rubber sheet were removed. To keep the width of the fracture constant under confining pressures, two Teflon strips were glued along the edge of fracture plane (Figure 2.2e). Because of the compression, the Teflon thickness measured after experiments were roughly 0.1 mm thinner than their original form (1.6 mm).

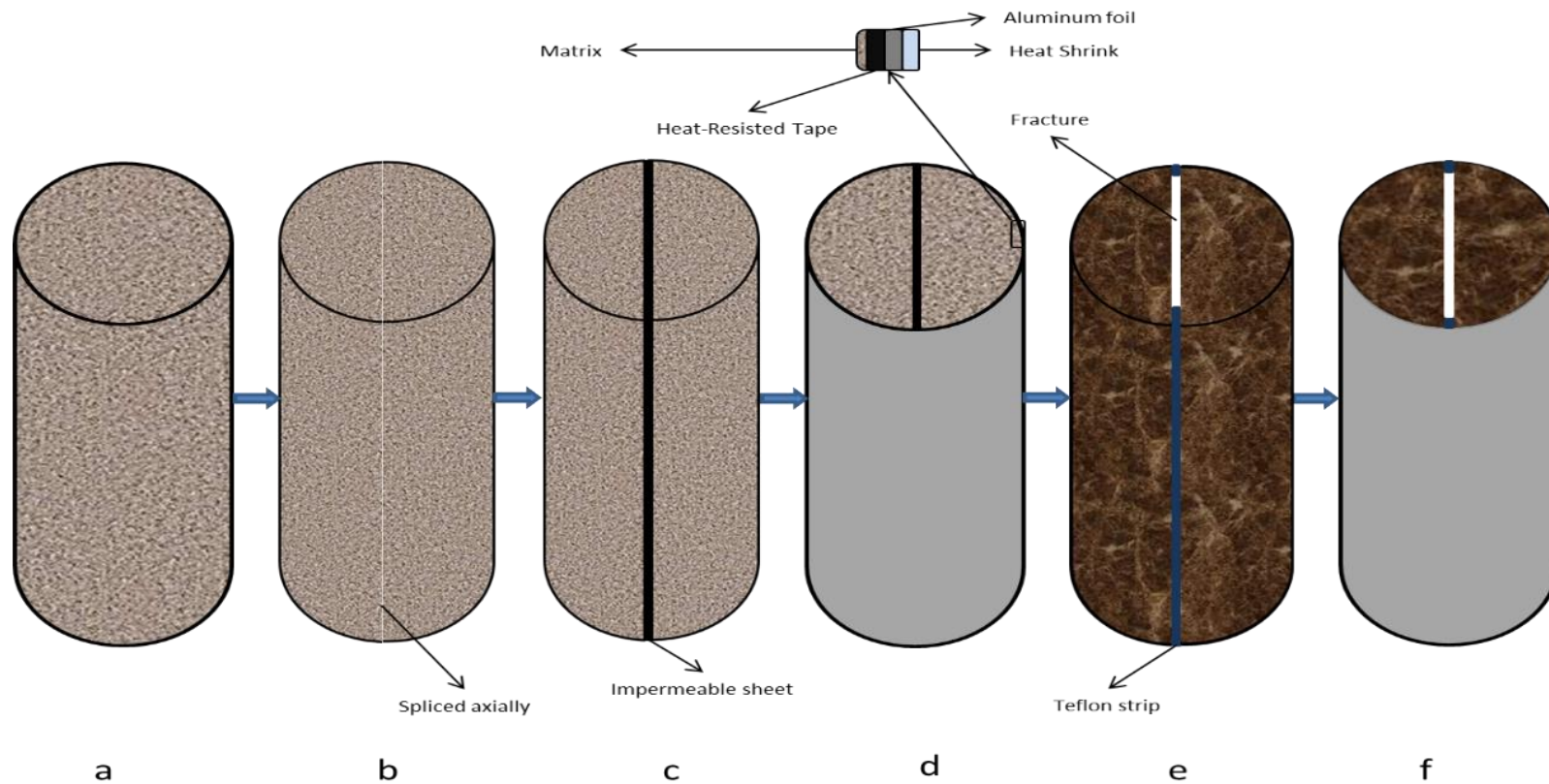


Figure 2.2: Illustration of Core Preparation Process (not to scale). 3a. Cores were cut from Idaho Gray sand stone. 3b. Cores were spliced axially to create the fracture. 3c. Impermeable rubber sheet was placed in the fracture during oil saturation to seal the fracture. 3d. Two blue Teflon strips were glued along the edge of the fracture plane to avoid compression during confine pressure of the saturated core. 3f. Core tightly wrapped with heat-resisted tape, aluminum foil, and heat shrinks.

The core was tightly wrapped with temperature resistant tape, aluminum foil, and heat shrinks. The core holder was cleaned with high-pressure nitrogen and distilled water to remove any excess oil from the saturation process. Once the core was loaded, confining pressure was applied. To measure the fracture volume after compression, 3% by mass of NaCl brine was injected from the bottom of the core at ambient conditions, until brine was produced at the end of the core holder. The volume required to fill the fracture gap after compression is roughly 35 cc, which helps verify the dimension of the fracture as 0.15cm x. 3.9 cm. x 60.01cm.

Next, the core holder was heated to the experimental condition. While heating, the top valve of the core holder was opened to allow for the collection of the water displaced by the thermal expansion of the oil. The amount of thermal oil expansion, reported in Table 2.2, assumes that the volume of water collected equals the volume of oil expansion.

Case #	Volume water collect (cm³)	Thermal Expansions of oil (% of OOIP)
1	26	8.77
2	29	8.79
3	28	8.74
4	27	8.56
5	29	9.04

Table 2.1: Thermal expansion of oil during heating (25°C to 50°C)

2.2.2 Solvent Injection

The pressure of the systems in all our experiments were 1 MPa. The temperature was chosen so that the diluent was in liquid phase. At 50°C and 1 Mpa, n-Butane is liquid. The parameters schedule for each case was summarized in Table 2.3. During the 24-hour heating of the core holder, the solvent accumulator Figure. 2.1- (6) was filled to prepare for the next stage: solvent injection. The 99.98 % purity n-butane was compressed into liquid form and stored in a three-liter, high-pressure stainless steel piston accumulator Figure. 2.1- (6) using a booster pump. The injection pressure was controlled by a BPR connected right at the outlet of the accumulator. The pressure was set at 0.5 to 0.7 MPa above the production system's pressure to serve as a choke valve that can prevent oil and solvent mixture from flowing back.

A Quizix pump Figure. 2.1- (3) displaced the solvent in the piston accumulator using distilled (DI) water at 25 °C and 1.72 MPa. The solvent went through long coiled tubing set in a heated bath to ensure that the targeted injection temperature was achieved. At the time of the injection, the data acquisition was activated to record the temperature and pressure. The production rate for water and oil was calculated by recording the time for every five-cm³ increment to collect in the glass collector. Produced n-butane gas rates were measured using the wet test meter. After the liquid production stopped, the core was cooled to ambient temperature for further analysis.

Table 2.3: Experimental parameters

Case #	Temperature (°C)	Pressure (MPa)	Solvent Type	Injection Rate (cm ³ /min)
1	50	1	n-Butane	2
2	50	1	n-Butane	0.5
3	50	1	n-Butane	4
4	50	1	n-Butane	10
5	50	1	n-Butane	6

For visualization, a chart where the experiments parameter compares to vapor pressure of vapor pressure where provided on the Figure 2.3 below.

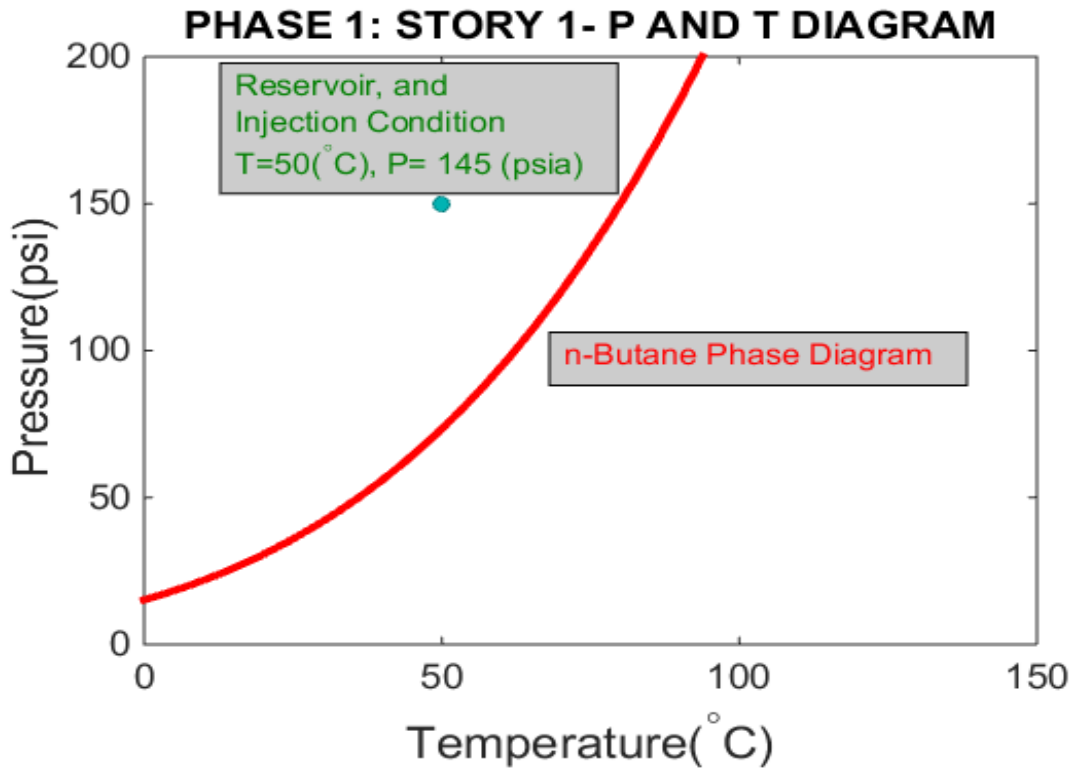


Figure 2.3: Summary of Chapter 1 parameter with visual demonstration.

2.2.3 Asphaltene Analysis

After releasing the confining pressure on the core holder, the residual solvent was vented to the fume hood, and the core was removed. The outer wrappings were removed, and the core was divided into four sections from top to bottom: top, 2, 3, and bottom. The asphaltene deposited on the fracture plane of each section was scraped off and added to the final asphaltene mass of each section accordingly. To determine the mass and asphaltene content of the residual oil in the matrix, each section of the core was crushed into grain-sized particles to help speed up extraction from the Soxhlet extraction process.

Toluene was chosen to be the solvent to extract the residual oil from the sand. Toluene was repeatedly vaporized and condensed in the condensing unit to create heated, pure liquid toluene when in contact with sand. Sand grains from each section were put into a 100-micron filter bag to ensure no loss in mass during extraction. A Buchi Rotavapor was used to remove the liquid toluene from the oil-toluene mixture collected from the Soxhlet process. The oil was then collected for asphaltene content analysis. The mass of each sample was recorded for use in the calculation of the residual oil volume for each section. Finally, the residual's asphaltene content was analyzed by the standard procedure from Wang and Buckley (2002) using n-Heptane. The composition and viscosity of produced oil were determined. Material balance of the oil, solvent, and asphaltene are discussed in the next section.

As the term asphaltene and maltene are intensively used, I wanted to try defining the most complex compounds here to help reader follow easier. Asphaltene are complex hydrocarbon having condensed aromatic compound with side chain of C_{30+} with sulfur

present in bithiophene ring and nitrogen in pyrrole and pyridine ring. Most importantly, bi or polyfunctional molecules with nitrogen as amines, amides, and oxygen in ketones, amides, phenols and carboxylic acids. They also contain heavy metal such as nickels, and vanadium complexed with pyrrole nitrogen atom in porphyrin structure. The compounds that soluble in n-alkane solvent constitute a fraction of asphalt, namely maltene. Maltenes contains smaller molecular weight of asphaltene called resin. Resin/ wax is the main cause of oil viscous. They also contain aromatic hydrocarbon, oleifins, naphthenes, saturated.

2.2.4 Permeability and Porosity Reduction Measurement

Before the core was divided and crushed into small sand grains, the asphaltene cleaned in the fracture core was reloaded into the core holder. In order to eliminate fracture flow, a thin rubber sheet was used to fill the fracture space. The core was again vacuumed to prepare for the injection of NaCl 3% from the bottom to determine porosity and permeability.

2.3 RESULTS

Experiments were conducted with five different injection rates, starting at the injection rate of 2cc/min as the base case. The first four experiments studied the effect of solvent rate; while the last two provide a better understanding on deasphaltene process (see the rate of injection for each case in Table 2.3).

2.3.1 Base Case -2cc/min

The base case experiment injects butane at 50°C and 1 MPa. Figure 2.4 shows the pressure profile for the entire core flood duration. The inlet pressure in dashed yellow and

the outlet pressure in dashed green, shown on the upper right y-axis, are above the vapor pressure of butane at 50°C, indicating solvent exists under liquid phase. The difference between and the inlet and the outlet pressure are calculated and shown in the solid purple line. The volume of oil production and its dimensionless recovery fraction are shown on the lower left and right y-axis, respectively.

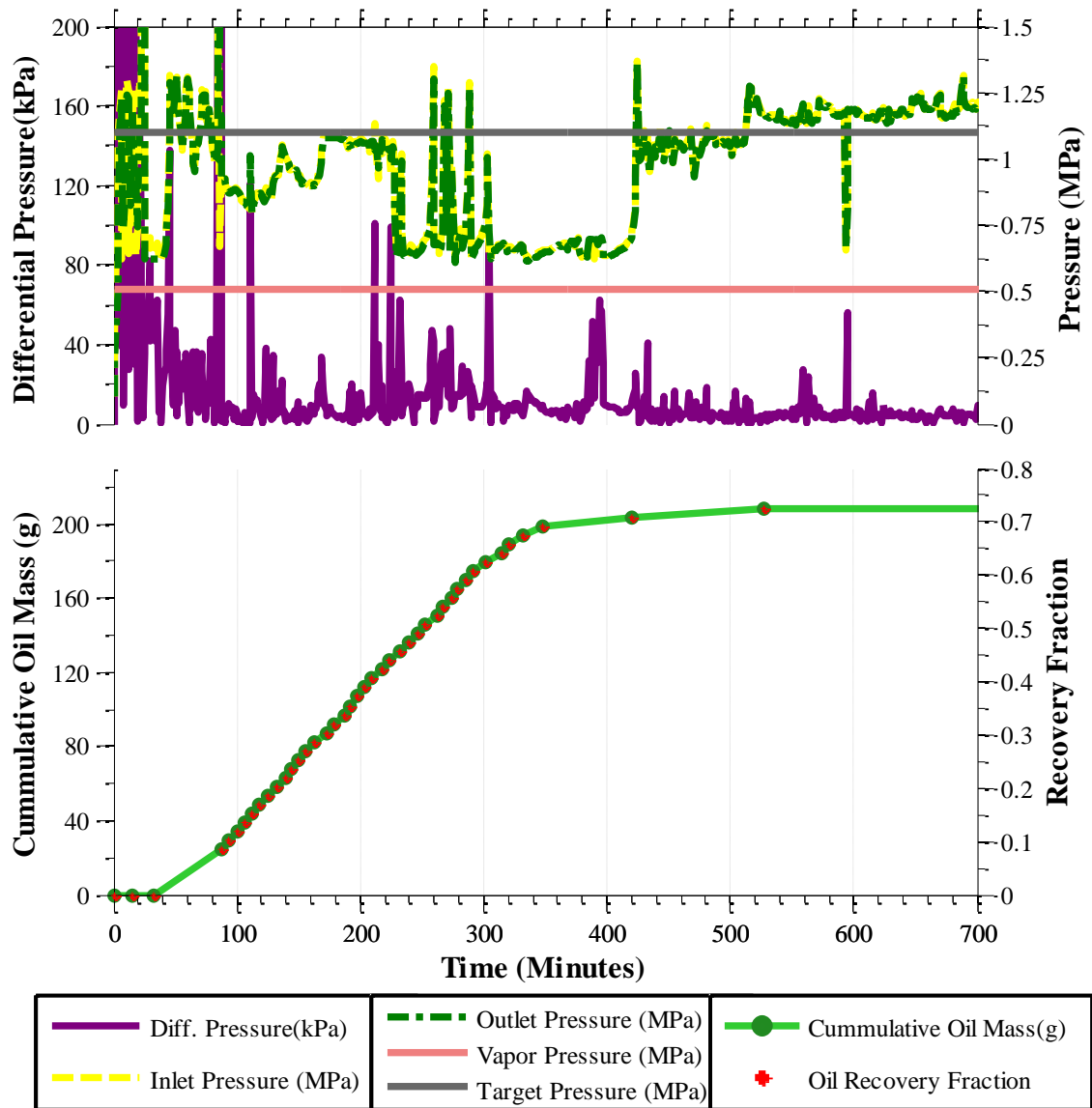
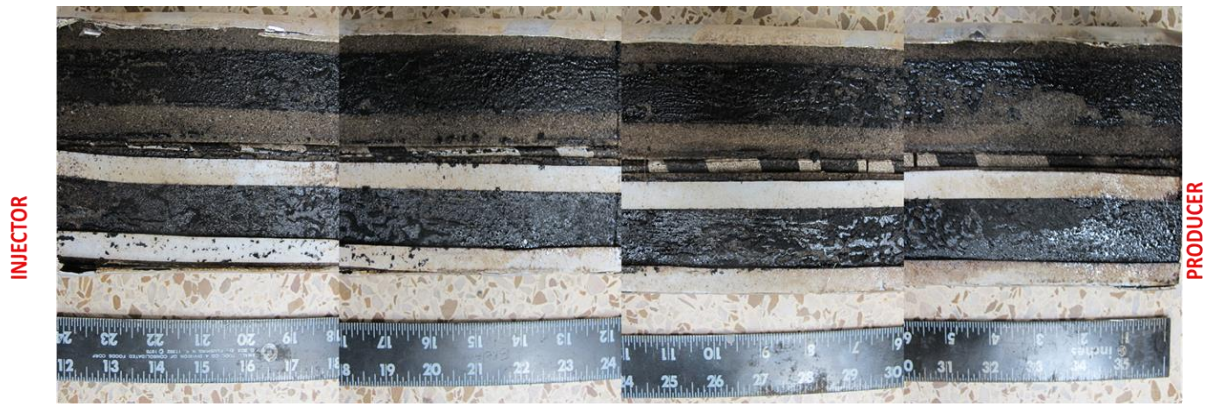


Figure 2.4: Results from the injection rate of 2 cc/min experiment.

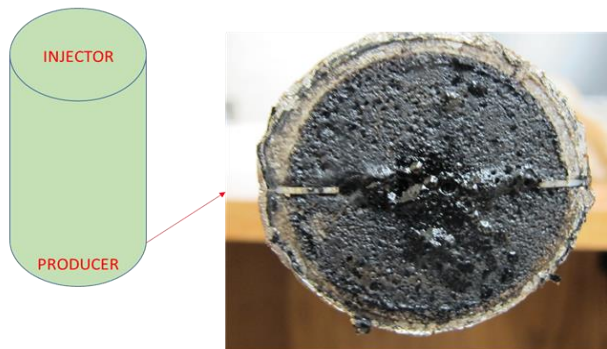
When the liquid solvent was injected into such a high permeability contrast environment, the diluent preferred flowing in the fracture and bypassing the matrix. The differential pressure measured across the 2-ft. long core in such a scenario could be estimated based on hydrostatic pressure of the liquid diluent column and friction loss. The

hydrostatic pressure for the diluent column is approximately 10 kPa. The purple differential pressure recorded during the core flood greatly fluctuated above the expected value. It took 32 minutes after the diluent injection was turned on before observing the first drop of oil coming out. Because it was partially filled with thermally expanded oil, the first measurement point was solely due to oil preoccupied in the fracture. After about 90 minutes of injection, the mass transfer between the oil and the diluent was fully established through the fracture system; hence the oil production mechanism of interest began. The rate of oil production stayed constant around 0.71 cc/min until the production reached 200 cc (RF=0.73) after 350 min.

As heavy oil contains high concentrations of asphaltene, asphaltene destabilization phenomena will occur once oil is exposed to the diluent. As a result, the effluent oil contains a lower percentage of asphaltene than the original heavy oil, 7.46% compared to 13.6%, and a solid asphaltene deposition on the fracture as the core is taken apart after the experiment as shown in Figure 2.5.



a



b

Figure 2.5: Asphaltene deposited after core flooding, a) Four sections of the core with asphaltene deposited on the fracture plan, b) Asphaltene on the production end of the core

Diluent dispersion is comprised of molecular diffusion and mechanical dispersion. Dispersion is caused by variation in the velocity of fluid elements as they move through a porous system. These two mechanisms determine how quickly the diluent penetrates the bitumen body. The injection rate strongly impacts oil production as well as the quality of the effluent oil. The next experiments were designed to investigate this impact.

2.3.2 Lower Injection Rate effect- 0.5 cc/min

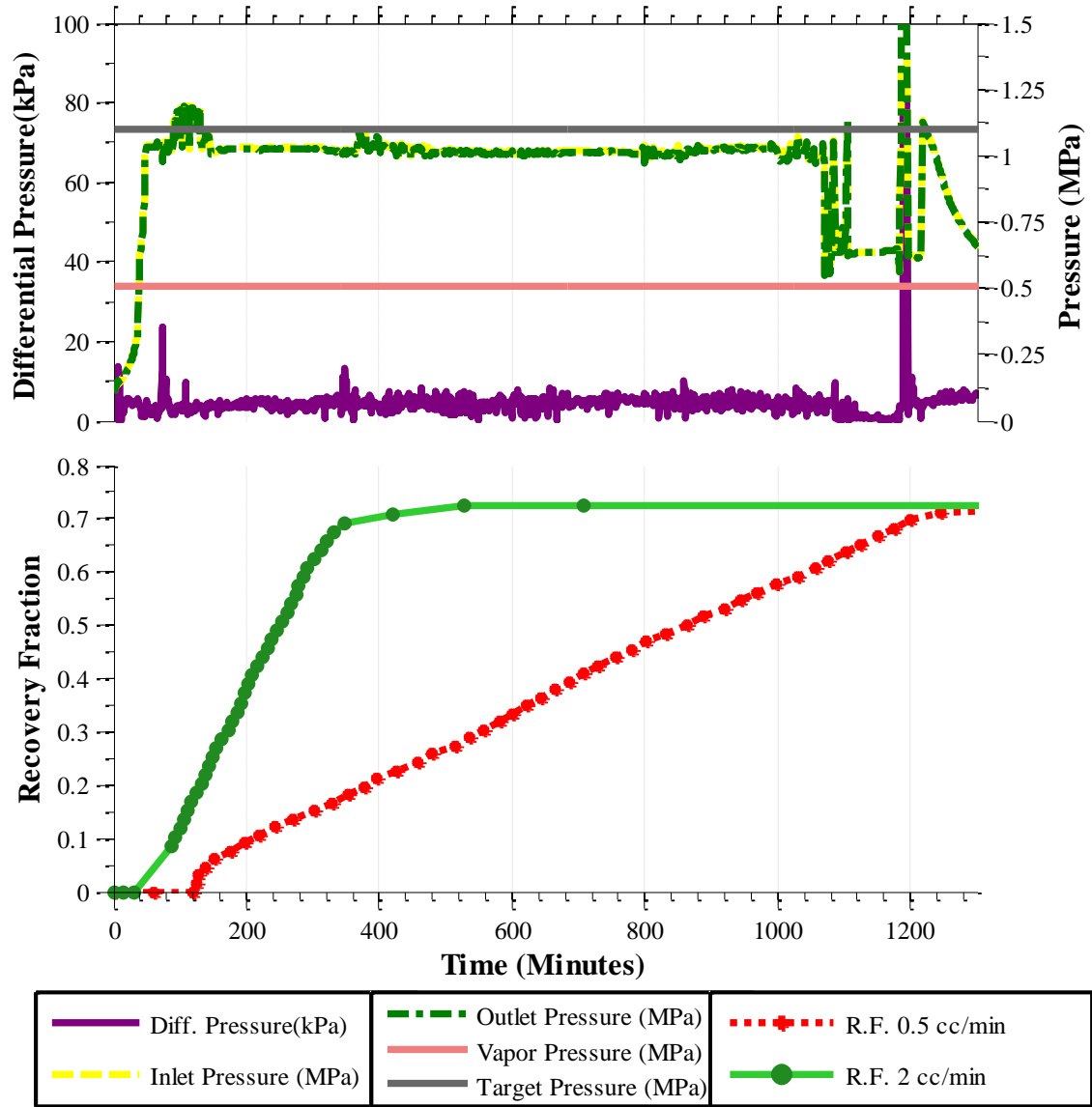


Figure 2.6: Results from the injection rate of 0.5 cc/min experiment.

We reduced the injection rate of butane in this case by four times compared to our base case, 0.5 cc/min. The inlet and outlet pressure of the system are shown in dashed yellow and dashed green, respectively as in Figure 2.6. The profile showed a more stable

behavior compared to the base case. As the rate is reduced, the diluent flow is further enriched by bitumen.

Rice University's chemical research lab successfully adapted the PC-SAFT equation of state from Gross and Sadwsi (2001) to fully predict the behavior of asphaltene precipitation. The results from their simulation indicated that an increased weight percent of n-alkane will increase the asphaltene unstable envelope. Hence, more asphaltene is precipitate with the increased injected n-alkane (Panuganti, 2013). The evidence indicated the stripping of heavy oil was not as strongly due to the lack of diluent as it was the effluent oil containing slightly higher asphaltene concentrations than the former case, 7.73%.

The drainage rate of oil into the fracture is influenced mass diffusion. Therefore, the oil production was expected to be reduced at lower diluent rate, as shown in Figure 2.7, 0.2-cc/min compared to 0.7 cc/min.

2.3.3 High Injection Rate Effect

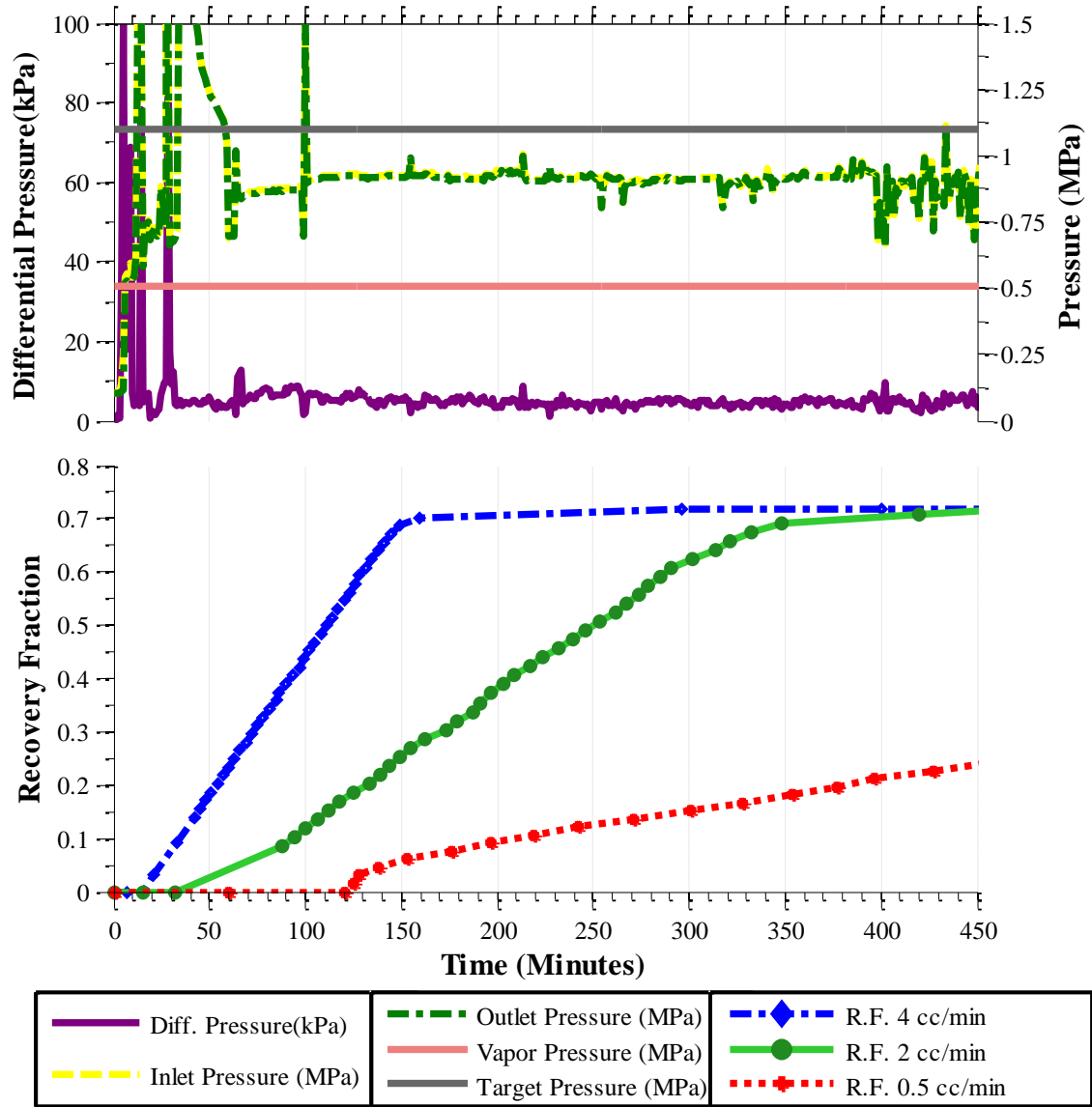


Figure 2.7: Results from the injection rate of 4 cc/min experiment.

In this experiment, the diluent injection was increased to 4cc/min. Figure 2.7 shows the pressure of the inlet and the outlet plotted in the same dashed yellow and dashed green. High diluent rate triggers the onset asphaltene precipitation at the early stage of the injection, causing the pressure profile to fluctuate wildly. As the production rate increased

by a factor of 2.3, while the injection rate increased by a factor of 2.230 cc of oil collected after 150 minutes of injection. The experiment was conducted for another 300 minutes; however, only 2 cc extra of oil was produced. The recovery of the three cases was plotted in green, red, and blue for the three experiments on the lower plot. Although in the experiment of 0.5 cc/min injection, the recovery fraction for the three cases was about 73%. Furthermore, the constant oil production rate in the three experiments proves that despite the unstable pressure profile, the in-situ oil production mechanism was not impacted.

According to Wang et al (2012), aggregation and deposition of asphaltene is because of changes in temperature (pressure) and the presence of an alien fluid, such as a diluent. When the equilibrium is disturbed, asphaltene can flocculate and adhere to the rock. The large flocs attach to the rock surface and can reduce permeability, as observed in Figure 2.5. The small flocs can flow with the fluid and cause bridge plugging, eventually reducing the permeability. The extent of de-asphaltene also depends on the amount of pure diluent exposed to the heavy oil.

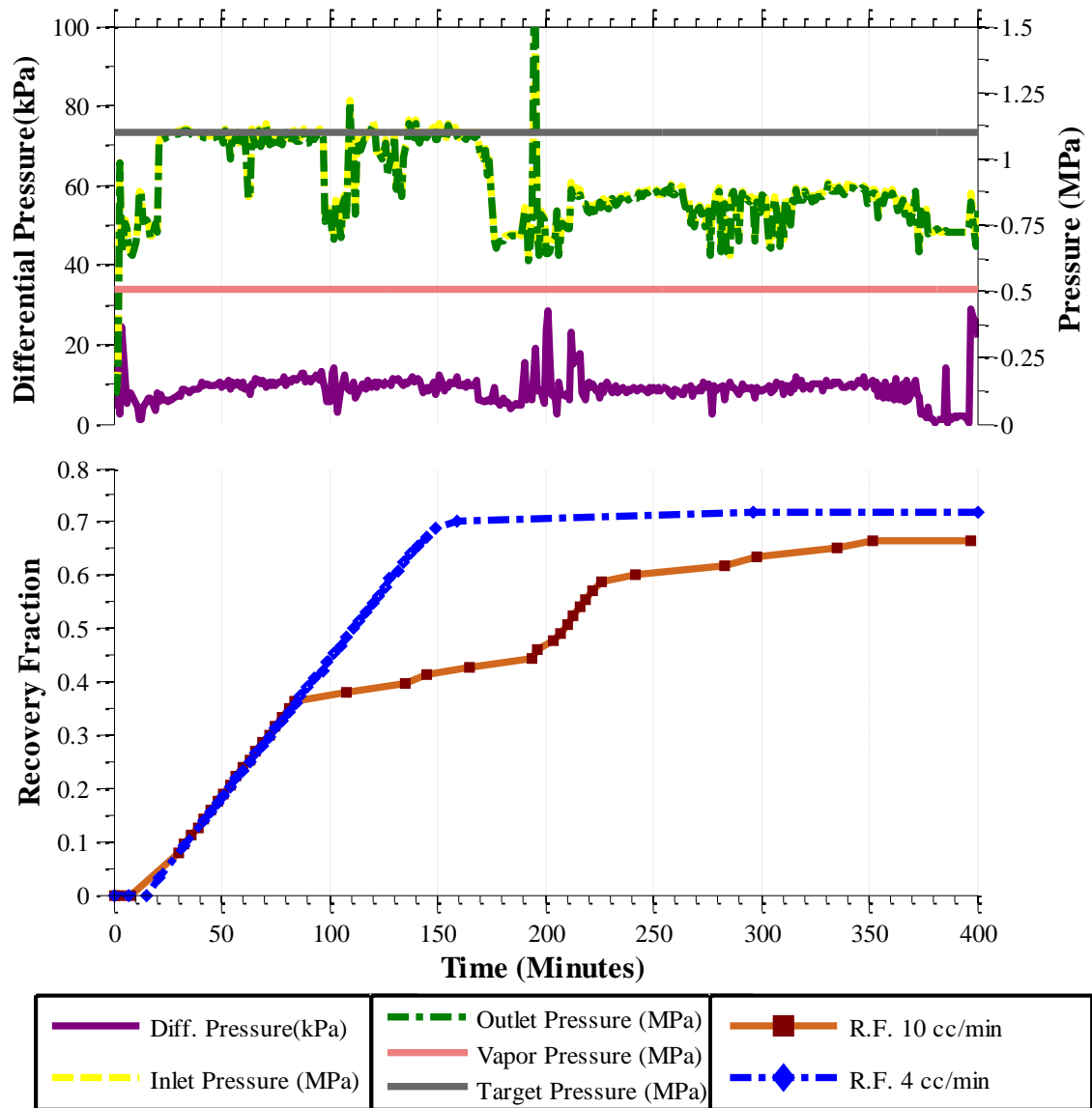


Figure 2.8: Results from the injection rate of 10 cc/min experiment.

The next experiment was designed with an injection rate five times larger than the base case. Figure 2.8 again provides the pressure profile of the experiment in the same layout as all the previous cases, dashed yellow and dashed green for inlet and outlet pressure. The pressure profiles display an unstable behavior, especially starting from the

80th minute. However, unlike the last three experiments, the oil production for this case, shown by the blue dotted line on the lower chart, was hindered for 118 minutes starting from the 80th minute, then returns back to the same production rate of 1.67 cc/min around the 160th minute. The pressure drop at that moment may indicate the dislodging of asphaltene that accumulated during the fast extraction period. The recovery fraction of the injection rate of 4 cc/min was also plotted as a brick dotted line on the lower chart for better comparison of the oil rate and ultimate recovery. At low injection rates, as observed in the 0.5 cc/min experiment, the oil production mechanism is a diffusion-limited regime, and therefore the oil production is a function of the injection rate.

Because of the asphaltene problem, the ultimate recovery was 6% less than the previous cases. To verify whether asphaltene precipitation can strongly impact the dilution process another experiment with injection rate of 6 cc/ min was conducted. The result of this experiment is shown on Figure 2.9.

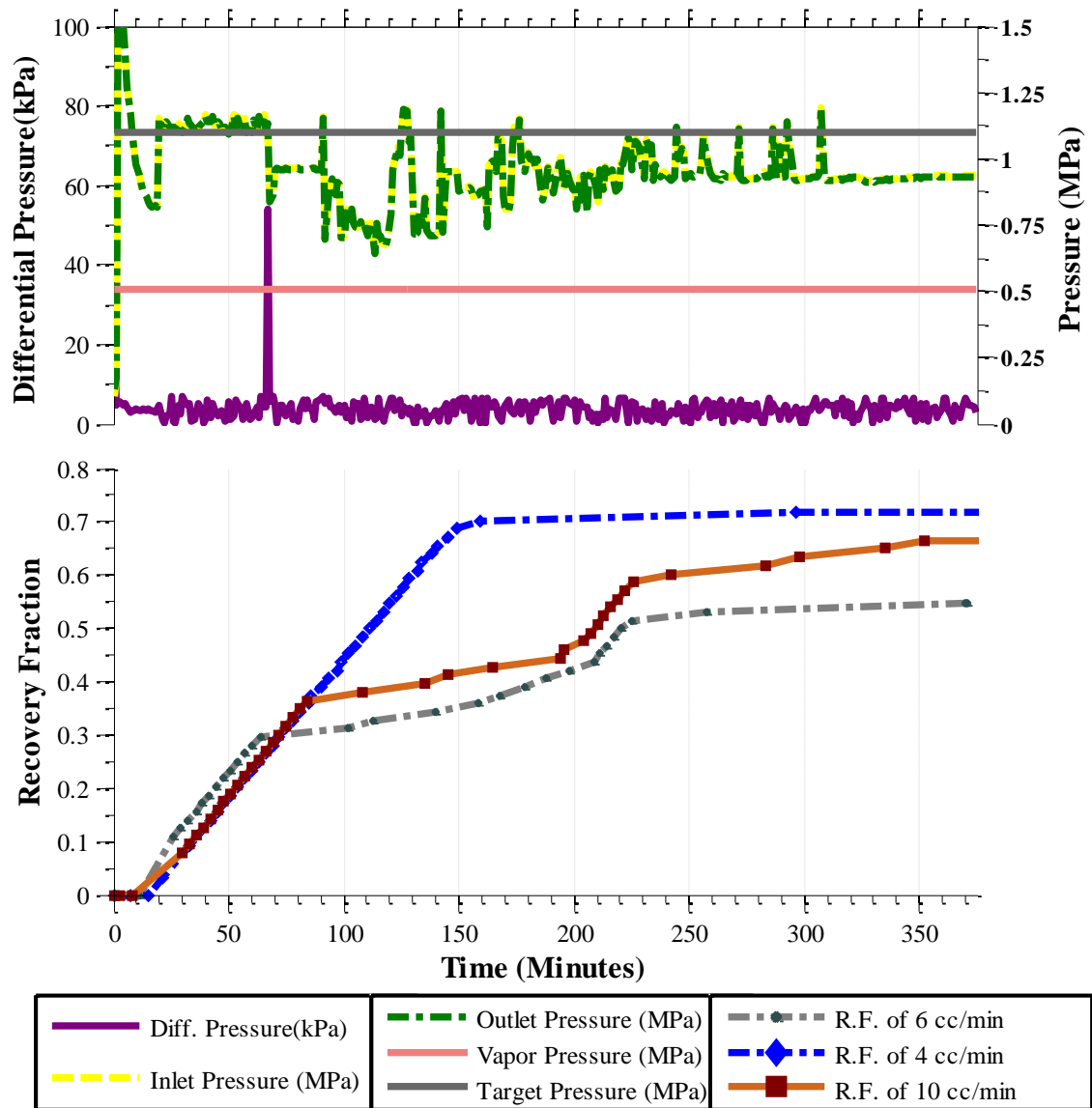


Figure 2.9: Results from the injection rate of 6 cc/min experiment.

Oil was produced at a stable rate of 1.59 cc/ min for around 42 minutes. A sharp decrease reappeared just like the previous case confirmed that asphaltene precipitation strongly impacted the dilution process. However, in this case, it took longer, almost 145

minutes, for the higher production rate to reestablish. The experiment was conducted for around 380 minutes, and 183 cc (R.F. =0.55) of oil was collected.

2.4 DISCUSSION

Molecular diffusion is a phenomenon whereby the transport of mass of a species occurs within a single fluid phase from one point to the other leading by a concentration of a different-driving force. Diffusion is a consequence of the random motion of molecules and can also take place in the absence of bulk movement or agitation. The spreading of a component in a phase due to microscopic variations in the velocity field is called convective or mechanical-dispersion. Optimizing operational conditions for a multicomponent fluid reservoir in a fractured system is an aching problem because of the unavailability of analytical models. Even though matrix, fracture, and fluid properties are also important in optimizing the process, the injection rate remains to be the most important controllable parameter. However, as heavy oil can contain up to 30% of asphaltene by weight, injection rates strongly impact the asphaltene aggregation and transportation, which can potentially impact the reservoir characteristics.

2.4.1 Injection Rate

Our results show that the higher injection rate of diluent, the faster the extraction of oil. However, after a certain injection rate, the oil production rates no longer depend on the diluent rate, the critical injection rate is 4 cc/min.

Figure 2.10 plots the oil production rate versus the diluent injection rate. The produced oil rate depends on an injection rate up to 4 cc/min and then the production rate becomes unchanged.

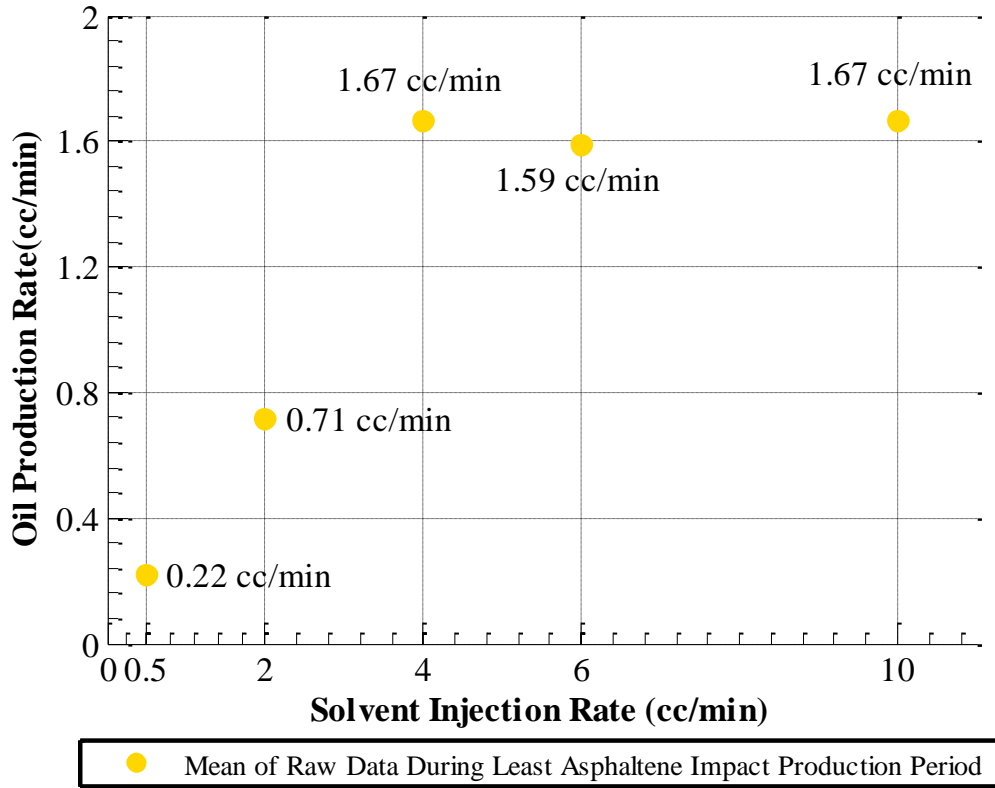


Figure 2.10: Produced rates of five experiments during stable condition, aka: no asphaltene disturbance.

Beside the oil production rate, the total amount of extracted oil as well as the time taken to reach the ultimate recovery in most enhanced oil recovery projects are the key factors. Figure 2.11 plots the recovery fraction of each experiment at different times for each injection rate. The lower the injection, the longer time it takes to achieve the ultimate . However, an increase in injection rate larger than 4 cc/min significantly reduced the ultimate recovery by asphaltene deposition.

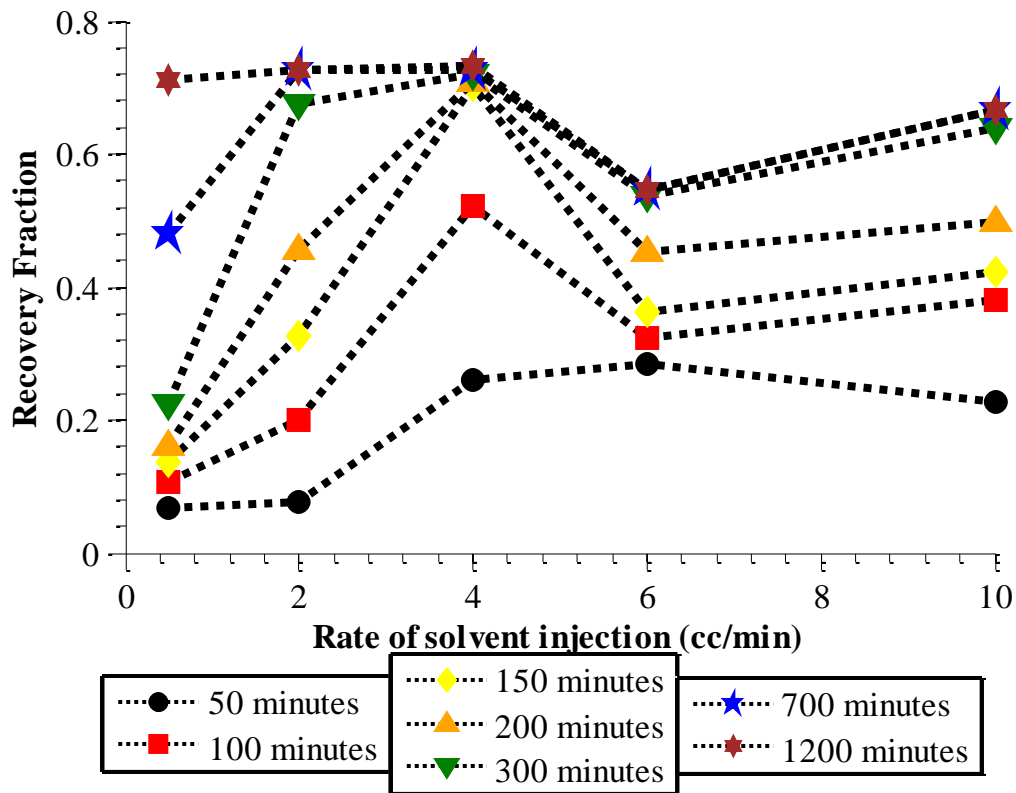


Figure 2.11: Recovery fraction of the five experiments at different times.

In terms of diluent oil ratio, the lowest injection rate yielded the best S_{or} of 2.3, indicating the lowest diluent required for the extraction process as show in Figure 2.12. The oil recovery curves shift systematically to the right with the increase in injection rate, indicating reduced bitumen recovery.

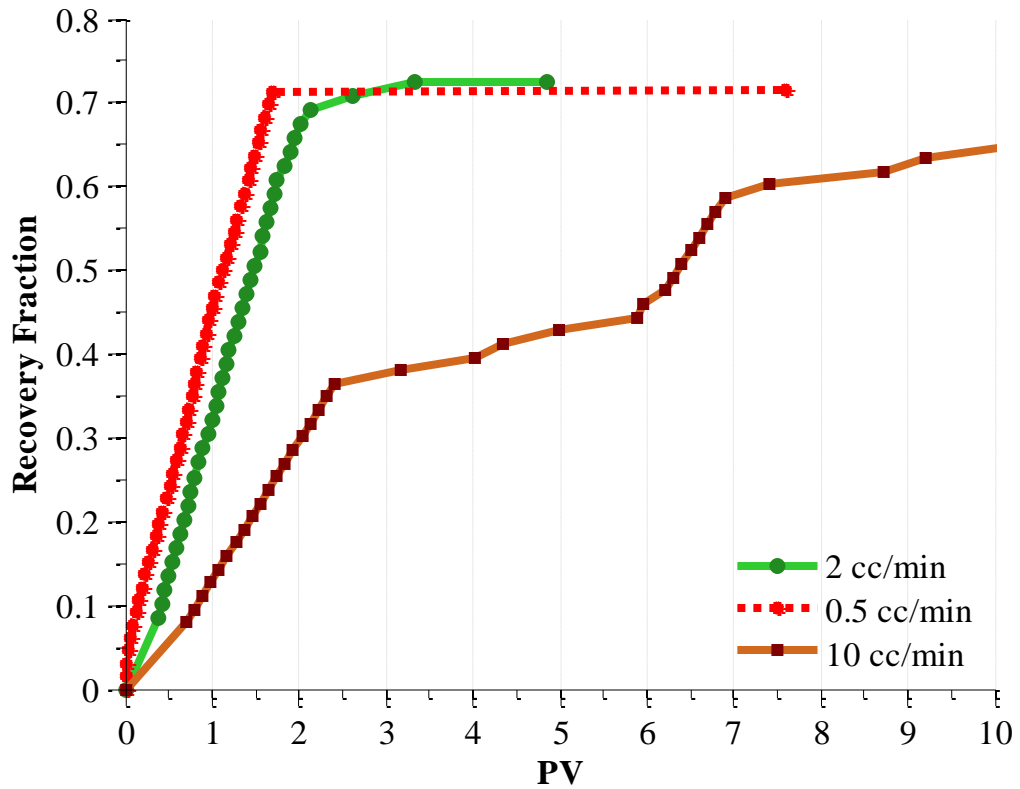


Figure 2.12: Recovery fraction of three experiments with the dimensionless recovery

2.4.2 Asphaltene

During the diluting oil production regime, more light components are produced as shown in Figure 2.13. The diluent processed oil has a lower concentration of asphaltene, which contains fewer large-carbon numbers - up to two times compared to the original oil. Because the smaller carbon number was extracted out by diluent, it leaves behind higher concentrations of higher carbon numbers than the original oil (Arciniegas 2014). One of the most obvious benefits of removing asphaltene from the oil is to reduce the viscosity of

the

produced

oil.

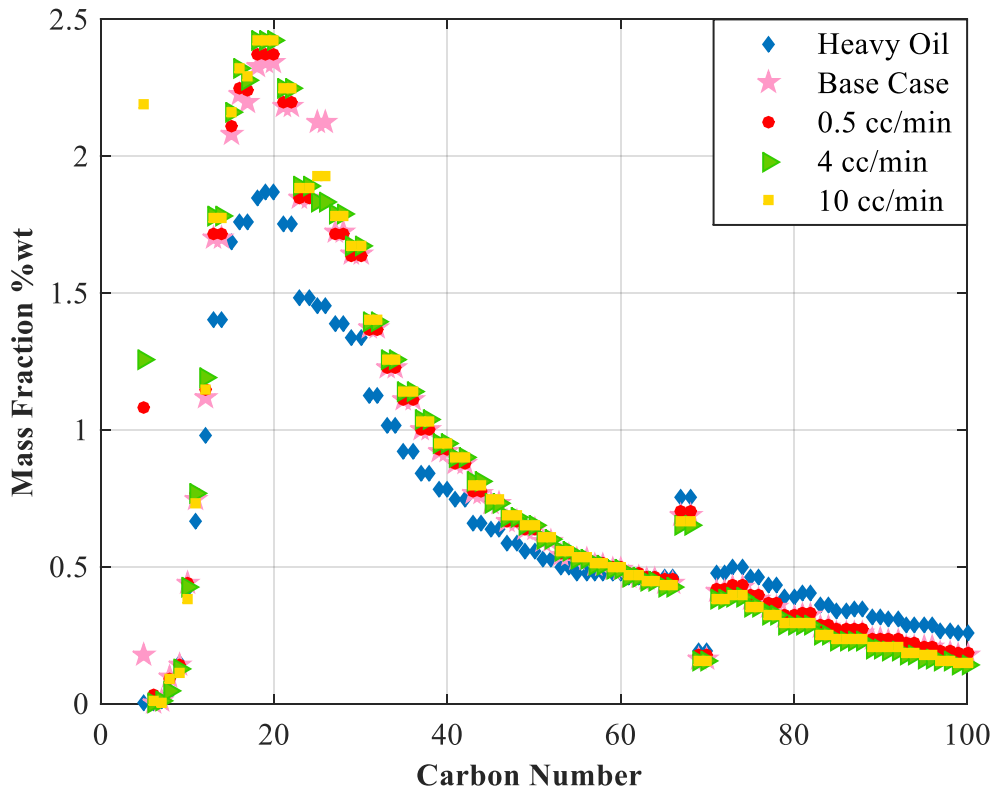


Figure 2.13: Effluent oils contain more of the small carbon number. This is a indicator of oil has been upgraded.

Figure 2.14 plots the viscosity of the heavy and the produced oil from the five experiments with the mass fraction of asphaltene using C7. By reducing the asphaltene contained in the oil by three times, the viscosity of the oil is reduced from up to 45 times for low temperature and up to 11 times for high temperature plots. In addition to the oil viscosity is improved, the process also helps upgrade the quality of oil, especially heavy metal concentrations of the effluent bitumen, are also reduced. The most important benefits are (1) to bring the oil closer to refinery specifications and (2) protect the catalysts in many

refining processes from deactivation (“poisoning”), resulting from prolonged contact with hetero-atoms. (Hart 2014)

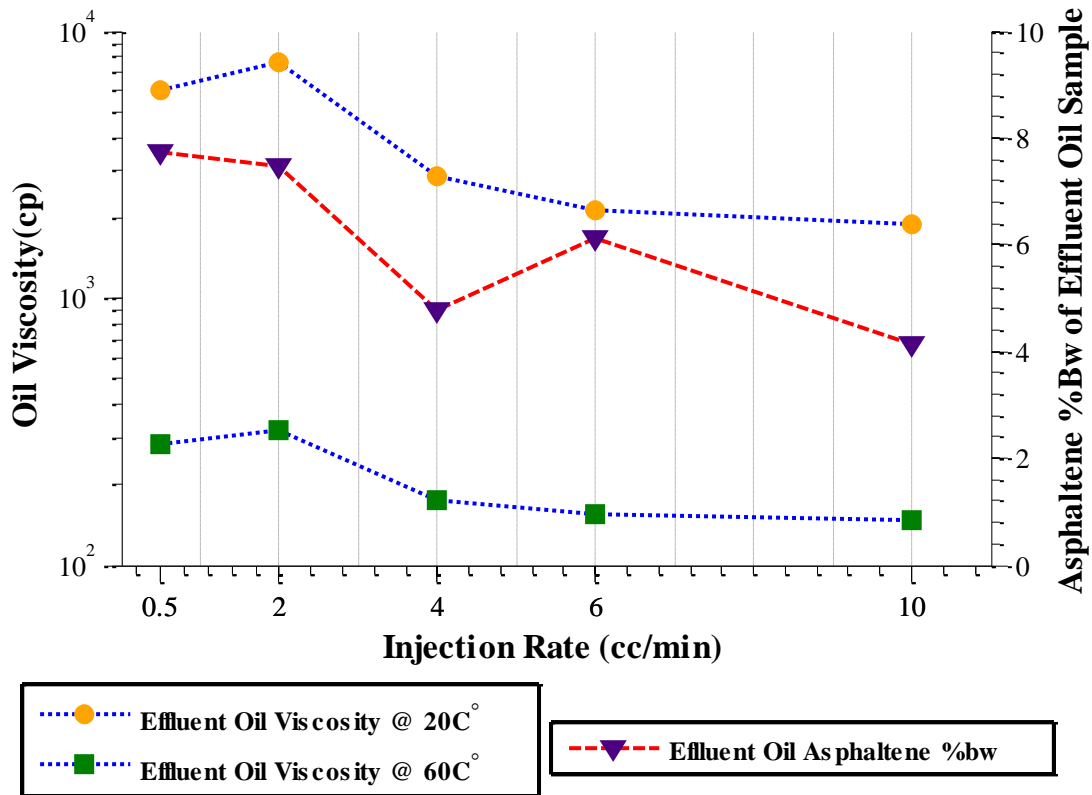


Figure 2.14: Viscosity of heavy oil is an exponential function of asphaltene content.

Suspended asphaltene particles have a tendency to aggregate and then flocculate and deposit, which can damage the formation’s permeability and porosity (Bedbahani, 2014) because, under a microscopic view, those asphaltene molecules carry a core of stacked flat sheets of condensed aromatic rings linked at their edges by chains of aliphatic and/or naphthenic-aromatic ring systems.

Rate (cc/min)	Porosity After (%)	$\frac{\phi}{\phi_{ori}}$	Brine Permeability (mD)	$\frac{k}{k_{ori}}$	C7 Asph. (%wt)
0.5	30.0	0.94	2.22	0.97	7.74
2	25.8	0.83	2.52	0.93	7.46
4	25.5	0.82	2.56	0.95	4.76
10	23.3	0.75	2.12	0.88	4.13
6	23.4	0.75	2.05	0.85	6.12*

Table 2.4: Permeability and porosity reductions after each experiment.

The more the diluent is exposed to the oil, the higher diluent-to-bitumen ratio, the more asphaltene aggregation occurs. Furthermore, Nazmul (2003) pointed out that increasing the diluent-to-bitumen ratio has a dominant effect on the kinetic of floc growth and the magnitude of aggregate break up. In other words, increasing the injection rate not only causes the greater quality of precipitated asphaltenes at a much faster speed, but it also introduces the larger mean average size of aggregate diameter of the particle. Hence, experiments with injection rates above critical rates trapped significant amounts of maltenes, which accounted for the porosity and permeability reduction.

Flory and Huggins (1942) predicted the onset of asphaltene precipitation based on the theory of polymer solution, while Hirschberg et al. (1984) assumed that asphaltene is a homogenous solid compound, neither assumption can completely describe the complexity of asphaltene in reliability. As mentioned earlier, the “hairy tennis balls” are

called micelles. The micelles and the diluent medium form a colloidal system. Those colloids are stabilized by resin adsorbed on their surface and the dispersion of colloid in the fluid form a two-phase system. Depending on the diluent-to-bitumen ratio, those colloids can be resin-like or more solid-like. The two forms have different behavior in nano-aggregate, precipitate, adherence to surface, and block rock pores. For example, injecting faster produces more solid-like particles that are harder to transport out of the matrix, while lower injection rates create a more polymer-like particle that can still drain out.

Figure 2.15 shows that the asphaltene deposited more in the inlet section compared to the outlet section. The trend also shows that the mass of oil retention tends to be more at the two last sections because the mass of the oil retained were proportional to the time of contact with cleaner diluent (Trivedi,2007). The suspended solid asphaltene is believed to have flocculated and adhered to the rock and created a “shield”, disconnecting the communication between the diluent and the oil. Because of the high injection rates, the asphaltene aggregation rate is much more rapid.

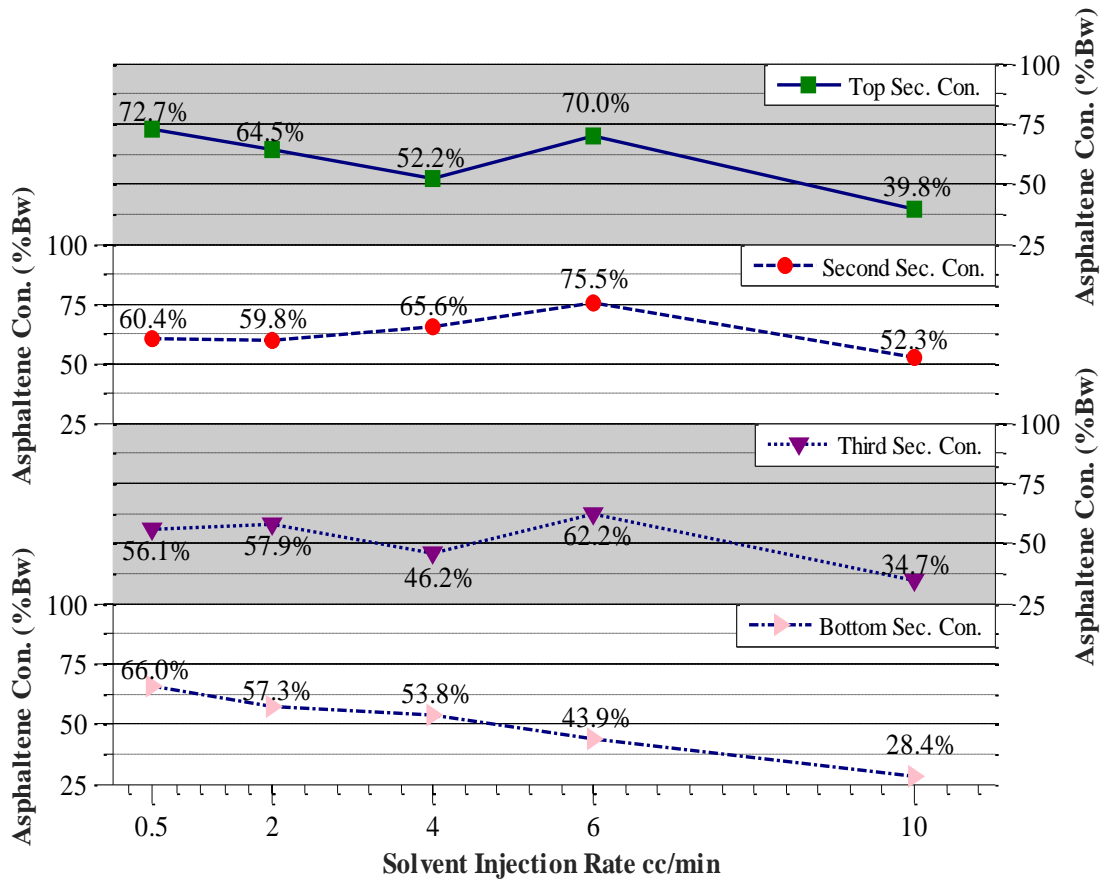


Figure 2.15: Asphaltene deposition of each section plot versus the injection velocity

When the good contact between the diluent and the oil was re-established, the production of oil returned to the original production rate. The building up of asphaltene deposition was observed to be repetitive with injection rates 6 cc/min and higher. Interestingly, the ability to produce large asphaltene floc by sheer force of high injection rates helped downfall the permeability reduction in 10 cc/min cases compared to permeability reduction in the 6 cc/min case. Similarly, Nazmul observed in his research in 2003 that increasing the injection rate increases the aggregation/growth rate and the higher fragmentation rate.

2.5 CHAPTER SUMMARY

Using liquid diluent to recover heavy oil in fractured reservoirs yielded promising results in terms of recovery factor (up to 73% of the original oil in place recovered) and rate of production. When liquid diluent is in contact with heavy oil, diffusion of oil into the diluent body, and vice versa, are both possible. However, because of the nature of mass transfer coefficients, it is faster for the oil to get into the diluent stream and produced out when the diluent is circulated. As a result, oil production strongly depends on the diluent injection rate up to a point, where the chemical potential is at a maximum. At this point the diluent is circulating faster than the rate the light oil components transfer into the diluent. If the injection rate is less than the described critical rate, there is enough time for the diluent to diffuse into the oil body, and the heavy oil's viscosity is reduced enough to drain into the diluent stream.

The two oil production regimes described above greatly differ in terms of de-asphaltene and deposition in the process of mixing n-Butane with a high asphaltene concentrated oil, such as with the Peace River bitumen. During the diluting limited regime, the oil production rate is optimum with better quality effluent oils, but due to the nature of rapid bleaching, the process can potentially cause unexpected behavior toward the whole process, as well as potentially damage the formation. While during the diffusion limited regime, the oil production rate is significantly lower, but as the process happens more slowly (less diluent availability), the asphaltene aggregation seems to slowly progress with time.

As found in this chapter, there exists an optimum diluent injection rate at which both the oil production rate and the asphaltene controlling aspects agree upon to deliver a technology that is economically feasible for future field pilot.

Chapter 3: The Effect of Temperature and Diluent Type

3.1 INTRODUCTION

Since the 1980s, many scientists have been tirelessly working on developing and improving the diluent based recovery technology of that was proven to be economically efficient in the lab. Providing that the diluent extraction process is similar to the shock mechanism, it is still unclear as to why the rate obtained from diluent extraction is 500 times larger than theoretical prediction from diffusion coefficient or dispersion., Neningen, after successfully deriving a correlation of bitumen production rate and dimensionless group of rock properties and oil viscosity, suggests that in the oil extraction process, the diluent type is not as critical as the raw oil viscosity. However, it is counterintuitive to conceive that diluent type insensitivity applies in all diluent based gravity drainage. For example, in a diffusion- dominant mechanism such as diluent assisted controlled gravity where rates controlled the drainage rate (Boerrigter et al., 2007). It is hard to believe that the rate of diluent transfer into the viscous oil is mainly controlled by solubility, mixture viscosity, and phase equilibria.

Even if the diluent type does not impact the extraction process, there is no doubt that the diluent composition and temperature has tremendous influences on the process of asphaltene aggregation, transportation and deposition.

3.2 MATERIAL AND METHODS

This section discusses the materials and the experimental procedure.

3.2.1 Materials

The oil used in this experiment is dewatered bitumen. N-Butane is supplied by Matheson. The n-Pentane is technical grade (95%) purity from Acros Organics. Methylene Chloride (DCM) is also of technical grade with purity of 99.5%, and based on the viscosity provided on the label, we use Walter's model to extrapolate for viscosities at various conditions. The viscosity of crude oil was measured using a double-walled column. The viscosity of liquid butane is predicted using Vogel et al. model, while Pentane's viscosity is computed based on Span's EOS. The viscosities of those diluents and bitumen at the temperature of interest are shown in the Table 3.1.

Temperature (C)	Viscosity (cp.)			
	P.R. bitumen	n-Butane	Pentane	DCM
25	51255	0.160	0.221	0.413
40	8519	0.139	-	-
50	3165	0.126	0.179	0.342

Table 3.1: Thermodynamic Parameters of the liquids used in the experiment.

3.2.2 Procedure

The experiments were designed to continue the investigation of the different diluent types, and the study of temperature effect on asphaltenes aggregation and deposition in the process of extracting heavy oil via diffusion in a fractured system. The set up comprised of two feet long, and two inches' diameter core holder that was placed in the oven. The diluent was injected into the system using Quizix pump to help displacing a three-liter

accumulator of liquid diluent. When the diluent was n-butane, the injection accumulator was compressed up to 250 psi. After passing through a back-pressure regulator, the diluent was going through a long coiled tubing at the oven temperature to ensure that the experiment was conducted isothermally.

The rock cores were drilled from a 1 foot by 1 foot Idaho Gray block. Because of the high viscosity of the bitumen, the saturation process was done at elevated temperature of 50°C. Furthermore, to force the oil to invade the matrix only, the fracture was closed using flexible tubing. We created a two-foot long core with a fracture in the middle by splitting the cores axially then glue them back together with two incompressible Teflon strips at the edge of the fracture after removing the tubing.

The pressure and the temperature of the system was measured 18” from the inlet of the core and 12” from the outlet of the core. Those data were recorded in a computer using Labview. The experiments were designed to run at 1 MPa, and summary of the key parameters is shown in Table 3.2. In order to gain more understanding, data from previous work are loaned and marked with asterisk.

No.	Diluent Type	Temperature (°C)	Injection Rate (cc/min)	Goal of Study
1	DCM	25	6	Base case
2	DCM	50	6	Temperature Effect+ Diluent Type
3	Pentane	50	6	Diluent Type
*	Butane	50	6	Diluent Type
4	Butane	25	6	Asphaltenes
5	Butane	40	2	Subcritical rate and Temperature
*	Butane	50	2	Subcritical rate and Temperature

Table 3.2: Experiment Grid of this experiment and loaned data from previous work

For visualization effect, the parameters for the experiment was plot on the vapor pressure curves for the two diluents as in Figure 3.1.

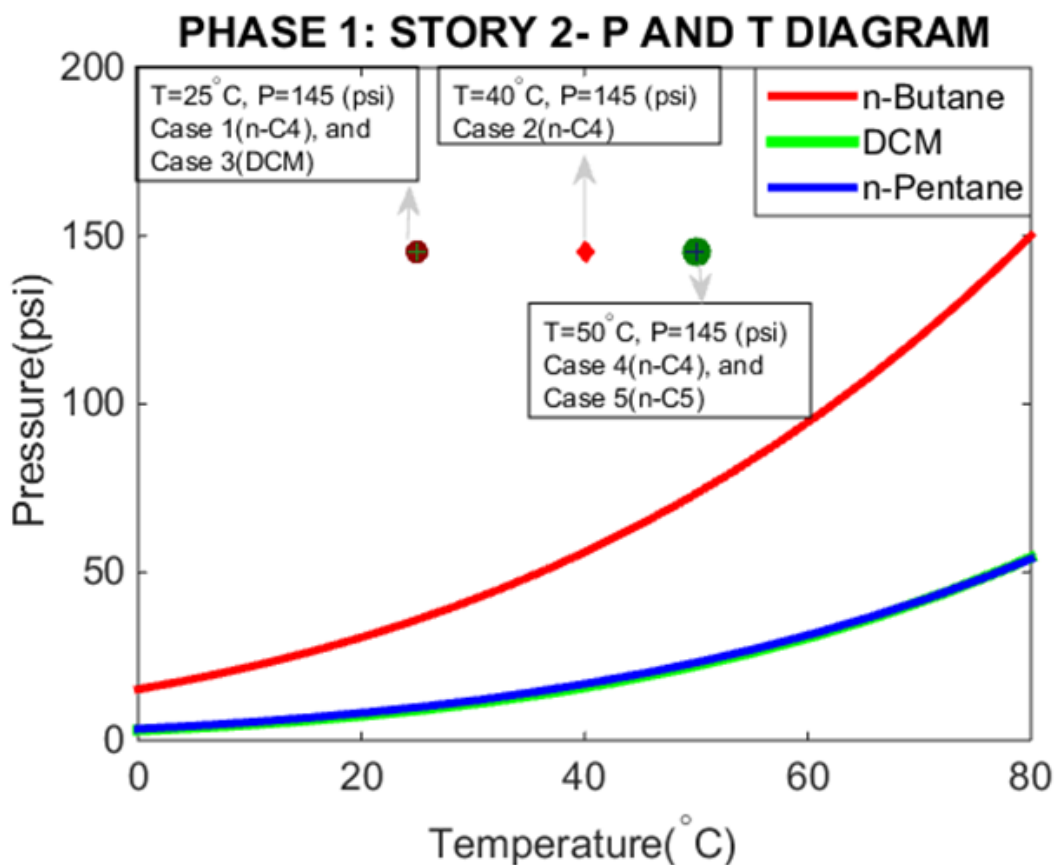


Figure 3.1: Summary of Chapter 3 parameter with visual demonstration.

The effluent was collected in a glass accumulator. For butane cases, most of the diluent in the mixture flashed and became gaseous at ambient condition, and the small amount of diluent remaining in the effluent was neglected during the accounting of oil production rate. For diluent that is liquid at room condition, the collecting apparatus was modified so that the true oil production rate is captured. The effluent mixture went through a 22-in-long heating tubing to boil off the diluent. The vapor was then forced to go through a super condenser; liquid diluent was collected and measured at the end of the condenser. For all the cases except Pentane, a vacuum condition was created during the experiment in the collector apparatus to enhance the boiling of the diluent. The vacuum was connecting

at the diluent collector. The separated effluent's volume and mass were then measured to calculate the density. In reality, the mixing of diluent and bitumen is non-ideal, however there is a small deviation from the real mixing and ideal mixing after the primary experiment of mixing the two components as shown in Figure 3.2. For simplicity, the mixture density of the diluent and bitumen is assumed to be ideal.

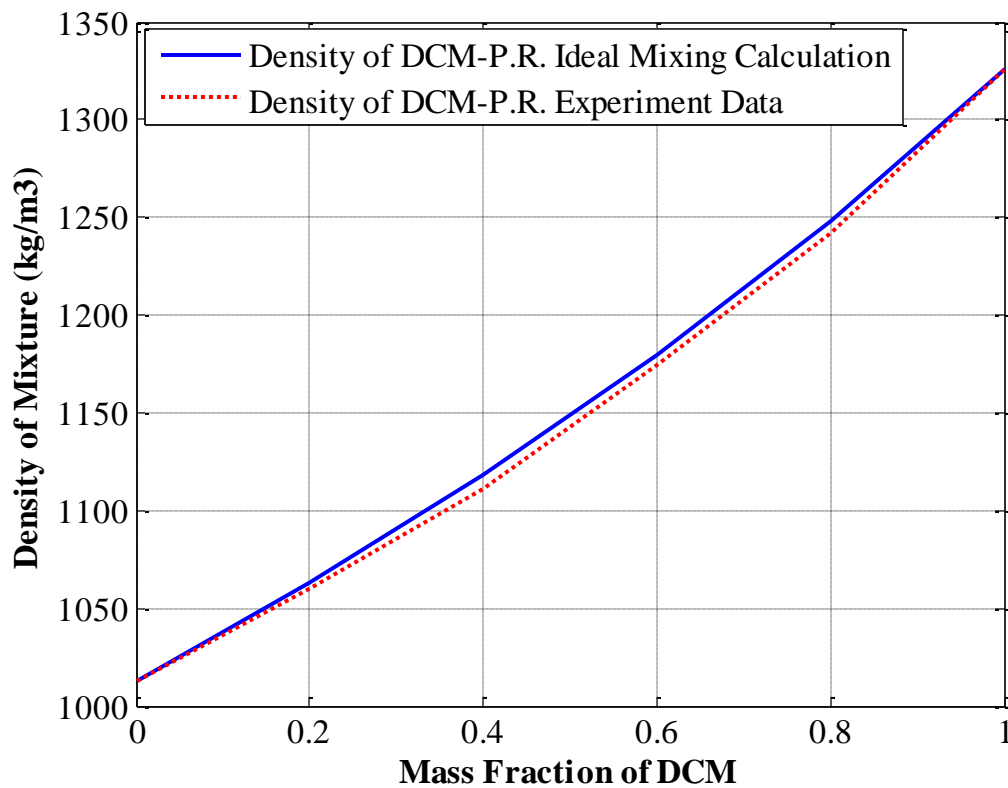


Figure 3.2: Density of P.R. and DCM

After the experiments were finished, the cores were divided into four sections to analyze and quantify the residues and asphaltenes content. Using toluene in Soxhlet Extractor process, the mixture of residual oil and toluene was then separated using Rotary Evaporator. The residual oil was undergoing the asphaltenes analysis procedure from

Wang (2002) to quantify for asphaltene mass fraction. 10 cm³ of the effluent oil from each experiment was exposed to the same procedure to analyze their asphaltenes containment.

3.3 RESULTS AND DISCUSSION

Five experiments with 2 data sets from previous work are shown here to study the effect of temperature, diluent type on the asphaltenes aggregation, one of the most important factors that influence the extraction of heavy oil in fractured system via mass transfer.

3.3.1 Base Case

In this experiment, DCM was injected into the fracture at 6 cc/min at ambient temperature. The vapor pressure of DCM at the injection temperature is shown in solid pink line in Figure 3.3. The inlet and outlet pressures are plotted as yellow dash and green dash on the right y- axis of the upper chart, respectively. Both inlet and outlet pressures indicate that the diluent existed in the liquid phase. The oil production rates, shown as green dotted line in the lower chart, were calculated from the cumulative produced volumes. Both charts share the same x-axis of time in minute. The oil production appears to have an unsymmetrical s-shape curve, where the rate was constant for about 420 minutes at 0.29 cc/min then gradually declined with time. The total oil drainage for the period of 1450 minutes was 228.1 cc.

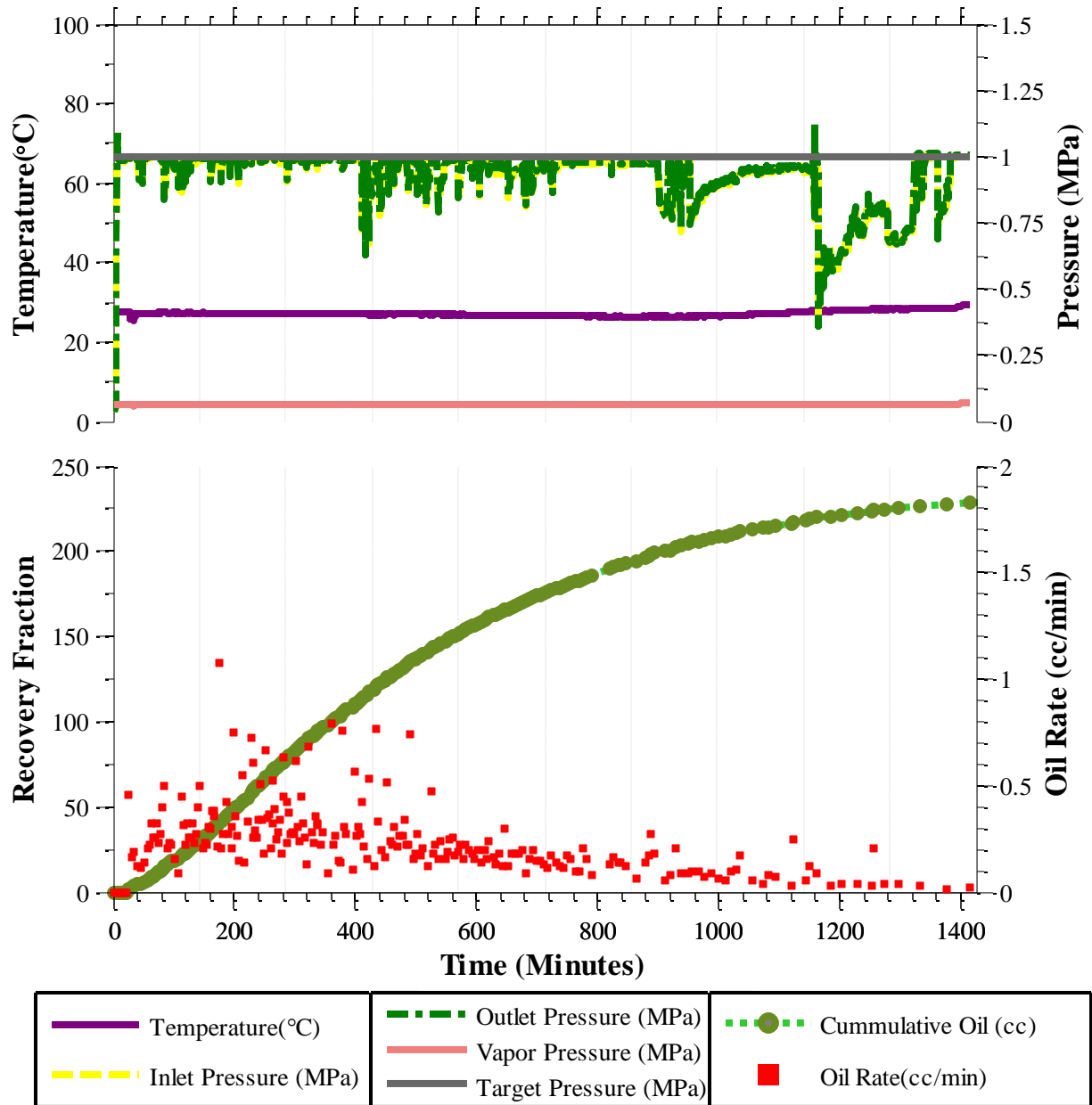


Figure 3.3: Experiment data for Base Case-DCM 25°C

Initially when the pure diluent in the fracture is in contact with pure bitumen in the matrix, the concentration difference activates the molecular diffusion between the two media. With sufficient diluent dissolving into the body of bitumen, the viscosity of the

mixture reduces exponentially such that the mixture can overcome the viscous forces and drain down to the fracture under natural convection due to density difference. Furthermore, the extraction of the bitumen by the flowing diluent stream also contributes to the production flux. Theoretically, the amount of bitumen diffuses into the diluent stream is at least two orders of magnitude higher than the reverse path, due to the inverse relationship between diffusion and viscosity. When sufficient bitumen is removed from the matrix to yields space for diluent to flow in the matrix, an increase in mixing by uneven flow occurs marking the beginning of dispersion dominated flow.

Hydrodynamic dispersion in porous media consists of effective molecular diffusion and mechanic dispersion (Perkin and Johnston, 1963). Effective diffusion is the apparent molecular diffusion taken place in porous media, and is found to be inversely proportional to the electrical conductivity and porosity of the media while the mechanical dispersion is a function of the interstitial velocity and dispersitivity. It is important to recall that this type of experimental set up is a controlled gravity drainage in fractured system, that is, build-up of the lower- viscosity mixture in the fracture does not occur if injecting diluent above the critical rate. Hence, the rate of oil production is only constrained by the factors that influence molecular diffusion of the dispersive mixing such as particle sizes, temperature, concentration difference, surface area, and permeability. Those parameters play important roles in determining the speed of creating a mixture that is able to drain down the fracture. Thus, the correlation between the oil mass flux and the ratio of bitumen viscosity and the product of porosity and permeability is misleading when evaluating diluent drainage process without other important parameters of hydrodynamic dispersion.

3.3.2 Effect of Temperature – DCM 50°C

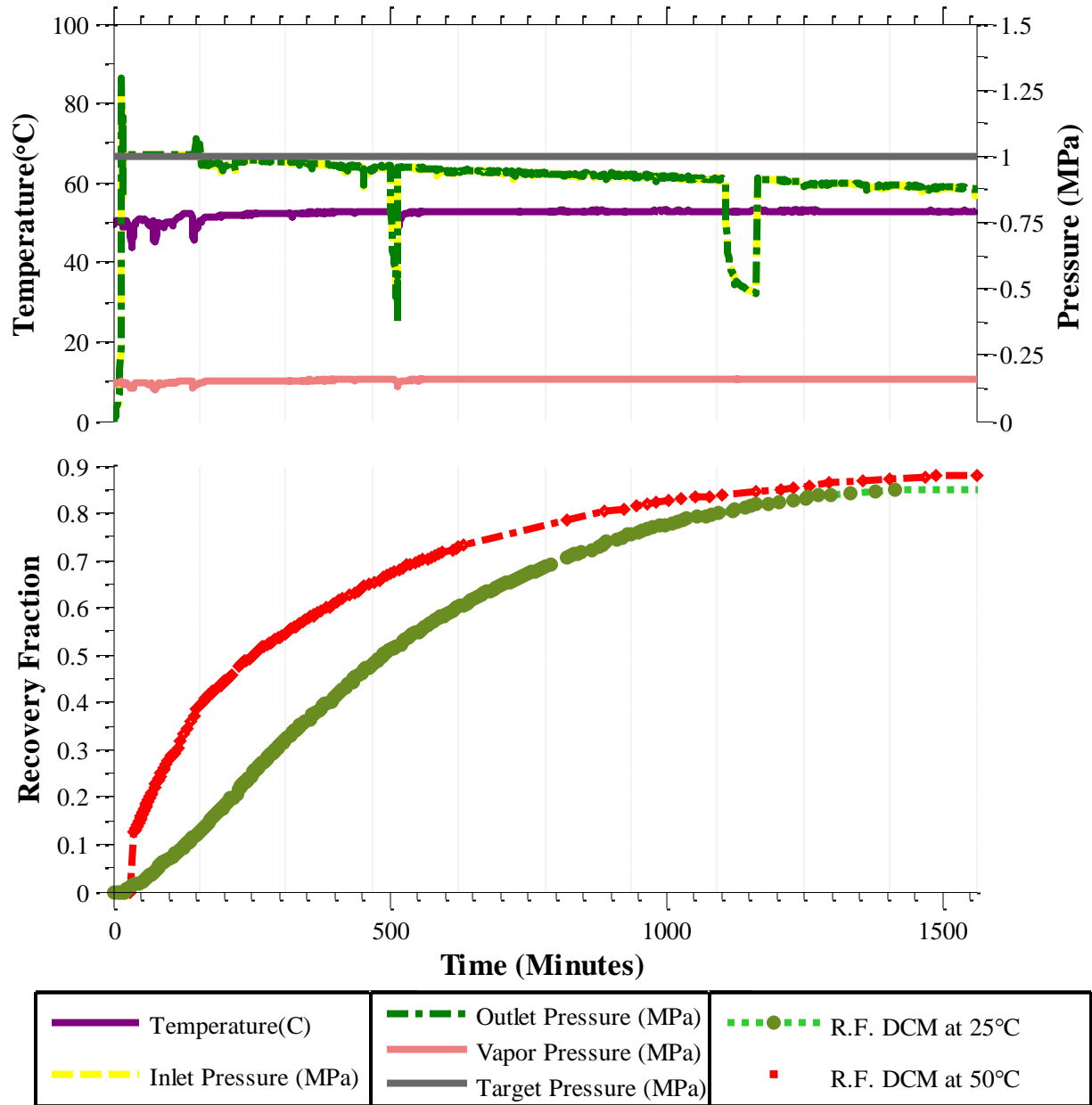


Figure 3.4: Experiment data of DCM at 50°C

This experiment was designed to study the effect of temperature. The parameters used were picked from the previous base case except that temperature has been increased

from 25°C to 50°C. Figure 3.4 shows the temperature and pressure profile in the duration of 1570 minutes of the total experiment. The inlet and outlet pressures of the system appear to be more stable than the base case. On the lower chart of the same graph, the oil recovery fraction is shown in red and the base case in green. Overall, the oil production rate of the 50°C case is higher than that of the 25°C case. The thermal expansion of the fluid occupying (~9%) the fracture in the 50°C case explains the incremental production. The decrease of mixture viscosity and the increase of diffusivity of diluent into bitumen as temperature increases are the main factors for the increase in oil recovery.

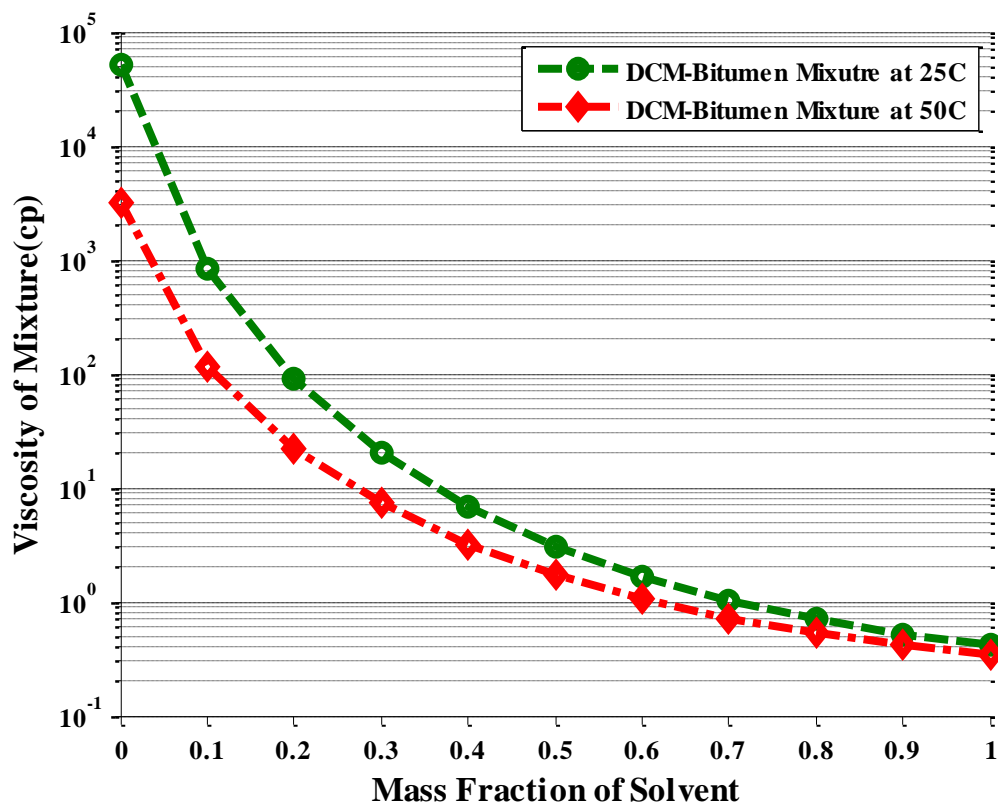


Figure 3.5: DCM and P.R. viscosity at 25 and 50°C generate using double log model

We used Miadonye's double log mixing rule for diluent and heavy oil to generate Figure 3.5. In the figure, mixture viscosities as function of mass fraction of diluent are shown in green and red for the 25°C and 50°C cases, respectively. Heating from 25°C to 50°C not only lowers the pure bitumen viscosity from 51255.49 cp. to 3165.3 cp but also decreases the diluent viscosity from 0.34 cp to 0.17 cp. With reduced pure component viscosity, the mixture viscosity becomes smaller thus entailing a higher drainage rate. Additionally, temperature promotes the mass transfer rate. Stokes- Einstein(1905), Wilke and Chang(1955), Sitaraman et al. (1963), and King et al.(1965). derived different correlations to estimate diffusion coefficient but interestingly, they arrive at the same conclusion that diffusion coefficient is directly proportional to temperature and inversely proportional to viscosity. Increasing temperature provides more kinetic energy for molecules to diffuse faster as diffusion involves random molecular movement. According to Hayduk et al. (1982), diffusivity and diluent viscosity were not inversely proportional, but they are correlated by a power law in which the exponent varies by the oil and not diluent composition. For infinite dilution case, the effectiveness of diffusion coefficient due to temperature difference is calculated as:

$$\frac{D_{50^{\circ}C}}{D_{25^{\circ}C}} = \left(\frac{50 + 273}{25 + 273} \times \frac{0.413}{0.342} \right)^B = 1.309^B, \text{ where B is determined experimentally on specific pair}$$

of diluent and bitumen and usually larger than 1. Reduced viscosity not only impacts diffusion but also affects dispersion. At low temperature where the difference in diluent and bitumen viscosities is much larger, the dispersion coefficient is larger than that when

the viscosity ratio is small (Jiao, 2013). Overall, that combination boosts the oil production rate from 0.24 cc/min at 25C to 0.60 cc/min at 50°C.

3.3.3 Diluent type effect- Pentane 50°C

In this experiment, Pentane was injected into the core at 6 cc/min at isothermal condition of 50°C. This experiment was designed to test the effect of diluent type on the mass transfer. Figure 3.6 shows the temperature and pressure profiles in the total duration of the experiment. Again, the yellow and green dashed lines show the inlet and outlet pressures of the system, respectively. The target pressure and temperature are also shown in the same graph. The pressure of the system comes quite close to the target pressure despite some fluctuation. The oil recovery fraction of this case is plotted on the same graph in dotted blue line with two other experiments that have the same parameters as the current case except for the diluent types. The experiment with DCM is shown in dotted red line, and the case in which n-Butane was injected at 6cc/min at 50°C.

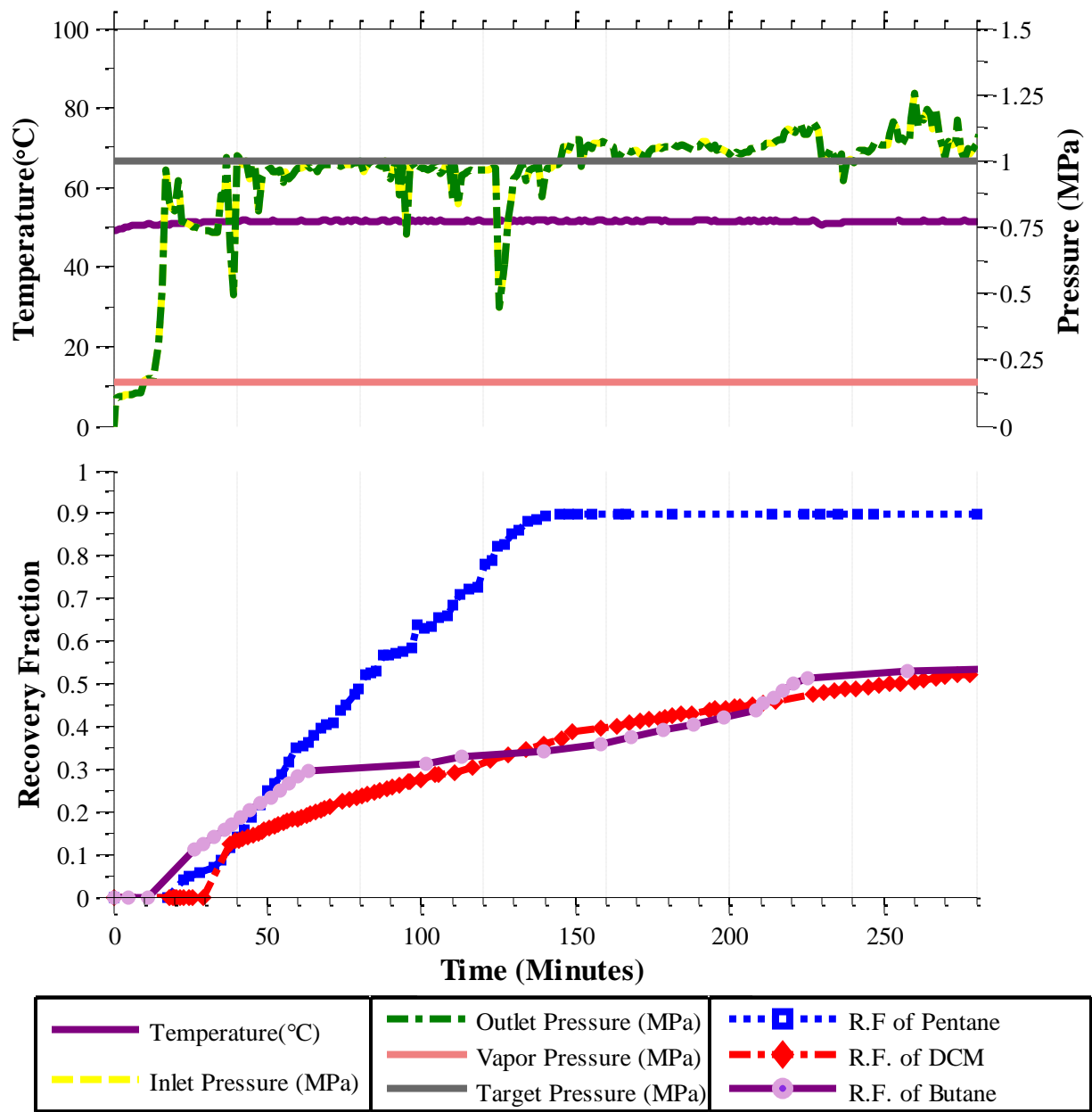


Figure 3.6: Experimental data from Pentane at 50°C

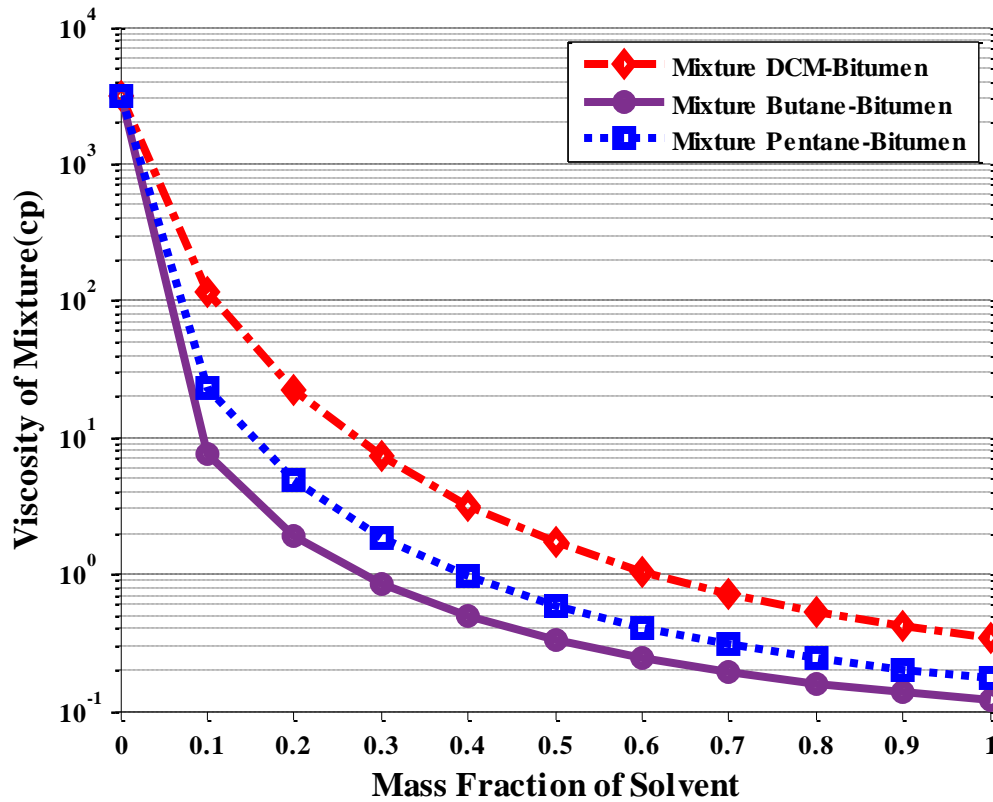


Figure 3.7: Viscosity of P.R and various of diluent

Again, we use the double log mixing rule to graph the mixture viscosity versus the mass fraction of the diluent for three different types as shown in Figure 3.7. For consistency, the color of each line is matching with the oil production curve. As shown in the chart, the pure diluent viscosity has a strong impact on the mixture viscosity. As a result, mixture of DCM is the most viscous and n-Butane is the least viscous. Furthermore, assuming that the mixing of the liquid diluent and crude oil is ideal, the mixture density should be a linear function of mass fraction of diluent. By showing the density difference

of the mixture with the pure diluent in Figure 3.8, one can illustrate the driving force for the drainage rate of the diluted mixture.

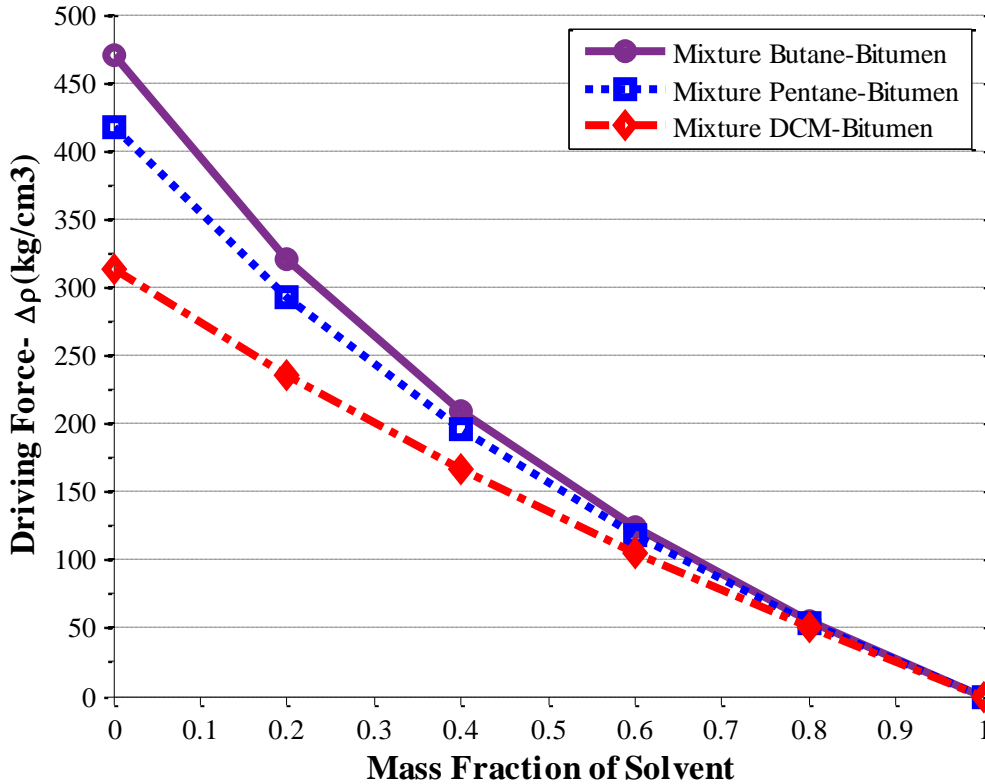


Figure 3.8: Driving force of P.R and various of diluent

The graph above indicates that the force that drives the oil from matrix to fracture is highest in n-Butane and lowest in DCM. The Butane case has a more favorable mixture viscosity than the Pentane case, nevertheless, because permeability in the Butane case was significantly lower than the Pentane case, 2.4 Darcy versus to 3.1 Darcy, the oil production of the Butane case is significantly lower. Hence, the oil extraction rate is more sensitive to permeability than mixture viscosity

The images of the cores after each experiment are also put together for illustration of the fracture surfaces in Figure 3.9. In the DCM case, the surface was completely clean of solid particles. We observed presence of solid asphaltenes in the fracture surfaces of the Butane and Pentane cases.

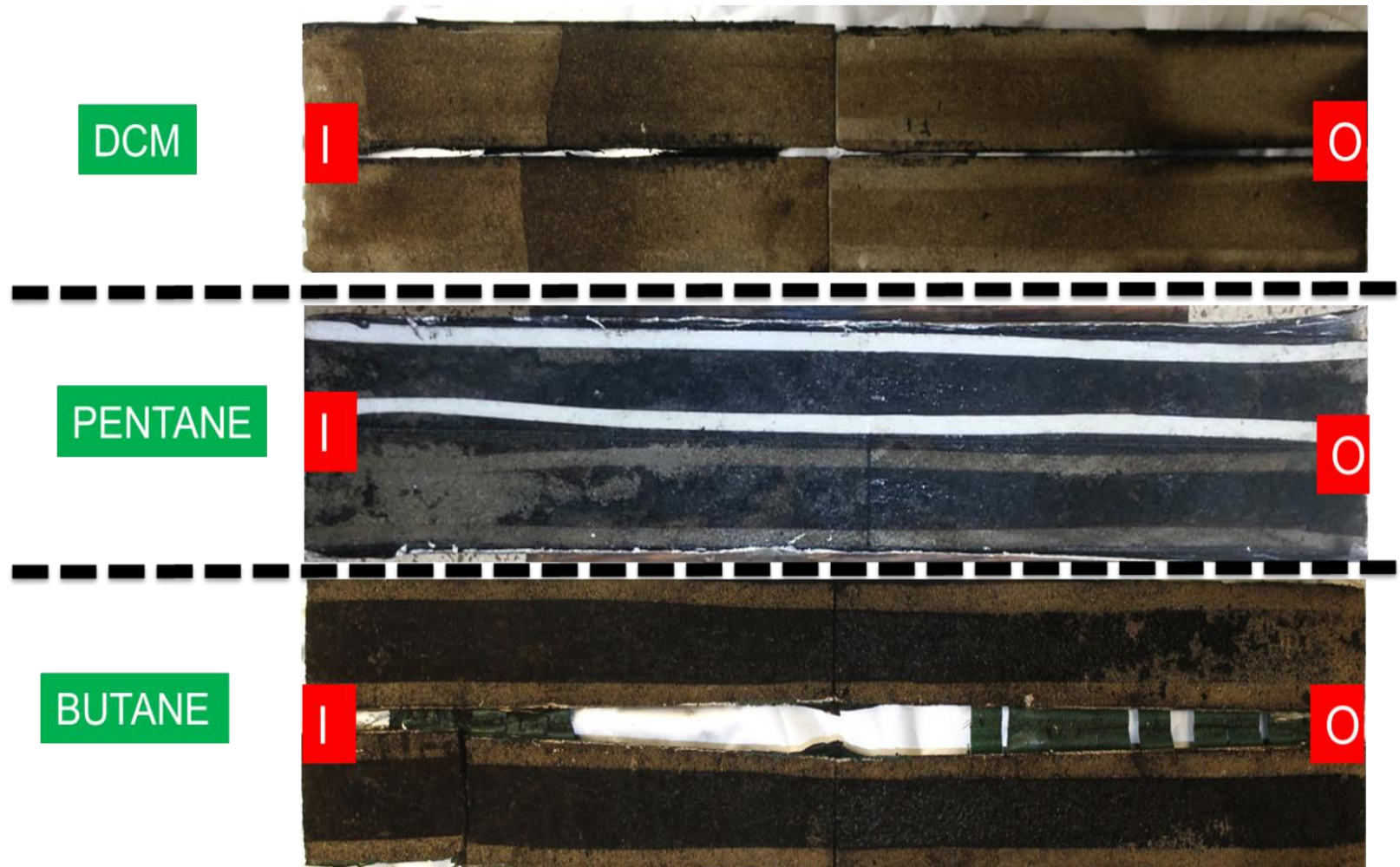


Figure 3.9: Fracture of various diluent case after experiment

3.3.4 Asphaltenes Effect -Butane 25°C

Figure 3.10 has the same format as the graphs in previous cases: pressure and temperature profiles are shown in the top chart whereas the oil recovery is shown in the bottom chart. Additionally, three recovery fraction of DCM at 25°C, DCM 50°C, and butane at 50°C cases are plotted on the same graph to compare and contrast the effect of temperature on the oil extraction process. Pressure strongly fluctuates but does not compromise the results of the experiment as diluent is in the liquid phase. Increasing temperature enhances the oil production as observed in both pairs of DCM and n-Butane cases. However, because of asphaltenes aggregation in the n-Butane cases in the extraction process, their production profiles are only stable before asphaltenes deposition. The oil production in n-Butane at 25°C case was stable for almost 100 minutes then declined in the next 150 minutes, after which it returned to the original rates. At higher temperature of 50°C, the n-Butane case- displayed more severe asphaltenes deposition. The production almost ceased after 50 minutes then slowly increased, and finally rose sharply when the impermeable shield of asphaltenes that blocked the communication between oil and diluent was broken.

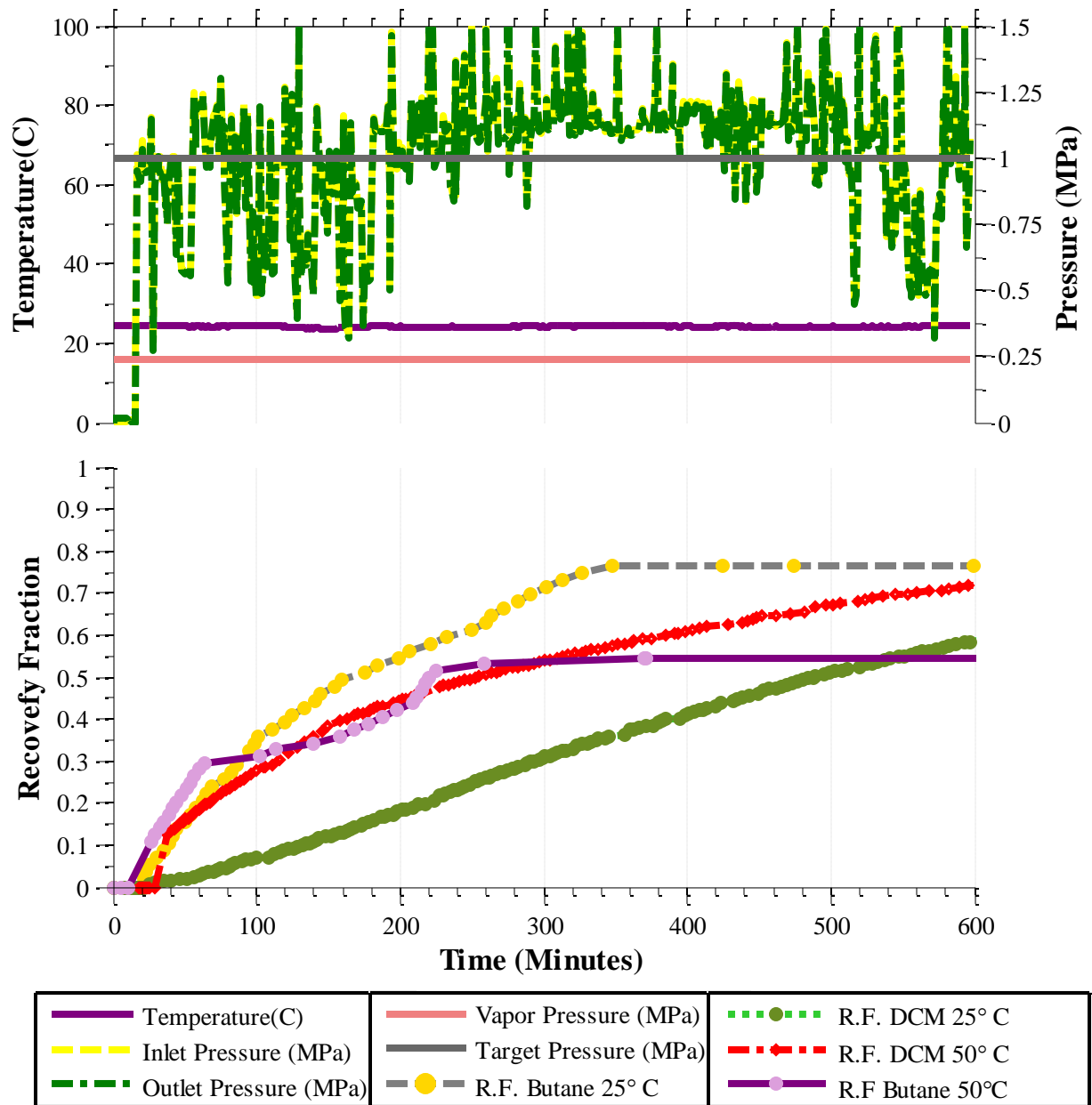


Figure 3.10: Experiment data of Butane at 25°C

David Ting (2009) pointed out that deasphalting process becomes increasingly unstable with temperature increase when using n-alkane. In other words, the asphaltenes precipitate faster at higher temperature despite the fact less asphaltenes in colloidal form

and more asphaltenes in soluble form with increase temperature. However, such observation only seen at temperature above 60°C. For our range of temperature, the onset time for precipitation was 1.6 hours at 50°C and 3.6 hours at 20°C. Maqbool et al. also confirmed asphaltenes aggregate more at 50°C than at 20°C but precipitation rate is lower due to lesser number of particle collisions because of the higher aggregate size. Furthermore, asphaltene cluster formation also needs to be taken into account. The residual mass analysis of the cores shown in Table 3.3 indicates that increasing temperature at a fixed pressure generates more asphaltenes at the top section. Because of the severe deposition of asphaltenes at high temperature, there is significant amount of oil left at the end sections making the mass fraction of asphaltenes even smaller. Arciniegas (2014) shows that higher temperature promotes cluster formation and flocculation ratios that causes severe blockage, similar to the phenomena observed in our production profile.

Core Section	Mass fraction of asphaltenes extracted from residual oils (% wt)		
	Butane at 25C	Butane at 50°C	Pentane at 50°C
Top	65.1	70.0	38.6
Section 2	69.6	75.5	66.6
Section 3	66.6	62.2	18.7
Bottom	69.6	43.9	18.4

Table 3.3: Mass fraction of asphaltenes in Butane 25°C and Butane 50°C

In Table 3.3, the mass fraction of asphaltene obtained from the residual core in Pentane case is significantly less than of what was found in the Butane cases. Asphaltene

agglomeration may change even when using different diluent types on the same crude oil. Despite their complication one common trend is that increasing the carbon number of the n-alkane diluent enhances the solubility of such diluent in heavy oil and results in lower asphaltenes flocculation (Buckley et al.). Wieche (1996) found that heavier molecular weight diluent tends to produce asphaltenes particles that are more resin.

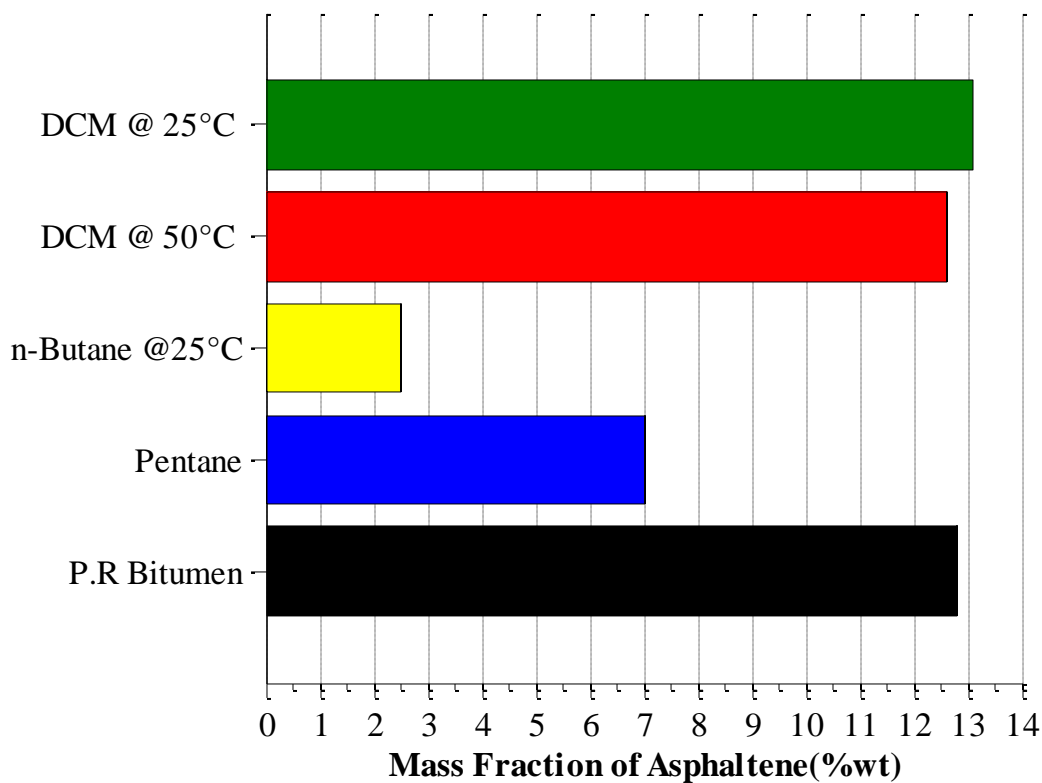


Figure 3.11: Effluent analysis

With lower carbon number, as in n-Butane, cluster of organic deposition forms super agglomeration which causes severe blockage and production tardiness when asphaltenes deposit onto the fracture preventing further penetration of fresh diluent. The

ability to aggregate and mobilize asphaltene particles of different diluent types is also reflected in the effluent asphaltene analysis. For example, when a diluent can dissolve more solid hydrocarbon, the effluent contains a larger fraction of asphaltene as shown in Figure 3.11. The asphaltene mass fraction of the original P.R is plotted in black. As DCM does not aggregate and precipitate any asphaltene, there is little compositional change in the effluent in both cases.

3.3.5 Sub-critical injection rate and temperature effect

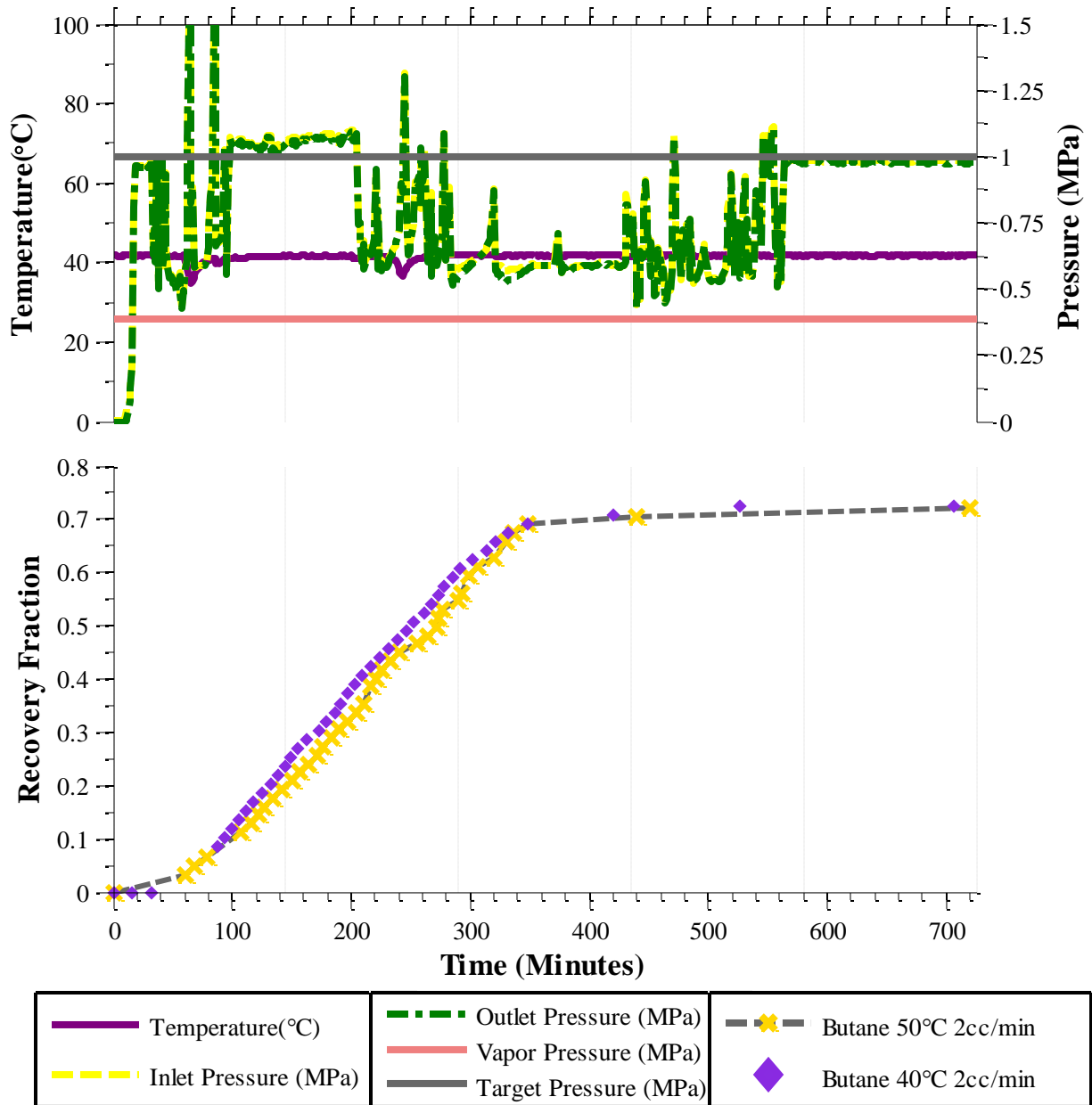


Figure 3.12: Experimental data of Butane at 40°C injection at 2 cc/min

In this experiment, n-Butane was pumped at sub critical rate of 2 cc/min at a temperature of 40°C. Similar graph structure is presented, where temperature and pressure profiles are shown at the top and the oil production profile at the bottom while sharing the

same x axis of time in Figure 3.12. The oil recovery fraction is shown alongside with a case published in the previous section with the same injection rate but at a slightly higher temperature of 50°C.

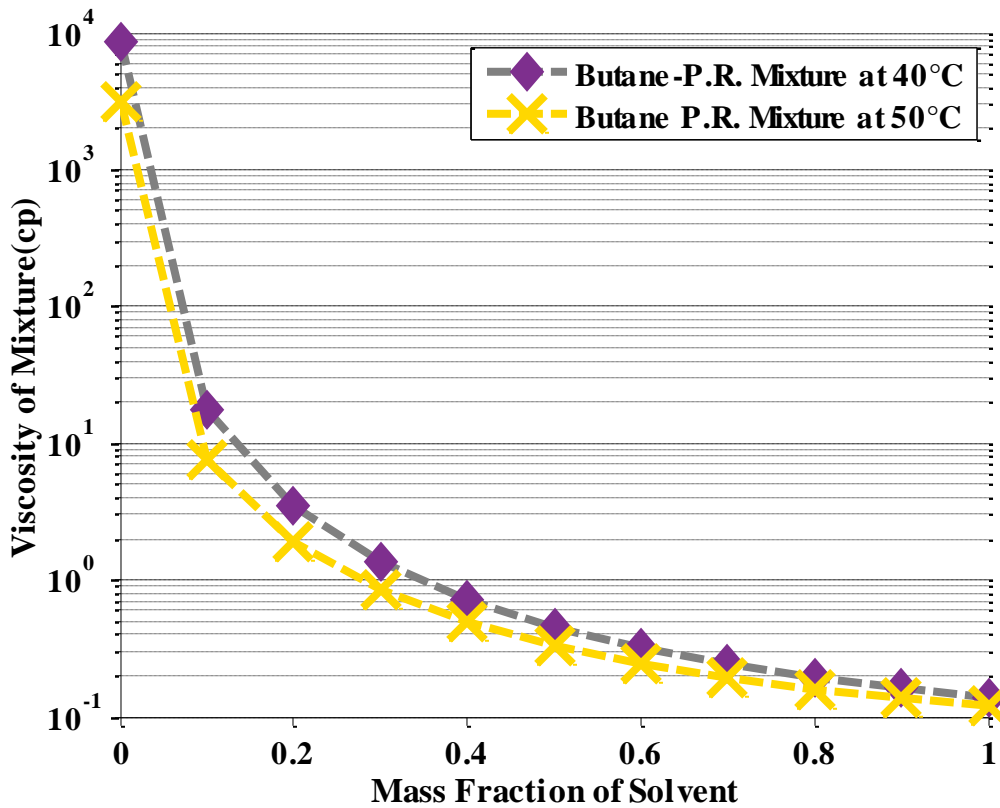


Figure 3.13: Viscosity of P.R and butane mixture at 50°C and 40°C

Figure 3.12 displays the viscosity of n-Butane mixture with P.R crude oil at 40°C and 50°C. As expected, mixture viscosity increases with decreasing temperature. As discussed above, lowering temperature actually retards the onset of asphaltene precipitation and also reduces the size of asphaltene aggregation which helps stabilizing the production profile. The data of mass fraction of asphaltene from the residual oil of

Butane at 50°C show that asphaltenes concentration is larger near the inlet in Table 3.4. While the asphaltene concentration of the Butane at 240°C is subtle, gradually increasing till the end. Only lower the temperature 10°C actually significantly change the aggregation of asphaltene in the matrix during the extraction. Compare the asphaltene concentration of the effluent conclude our hypothesis that despite the downturn of lower viscosity at lower temperature, the asphaltene aggregation can be beneficial as it becomes more controllable. For instance, at 40°C case, the effluent contain is 5.6% compare to 5.3% as in 50°C. It is surprise that even a small amount difference can cause the production profile to be less stable as observed in our experiment.

Core Section	Mass Fraction of asphaltene from residual oil(%wt)	
	Butane at 40°C @2 cc/min	Butane at 50°C @ 2cc/min
Top	56.3	72.7
Section 2	57.9	60.4
Section 3	62.1	56.1
Bottom	68.6	66.6

Table 3.4: The asphaltene analysis of sub-critical cases of butane at 40 and 50°C

3.3.6 Residual Oil Summary

In this section the residual oil in the cores of the five experiments are provided in Figure 3.14. Each of the five cores is separated into four sections, and each section is colored by a special color designated to its experiment. The weight percentage of asphaltenes in each section is plotted together with corresponding residual oil in the same bar, with the number at the top of each bar indicating the asphaltenes weight percent.

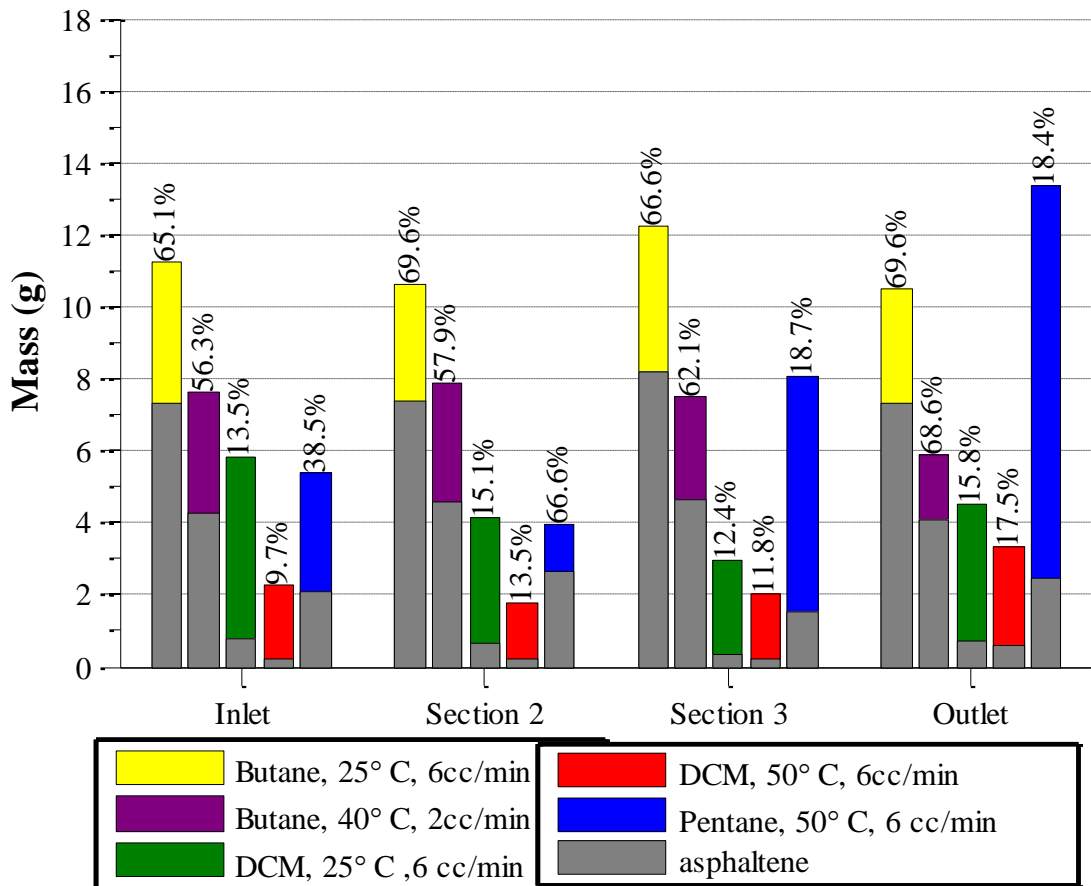


Figure 3.14: Summary of residual oil of all the experiment

In DCM cases, from the effluent analysis point of view, the composition of the effluent is unchanging. Therefore, DCM and bitumen are considered first contact miscible fluids at the injection condition. Theoretically, the diluent can extract all the bitumen in the matrix. However, after 1600 minutes of injection, the oil extraction rate approached zero while there was still some residual oil left. Such phenomenon is also observed from other diluent-based gravity drainage in fractured system. As diluent displaces bitumen in matrix, some part of the diluent is directly in contact with the oil, however the rest of the diluent is in dead end pocket.

3.4 CHAPTER SUMMARY

Without a doubt, diluent type has pronounced impacts on the process of extracting heavy oil in a fractured system using n-alkane diluent. From the mass transfer standpoint, diluent types might not affect the extraction rate as strongly as other parameters such as permeability of the media or viscosity of the raw liquids, it can be game-changing solution when controlling the asphaltenes deposition aspect.

Lowering temperature decreases the mass transfer rate as it decreases the diffusion coefficient and increases viscosity. However, it delays the onset aggregation of asphaltenes and helps prolonging the production life.

The production strategy for diluent-based process involving high-concentration bitumen must be balancing between the extraction rate and asphaltenes aggregation. Aggressive extraction can cause damages to the reservoir.

PART 2: VAPOR DILUENT PROCESS

Chapter 4: Effects of Temperature and Injection Rates on Vapor Diluent Process

4.1 INTRODUCTION

One important aspect of heavy oil is its high concentration of asphaltenes: some researchers report that heavy oil might contain up to 22% of asphaltenes by weight. In the lab, acknowledgment of the presence of asphaltenes precipitation in the vaporized hydrocarbon recovery experiments is common, however a unified agreement regarding those asphaltene behavior during a solvent injection process has not yet met. For instances, Das concluded that increasing the pressure of the system will trigger asphaltenes deposition, and Rezaei found the maximum asphaltenes deposition when reaching the lowest reservoir temperature. Asphaltenes transportation and deposition can potentially cause problems in production of fractured reservoir such as reported by Nguyen et al., hence understanding the extent of asphaltenes deposition when using vaporized hydrocarbon in recovery heavy oil cannot be lightly regarded. The purpose of this study was to investigate the mechanism of asphaltenes deposition and transportation. More specifically, we want to understand how asphaltene drop out under different effects of temperature, and injection rate can impact the vaporized hydrocarbon diffusion process. The study was done by injecting vapor n-Butane into fractured sandstone cores at different temperatures and pressures, and injection rate while keeping partition pressure constant. As discussed in the previous chapter, the main bitumen production mechanisms are molecular diffusion, dispersion. Solid asphaltene drop out were also depend on those parameters. Hence, we isolated the effect of temperature, pressure, and rate on the main

mechanism before investigate the asphaltene precipitate perspective. The study was designed so that experiment can be compares into pairs, and each pair had one parameter changes at a time to highlight only the effect of the varying parameter.

4.2 MATERIAL AND METHODS

The same procedure for core preparation, and asphaltenes analysis described in previous chapter were used. The sandstone cores properties were measured independently on each plug and provided in Table 4.1

Case #	Porosity	Pore Volume (cc)	Permeability(Darcy)
1	33%	338.2	3.0
2	28%	283.7	2.9
3	28%	285.2	2.9
4	31%	313.3	3.1
5	28%	286.6	3.1

Table 4.1: Cores properties for Chapter 4

Furthermore, a few more twists have been added for these vaporized hydrocarbon cases. For instances, the BPR itself is not manufactured to handle bitumen, it was observed in the past that it requires higher pressure than the set pressure to push the viscous oil through the orifice. In such event, higher injection pressure could potentially cause condensation of vapor solvent that lead to experiment's failure. We learnt from past experiments that pressure build-up only occurs in the early periods when, diluent was first injected, it displaced brine and the thermal oil expands in the fracture. In order to avoid

pressure build-up in the course of diluent injection, the expand oil in the fracture was bypassed the BPR with brine before switching to diluent injection. The amount of bitumen collected is reported in mass as shown in Table 4.2.

Case #	Volume water collect (g)	Pre-solvent collected oil (% of OOIP)
1	63.4	18.7
2	55.2	19.4
3	62.1	21.7
4	43.8	15.8
5	58.9	20.6

Table 4.2: Thermal expansion of oil during heating (25°C to 50°C)

In order to achieve a better separation, the oil/solvent mixture was piped through a double-walled flask where the temperature was kept at 80°C. However, if the solvent is liquid under ambient conditions, a specially designed collecting apparatus was used to create a vacuum environment in the chamber to flash the solvent. If the solvent is gaseous, the standard volumetric flow rate was measured using a mass flow meter, and if the solvent is a liquid, the vaporized vapor solvent then went through a cooled condenser and was measured using a second accumulator. The production rate for water and oil was calculated by recording the time between each 5mL increment in the glass collector for the first liquid extraction. For the second liquid extraction and vapor diffusion, the oil was measured every 1 mL increment in volume for greater precision. The mass of the oil produced was also obtained to perform a density check in order to detect the existence of solvent in the oil.

There are total of five experiments in which different injection rates were implemented and summarized in the following Table 4.3. Detailed description of each case is described below:

Case #	Temperature (°C)	Target Pressure (Mpa)	Solvent Type	Injected Condition Rate (cc/min)	Injection Rate (cc/min)
1	50	0.37	n-Butane	3	198.60
2	80	0.78	n-Butane	3	95.44
3	80	0.78	n-Butane	1	31.82
4	50	0.37	n-Butane	1	66.20
5	80	0.22	DCM	3	--

Table 4.3: Experimental parameters for this chapter

One can visualize the set of experiments above as data points in a vapor pressure diagram, as shown in Figure 4.1

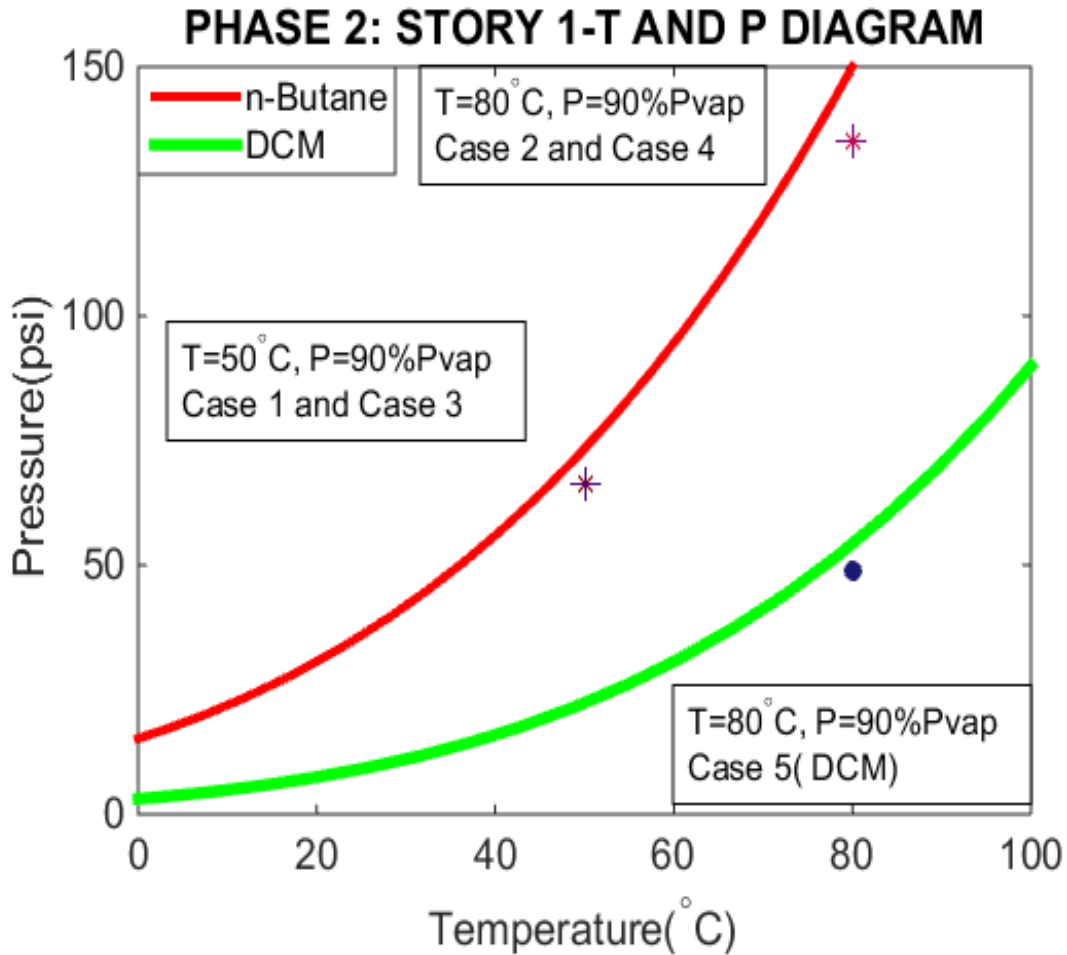


Figure 4.1: Chapter 4 parameter with visual demonstration with diluent vapor pressure line.

4.3 RESULTS AND DISCUSSION

This section discusses results and discussion of four experiment on systems pressure.

4.3.1 Base Case- *N-Butane at 50°C, 3cc/min*

In this experiment, vapor solvent was injected at 3 cc/min at $P=0.37$ Mpa and $T=50^{\circ}\text{C}$. The temperature (purple line) and pressure profile (dashed yellow line and dashed green line for inlet and outlet pressure, respectively) of this case indicated a successful run.

i.e. the solvent was in the vapor phase, or under the dew point (pink line) for Figure 4.2. The oil production rate shown in red saw a stable rate of approximately 0.288 cc/min for about 300 minutes before it starts declining. The oil accumulative column shown in green dotted line has a typical S- shape of a gravity drainage profile., We observed maximum recovery of 192 cc after 1800 minutes of solvent injection.

When the vapor solvent is in contact with the oil, the mechanism of oil recovery can be described as:

- molecular diffusion of the diluent within the body of bitumen bulk which helps reducing the viscosity of the mixture by diluting and upgrading
- Drainage of the reduced viscosity oil with the help of gravity

The physics behind this experiment can be simplified using the thin film theory, as illustrated in the diagram below (Figure 4.3), in which the mass transfer coefficient was denoted as K_v . The solvent concentration at the oil/gas interface is the maximum concentration of solvent diffusing into the oil, and the concentration of diluent at the liquid bulk interface is controlled by the diffusion coefficient and the time of diluent exposure. The thickness of δ_{ORS} is reported to be in the order of pore sizes (λ).

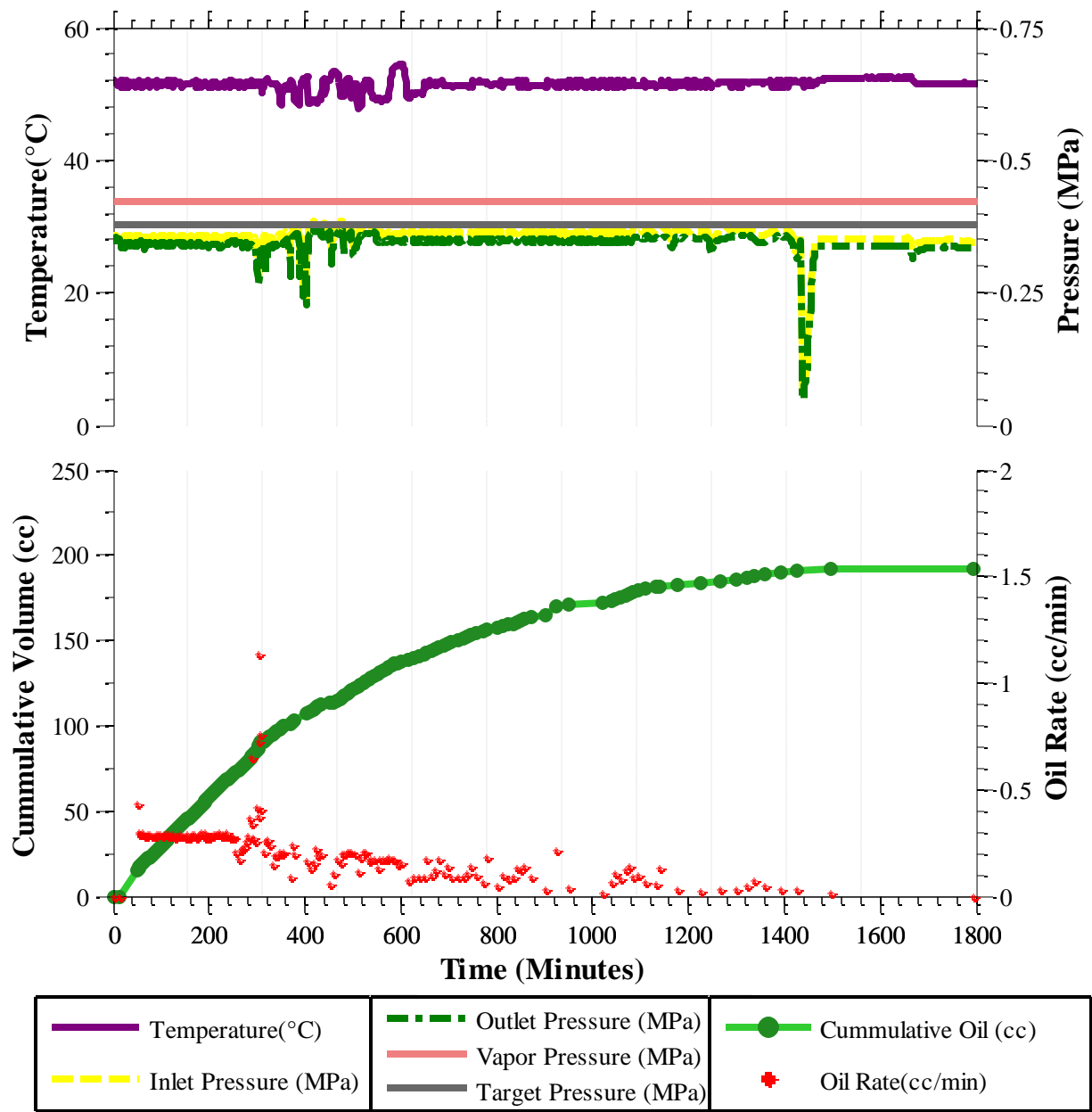


Figure 4.2: Results from experiment of Butane at 50 °C with injection rate of 3 cc/min

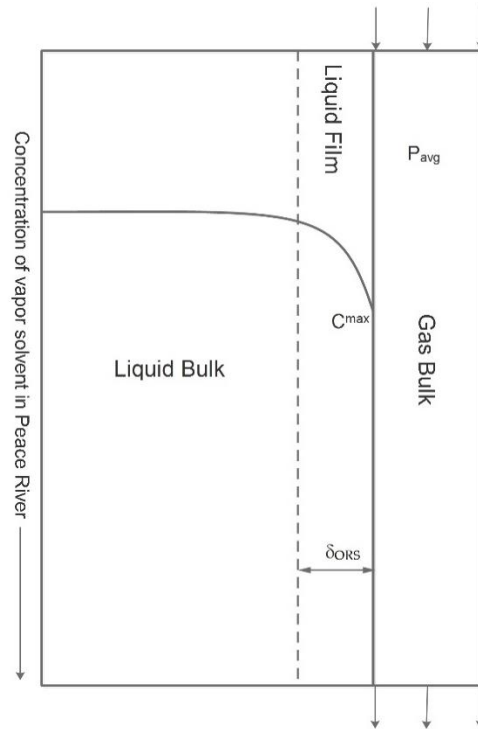


Figure 4.3: Schematic of penetration- film theory

C_{max} -the concentrations at the oil/diluent interface can be estimated by Henry's law assuming equilibrium of the oil and the vapor solvent at experimental conditions, as Wilhelm discussed that Henry's law approach appears to be naturally superior to the others. Henry's constant is not constant with respect to temperature. Henry's constant typically increases with temperature at lower temperatures, and after reaching a certain maximum, decreases with temperature. The temperature at which the maximum occurs depends on the solvent and oil pair. The interrelated temperature dependencies of Henry's constant are dictated by infinite dilution activity coefficient (diluent type) and solute vapor pressure.

When using the same diluent at the vapor pressure, Henry's constant increases with increasing temperature. Normally, the greater the Henry's constant, the less soluble the gas

in the oil, and the less effective the penetration of diluent gas molecules into bitumen body. However, oil viscosity decreases exponentially at higher temperature thus increasing molecular diffusion activity of the diluent in the bulk bitumen and enhancing the oil drainage rate. From previous chapter, we concluded the significance of temperature effect on the diluent process and the event of asphaltene precipitation. Therefore, it is essential to investigate the effect of temperature on the vapor diffusion.

4.3.2 Temperature Effect –Butane 80°C 3cc/min

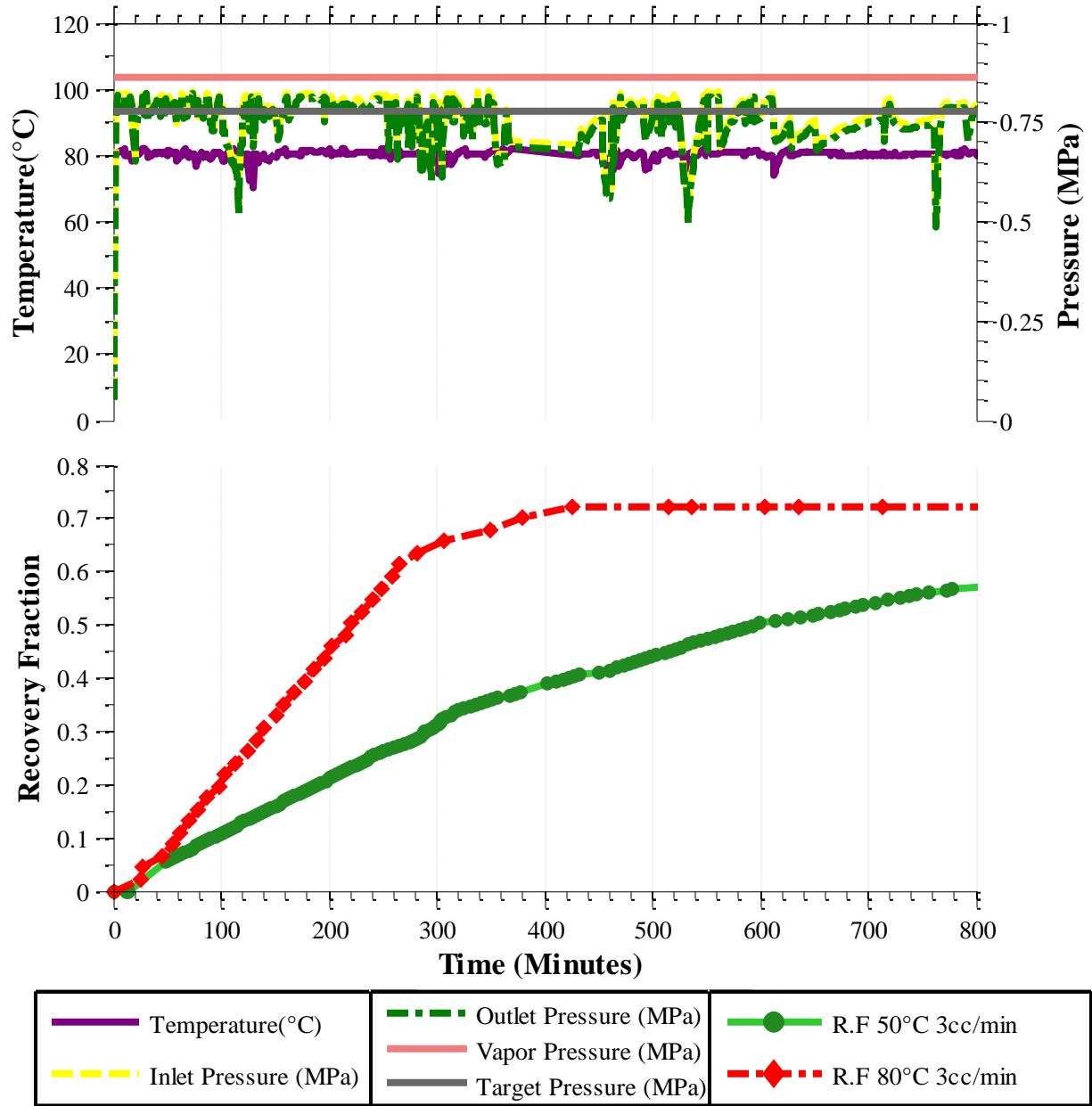


Figure 4.4: Results from experiment of Butane at 80°C with injection rate of 3cc/min

In this experiment, the same experimental conditions as the base case were applied except for the higher system temperature of 80°C as shown in Figure 4.4, The system

pressure (inlet and outlet) was fluctuating around the target pressure but stayed under the vapor pressure plotted in pink line. The oil rate in this experiment was constant at 0.5623 cc/min. For comparison purposes, the recovery fraction of this experiment was plotted in red whereas the base case results were in green. After offsetting the amount of oil recovered from cleaning the fracture, the oil recovery from this experiment is 72.2% compared to the base case at 69.8%.

The viscosity profile of the mixture is constructed using the double log model and is shown on the Figure 4.5. The viscosity of the bitumen reduced from 3165 cp. to 330.56 cp. when heating from 50°C to 80°C. Note that the viscosity of the vapor solvent did not change significantly between the two cases (0.00804 cp. versus 0.00888 cp.).

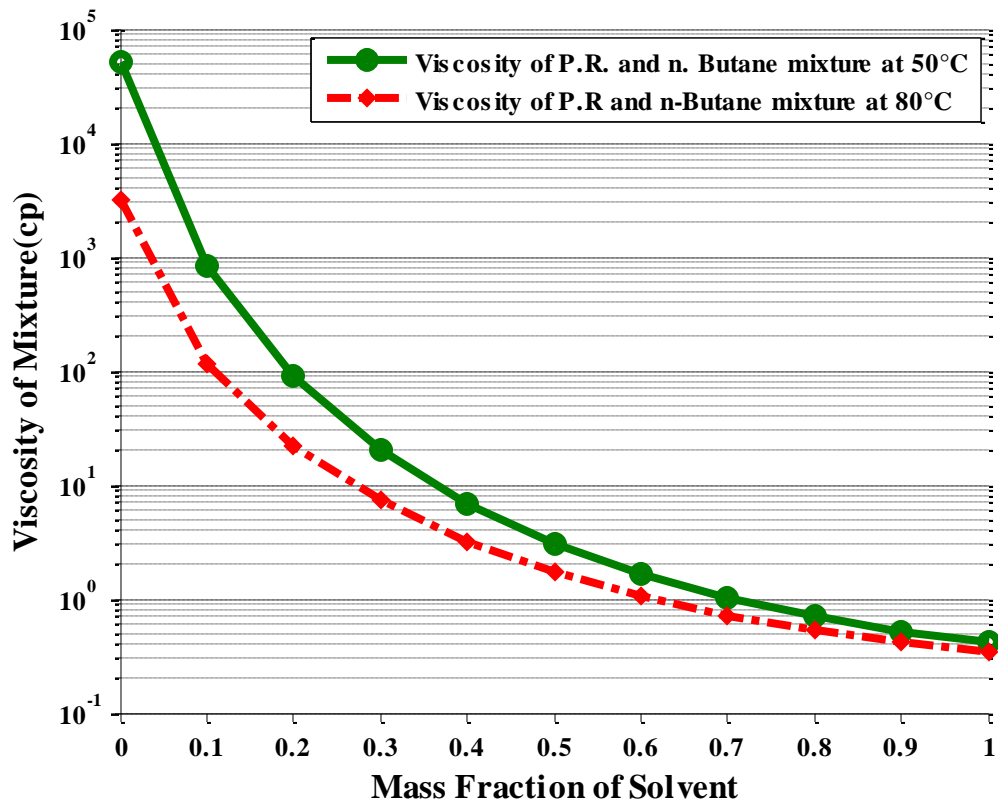


Figure 4.5: Viscosity of P.R bitumen and n-Butane

In a steady state process, the rate of recovery in the transition zone needs to be balanced with the leading front of the boundary layer. With that assumption, mass transfer of the diluent at the leading boundary layer is the limiting factor of the interfacial mass transfer. However, it is important to note that the steady state assumption of mass transfer of diluent into the bitumen in our study as the concentration gradient is changing in time due to the fact that the pressure gradient in the direction of flow within the diffusion layer was not steady state. In fact, most interfacial mass transfer study for bitumen overlooked the mass transfer due to such assumption. For instance, Das used apparent diffusion coefficient when calculating mass transfer coefficient in the porous media to account for: (1) the improved interfacial contact, (2) the increasing rate of solubility and the effective diffusivity, (3) and the enhanced surface renewal by capillary imbibition and development of transient mass flux at the bitumen surface.

4.3.3 Rate Effect on Mass Transfer

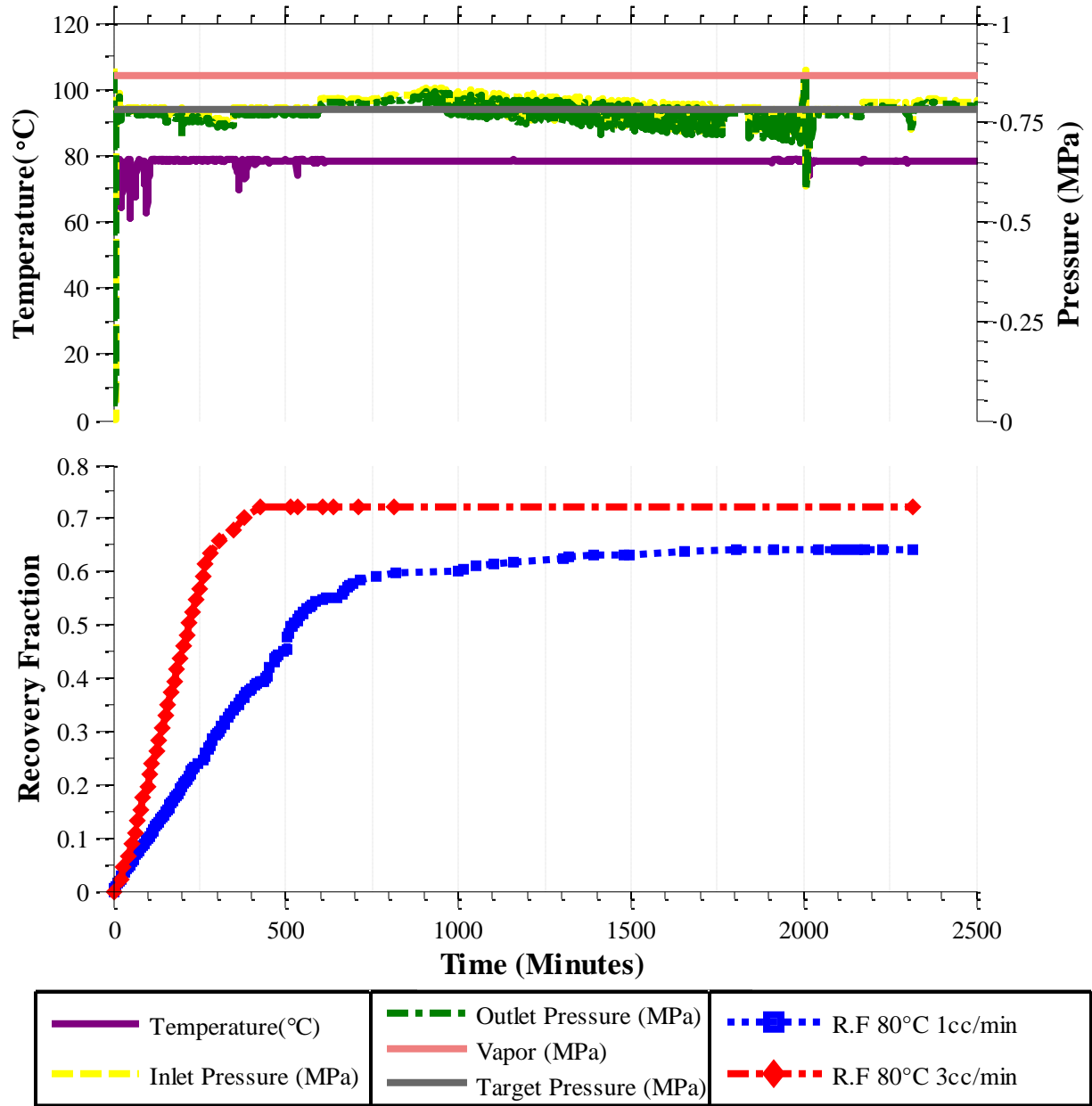


Figure 4.6 : Results from experiment of Butane at 80 °C with injection rate of 1 cc/min

In this experiment, n-Butane was injected into the fractured core with the same condition as the previous case ($T=80^{\circ}\text{C}$, $P=0.78\text{ MPa}$) at a much lower injection rate, 1

cc/min of cold water displacement. The same figure format for the system is shown in Figure 4.6. Both inlet and outlet pressures were fluctuating between the target pressure plot in the gray line. The oil recovery fraction in this case was plotted in blue in comparison with the recovery fraction of the higher injection rate in red.

Tripling the solvent injection rate increased the oil production rate from 0.267 cc/min to 0.600 cc/min. Increasing the injection rates increased the in-situ vapor phase velocity which directly impacted both the longitudinal and transverse dispersion (Blackwell 1992).

We ran another experiment similar to the Base Case except the injection rate of the in-situ velocity of the diluent is in the intermediate. The temperature and pressure profiles are presented in the same format in Figure 4.7. Pressure highly varied in the beginning but stabilize at a later time. The oil recovery fraction at higher injection rate was plotted in purple whereas that from the lower injection rate case was in green. Fortunately, the rock permeability of the two cases are relatively comparable, 3.1 Darcy versus 3.0 Darcy. In another word, in these two cases, diluent injection rate was the only significant difference. The oil production rate seemed stabilized and kept constant at 0.29 cc/min up to 600 minutes. This oil production rate is almost equal to our lower injection rate case at 0.288 cc/min. Now if we recall the volumetric solvent injection rate in Table 4.3, focusing on the higher temperature pair (80°C), the diluent rate on the lower injection rate get as low as 31 cc/min. And we observed a big production jumped as the diluent injection rate increased to 95 cc/min owing to the enhancement of dispersity that caused more mixing.

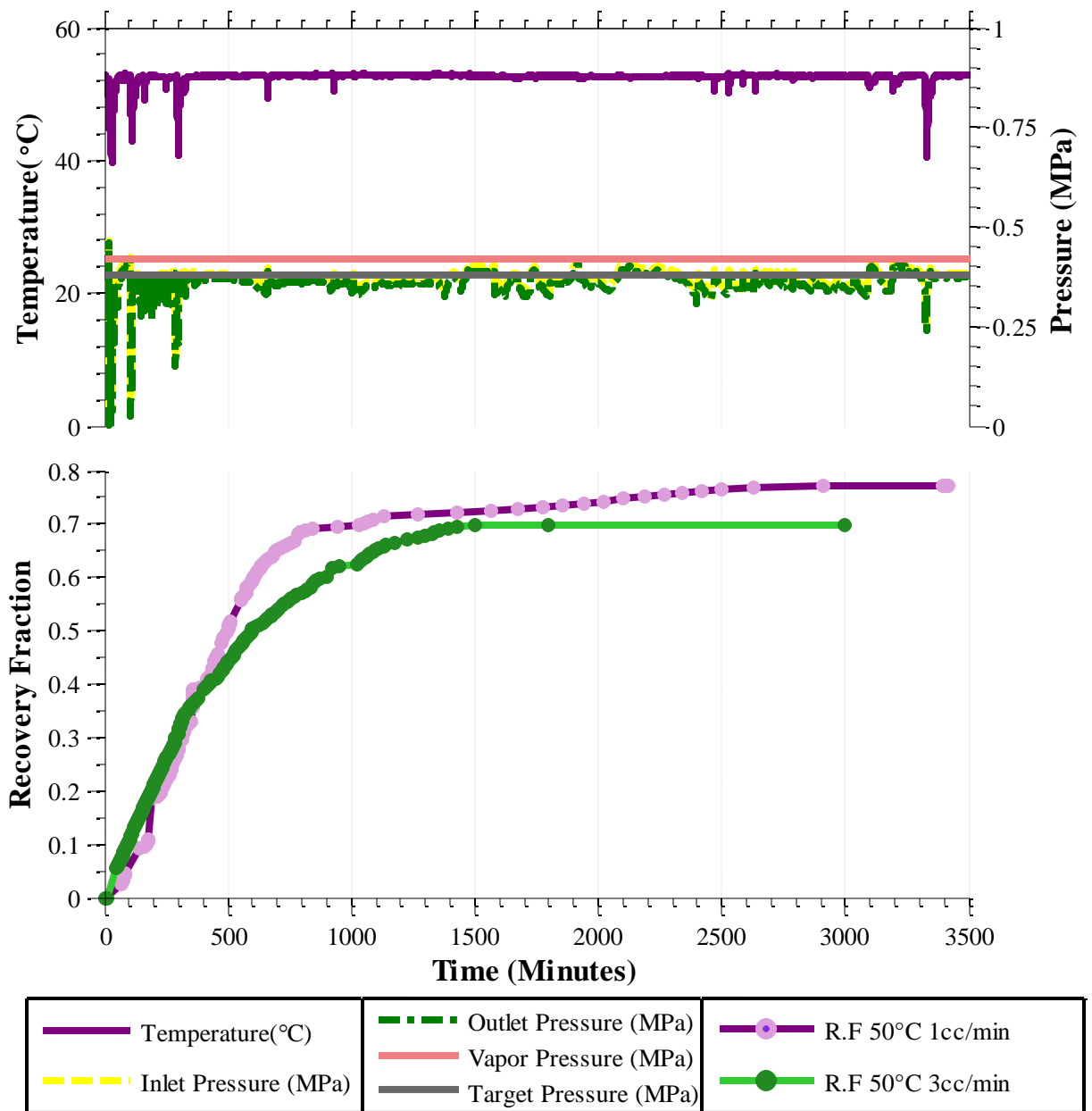


Figure 4.7: Results from experiment of Butane at 50 °C with injection rate of 1 cc/min

4.3.4 Asphaltene Effect-DCM 80°C 3 cc/min

After each experiment, the cores were taken out for the analysis of residual mass and asphaltenes as described in the chapter 2. The most notable observation was the lack

of solids deposited on the surface of the fracture face as shown in Figure 4.8. With asphaltene analysis, the asphaltene content of the residual oil ranges from 15.8% -22.1% where that of the original oil falls between 14.7%-16.2%.

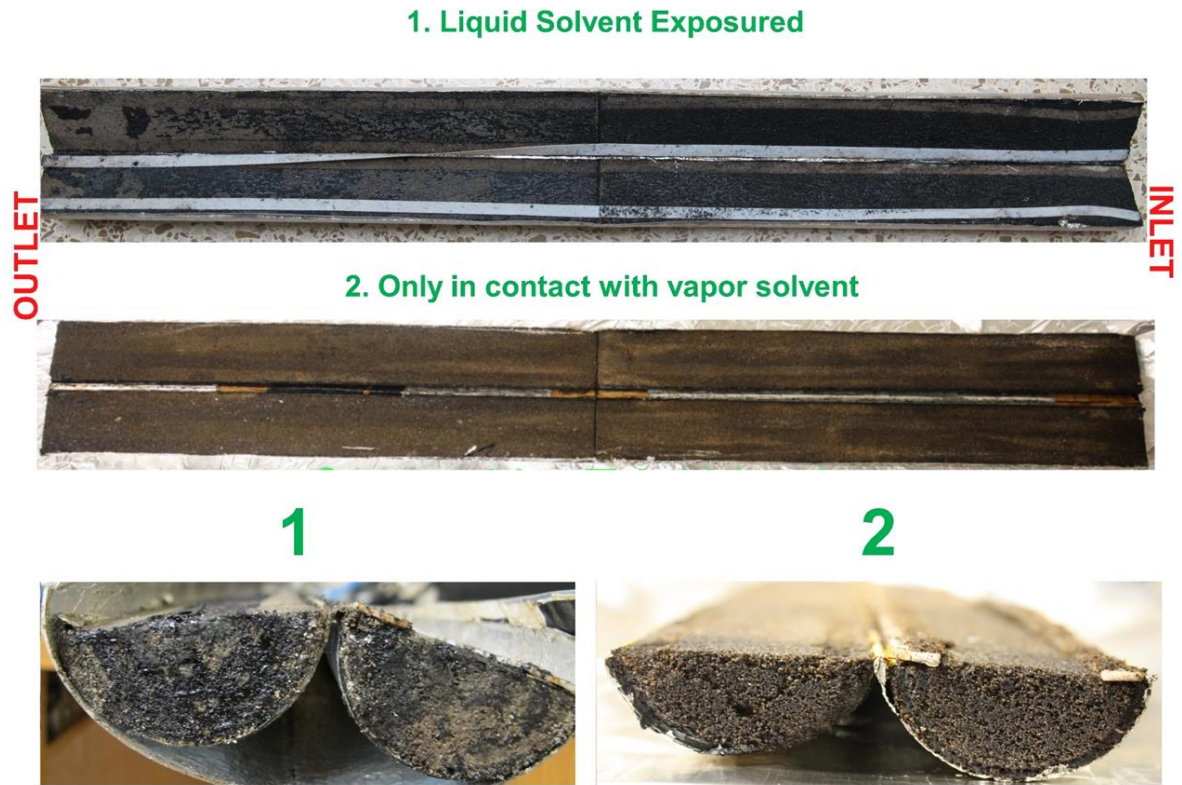


Figure 4.8: No asphaltene deposited after core flooding as in liquid

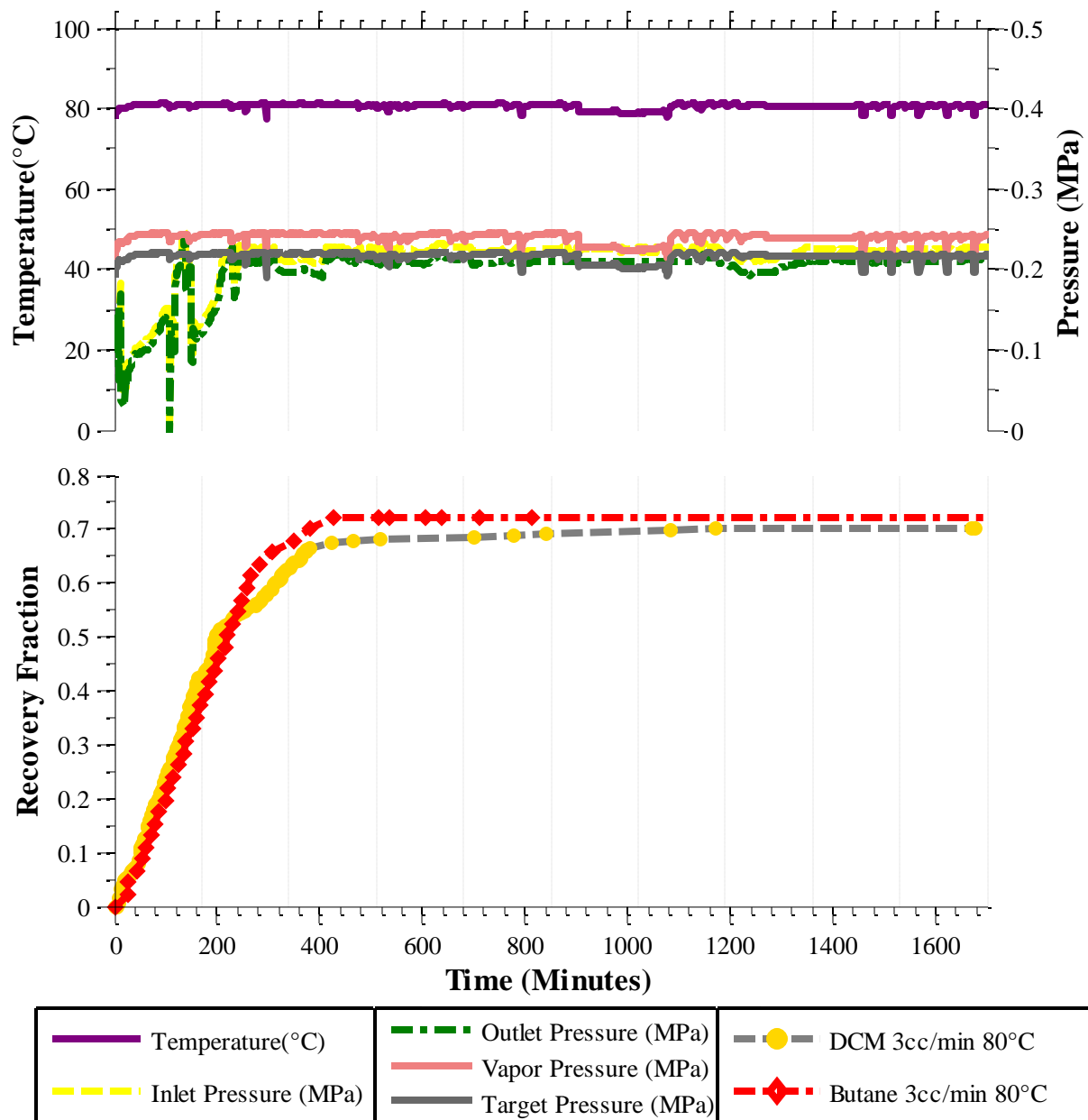


Figure 4.9: Results from experiment of DCM at 80 °C with injection rate of 3 cc/min

Figure 4.9 provides results for the DCM case. The effect of solvent type is highlighted by showing in red and purple for n-Butane and DCM on the same chart, respectively. Per expected, DCM drainage rate is higher than n-Butane at the same

condition, 0.8 cc/min compare to 0.6 cc/min. The better performance of vaporized DCM can also from the contribution of difference in mixtures viscosity of oil and diluent and/ or by permeability of the rock (3.1 Darcy-DCM compare to 2.9 in n-Butanes). The question of whether or not asphaltenes has impact on the process will be discussed along with residual and effluent analysis.

Mass of oil was plotted in four bars for each core flood, the mass of asphaltenes for that section was shaded in grey in Figure 4.10. The top section of the core contacted with the diluent longer, hence more mass was produced- less residual oil. All the cases shown in the graph below confirm that in vapor diffusion the asphaltenes deposition was not as severe as liquid extraction

When the diluent injection rates were above the critical rate, the effluent oil contains more asphaltenes in dissolution (n-Butane at 80°C). Furthermore, the excess of diluent in the higher injection rate of n-Butane showed a significant increase in concentration of asphaltenes in the rock compare to the 1 cc/min cases, Figure 4.11.

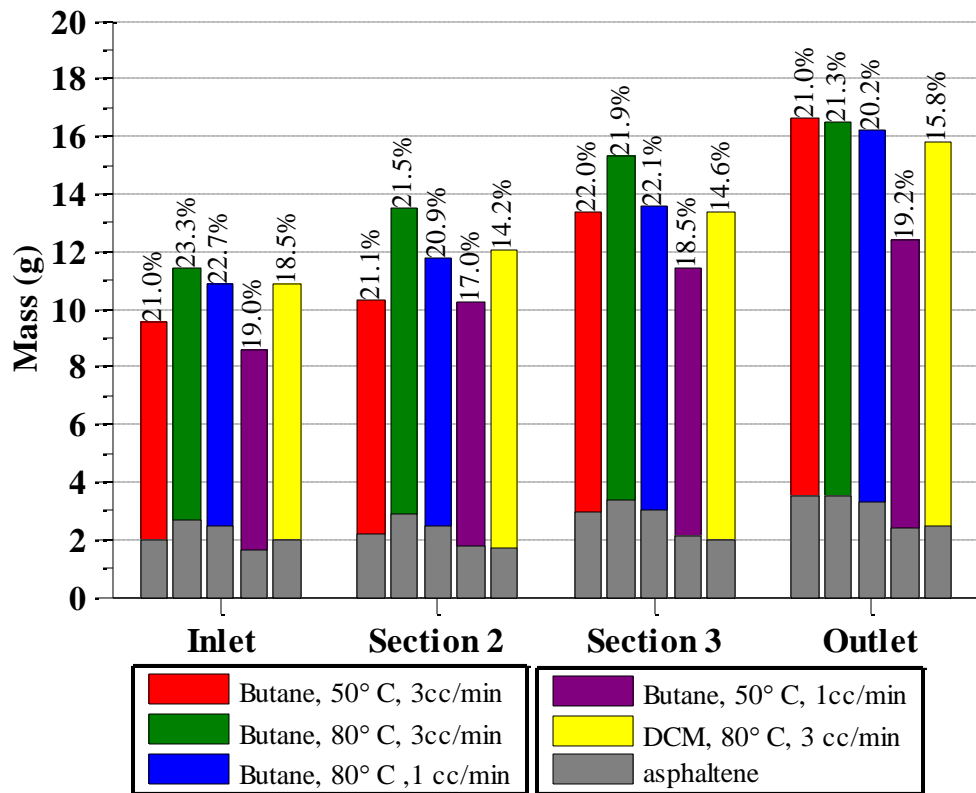


Figure 4.10: Mass of oil and mass of asphaltene of cores sample by sections.

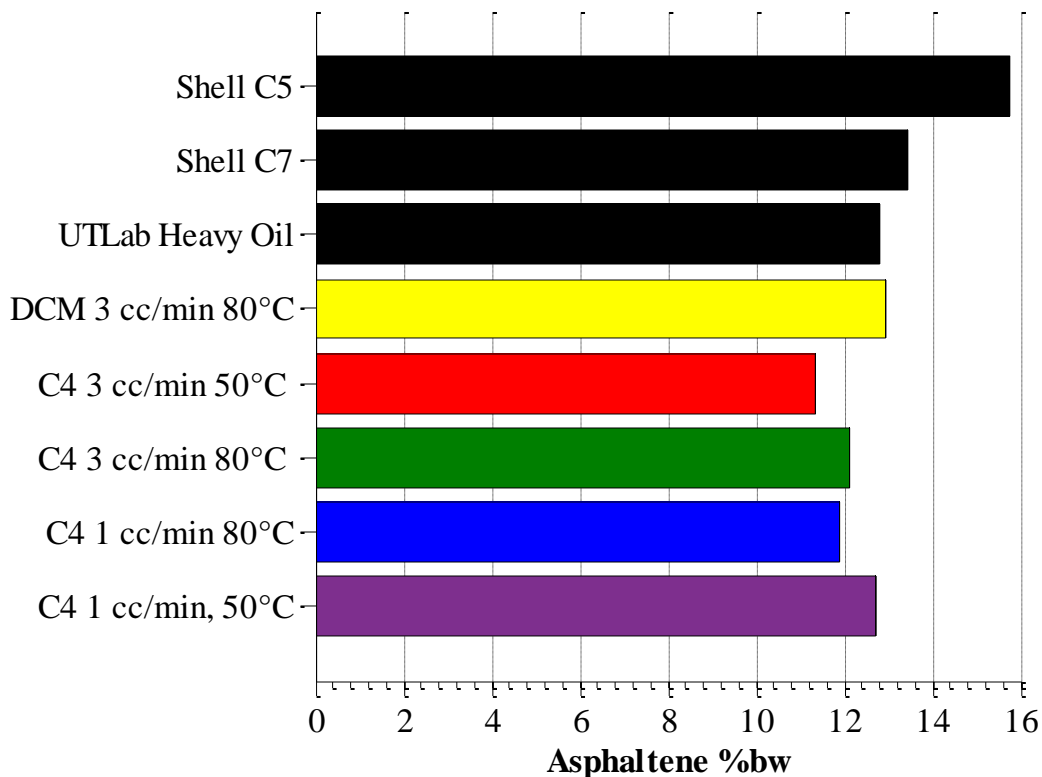


Figure 4.11: Asphaltene analysis for effluent samples

The dispersed asphaltenes colloids covered by resins are well peptized by the oils (maltene). At higher temperature, the colloidal asphaltenes are small in amount and tend not to form strong associations, because the resins effectively disperse the colloids (Branco et al., 2001; Hoepfner et al., 2013; Maqbool et al., 2011). This is because a fraction of asphaltenes is dissolved leaving enough mass of the resins and oil to keep the remaining smaller aggregates of asphaltenes well peptized in the oil at higher temperature. Fig. 6 shows that peptizability of asphaltenes decreases with increasing temperature because of possible phase transition, whereby, asphaltenes tends to dissolve in oil at higher temperature. Increase in peptizability means associations among

asphaltenes colloids is more extensive and they are not sufficiently solvated by the solvent, hence the tendency of asphaltenes to aggregate at lower temperature is higher which could result in precipitation and deposition on surfaces. Resins have strong tendency to associate with asphaltenes, this reduces the aggregation of asphaltenes which determine to large extent their solubility in crude oil. Resins are also reported to have a self-association tendency like asphaltenes and it can be assumed that at lower temperature, the resins self-associate strongly hence their tendency to associate with asphaltenes is reduced (Pereira et al., 2007).

To validate the experimental results, mass balance was performed on each experiment and the results are provided in Table 4.4 below. The error due to the loss of mass while crushing the rock can be up to 7%.

Case #	Mass oil original (cc≈g)	Mass Oil Produced (cc≈g)	Total Mass Oil Retrieve from Core (g)	Sum of oil recovered (g)	Rel. Error (%)
1	313.3	208.0	42.65	293.65	6.27
2	285.2	143.0	52.41	257.4	9.7
3	283.7	170.0	49.9	275.1	3.03
4	338.2	192.0	56.8	307.5	9.07
5	286.6	149.0	52.1	260.0	9.28

Table 4.4: Mass balance of Chapter 4 Experiments

4.4 CHAPTER SUMMARY

Condensation of vaporized hydrocarbon when utilizing to recover heavy oil can completely alternate the oil production mechanism and cause unwanted asphaltenes

precipitation and deposition. Asphalenes precipitation of pure vaporized extraction process is not as severe as reported in liquid diluent cases. We once shown that once the bitumen was in contact with liquid, deposition of asphaltene could potentially problematic to the reservoir especially fracture reservoir.

Below a critical injection rate, gravity drainage in fractured reservoir with vaporized solvent is sensitive to the volumetric injection rate of vapor. Increasing the temperature of the reservoir creates two counteracting effects: the decreased solubility of solvent into oil versus the lowered viscosity of the oil. With the results observed from the four cases of n-butane, effect of temperature on viscosity reduction seemed to be more dominant. Effect of the solvent type introduced no vivid increase in oil production between the DCM and n-Butanes. Solvent type contributes determine the maximum concentration of solvent at the interface which reduce the mixture viscosity. Furthermore, the diffusion of solvent within the bulk liquid depend on the liquid viscosity. However, without asphaltene problem, the use of diluent can only benefit from the mass transfer point of view.

Chapter 5: Effects of Diluent Pressure on Vapor Process

5.1 INTRODUCTION

From the previous Chapter 4, without a doubt, during vapor diffusion drainage process, asphaltene deposition was indeed less than of liquid diluent process asphaltene deposition was a less severe problem in vapor diffusion drainage process than in liquid diluent process. It is well known that the diluent concentration in heavy oil at equilibrium reaches a maximum value at the diluent vapor pressure. Increasing diluent concentration reduces bitumen viscosity resulting in higher drainage rate. Higher diluent concentration in the transition zone as pressure increases causing the asphaltene in the oil to become more unstable which cause increasing in precipitation. During field operations, the diluent injection pressure would vary away from the wellbore. Hence, it is important to fully understand the impact of pressure on the process for field optimization purposes. We run four experiments with two different types of diluent at two different partition pressures.

5.2 MATERIALS AND METHODS

In this series, we conducted four experiments with two different kinds of diluent: DCM and n-Butane. In all experiments, we injected diluent at the same cold water injection rate at isothermal condition of 80°C. We employed the same procedure and method from the previous chapters. The rocks properties were presented in the Table 5.1

Case #	Porosity	Pore Volume (cc)	Permeability(Darcy)
1	28%	338.2	3.0
2	29%	300.1	3.1
3	31%	301.1	3.3
4	31%	298.7	3.1

Table 5.1: Rock Properties from Chapter 5 experiment.

The experimental grid designed for each of the experiment are specified in Table 5.2 below. The pressure versus temperature plot is also displayed in Figure 5.1 to help visualizing where each of the experiment lies in the phase diagram.

Case #	Temperature (°C)	Target Pressure	Solvent Type	Injection Rate (cc/min)
1	80	0.75x P _{vap}	DCM	3
2	80	0.5 x P _{vap}	DCM	3
3	80	0.75x P _{vap}	n-Butane	3
4	80	0.5x P _{vap}	n-Butane	3

Table 5.2: Experiment grid for Chapter 5 experiments.

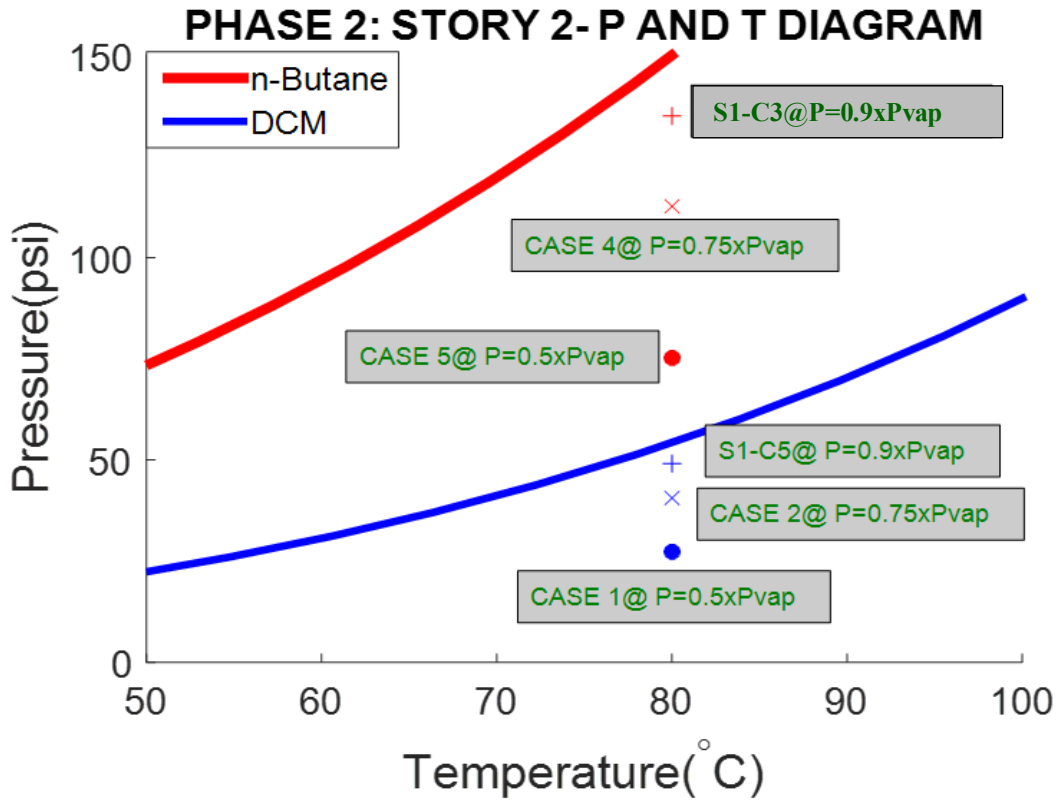


Figure 5.1: Summary of Chapter 5 parameters with visual demonstration.

5.3 RESULTS AND DISCUSSIONS

Four experiments with two diluents types were conducted at the same temperature of 80°C with pressure varying from 50% to 75% of the diluent vapor pressure.

5.3.1 DCM-80°C 75% Vapor Pressure

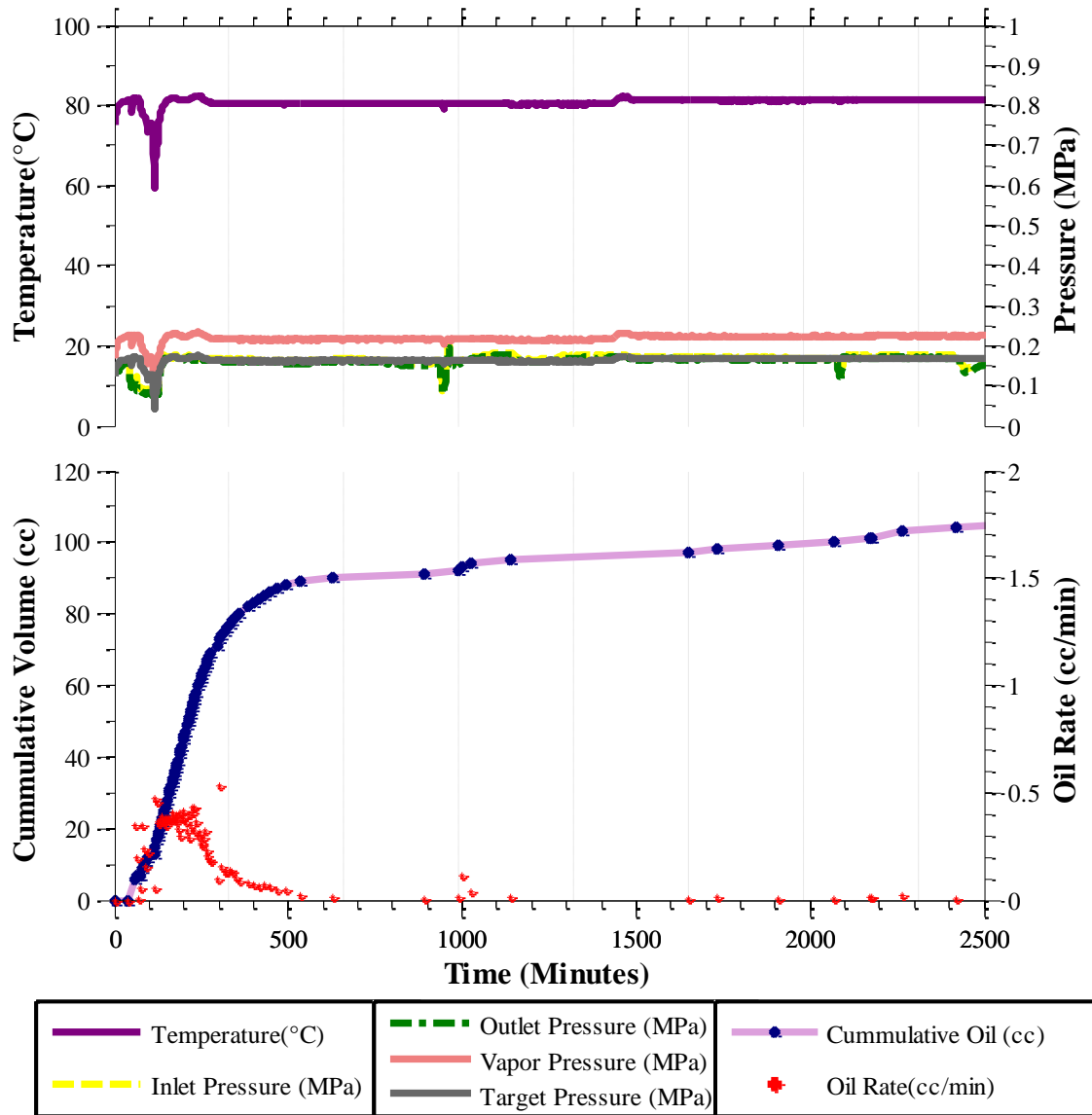


Figure 5.2: Results from experiment of DCM at 75% vapor pressure at 80 °C

In this experiment, DCM was injected at 3 cc/min at isothermal condition of 80°C, and 75 percent of DCM’s vapor pressure. The temperature profile plot follows the same template as all other the experiments. The temperature (solid purple) and the inlet and outlet pressures (dotted yellow and dotted green, respectively) were right at target of the solid gray line. The cumulative oil volume recovered was plotted in purple line with blue marker,

while the oil rate, calculated from dividing the equal incremental volume by the time it took for each increment, was shown in red dot. The oil production rate was stable at around 0.37 cc/min in the early times, and significantly changed at around 50% of OOIP. Such behavior can be due to some heterogeneity of the rock causing a sharp turn at around 250 minutes. Total oil recovery in this case is 46% while the experiment was run for 3200 minutes.

5.3.2 DCM-80°C 50% Vapor Pressure

In this experiment, DCM was injected into the core at 50% of the vapor pressure. Figure 14 indicated that the temperature and the pressure of the system were at target. The wavy behavior of the pressure of the system was because of the physical limitation of the BPR as discussed before. The oil rate peaked at 0.1 cc/min and then declined exponentially over the time of injection. For the total of more than 6000 minutes of injection only a total of 32% of OOIP was recovered.

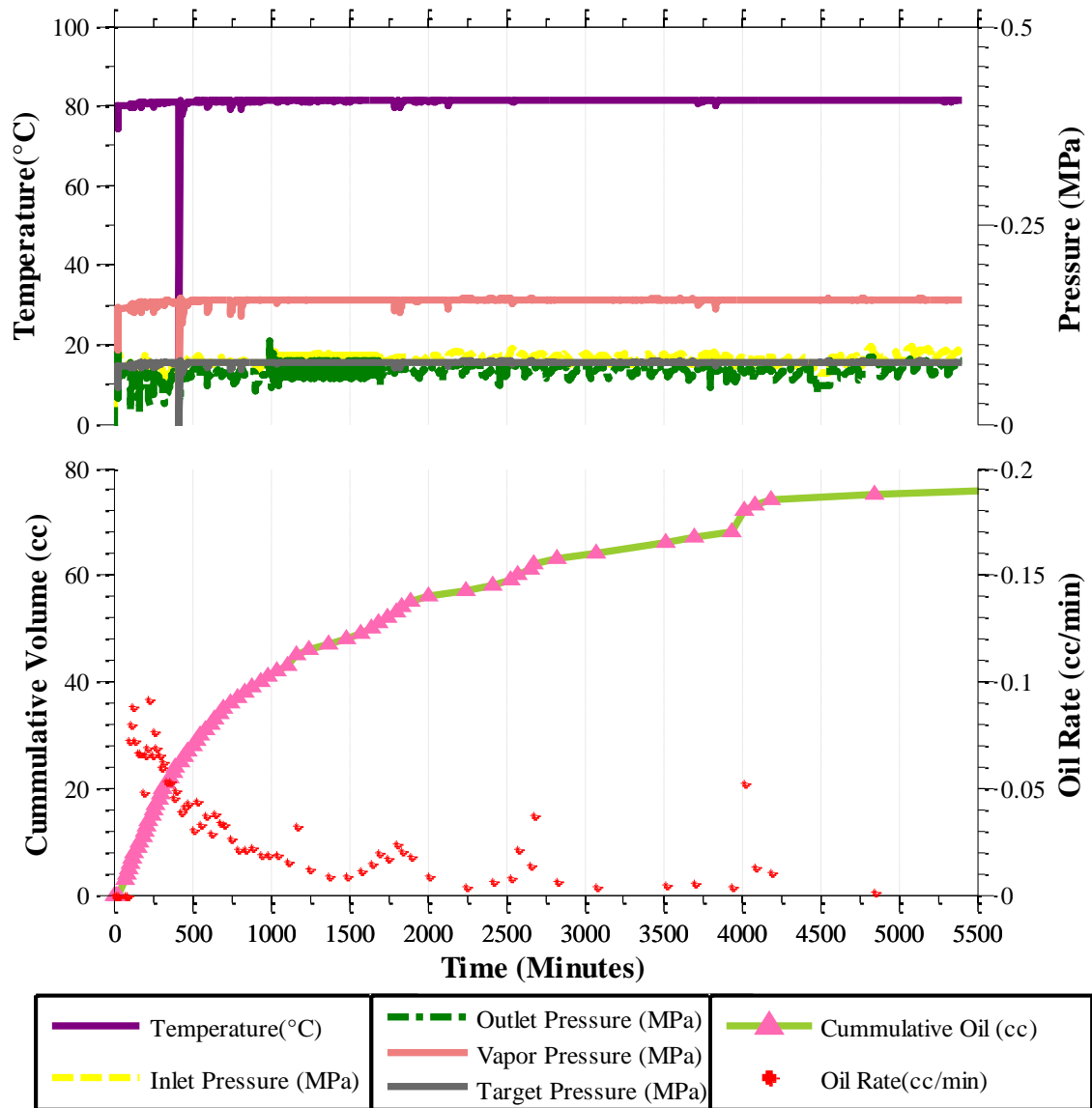


Figure 5.3: Results from experiment of DCM at 50% vapor pressure at 80 °C

5.3.3 n-Butane-80°C 75% Vapor Pressure

During this experiment, n-Butane was injected into the core at 75% of the vapor pressure. With the knowledge from the last two experiments, as prediction the oil production rate decrease as the vapor pressure decrease from the vapor pressure. The oil production rate in this case was initially around 0.2 cc/min and declined exponentially with time. The total oil recovery in this case was 68% in the timespan of 2000 minutes.

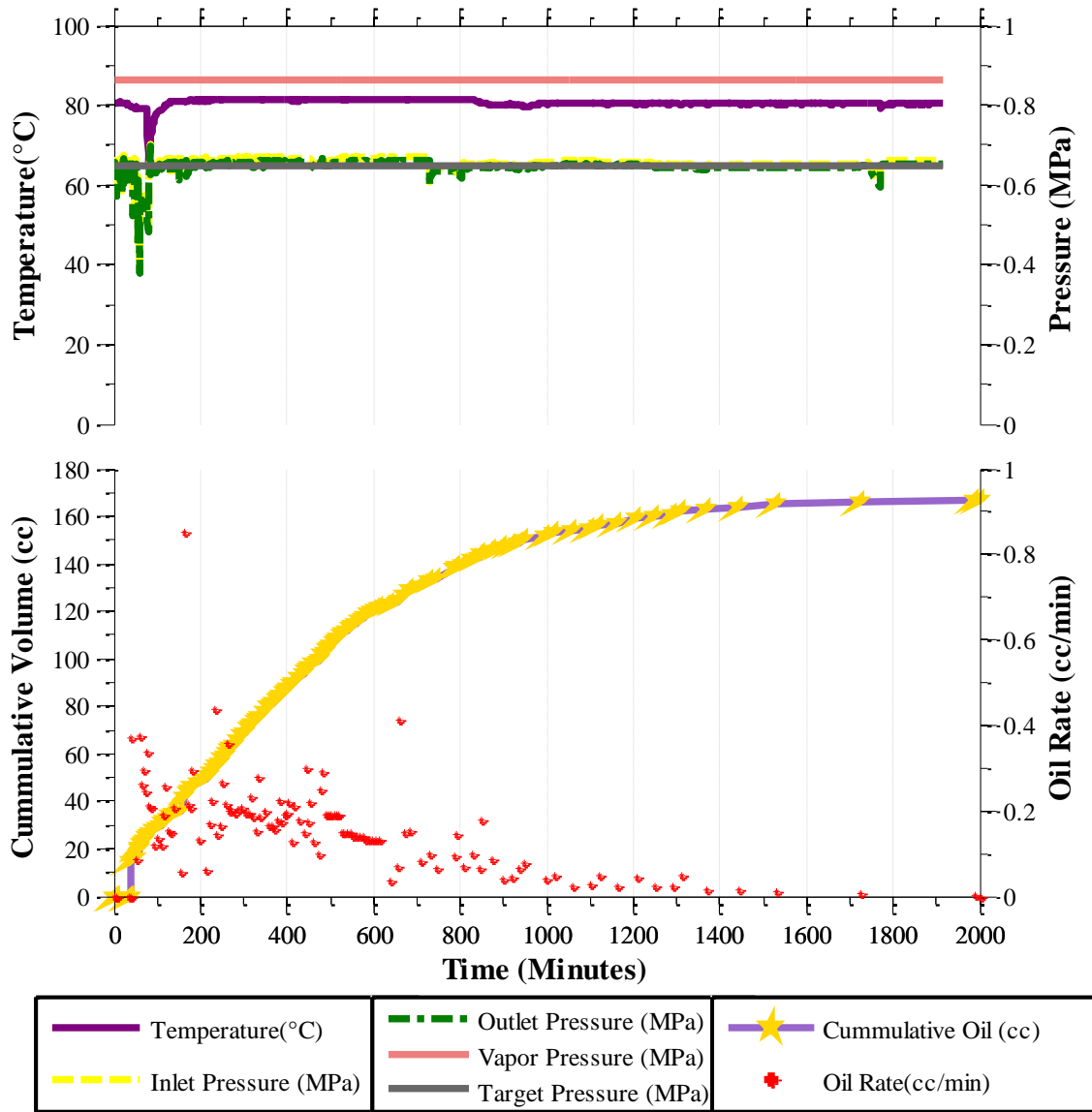


Figure 5.4: Results from experiment of n-Butane at 75% vapor pressure at 80 °C

5.3.4 n-Butane-80°C 50% Vapor Pressure

In this experiment, the system pressure was at 50% vapor pressure of n-butane at 50°C. Again, the parameters of the system were well-controlled. In this experiment, the results followed the formerly observed trend that as we lower system pressure, we were only able to recover 36% OOIP during the 3500 minutes of injection.

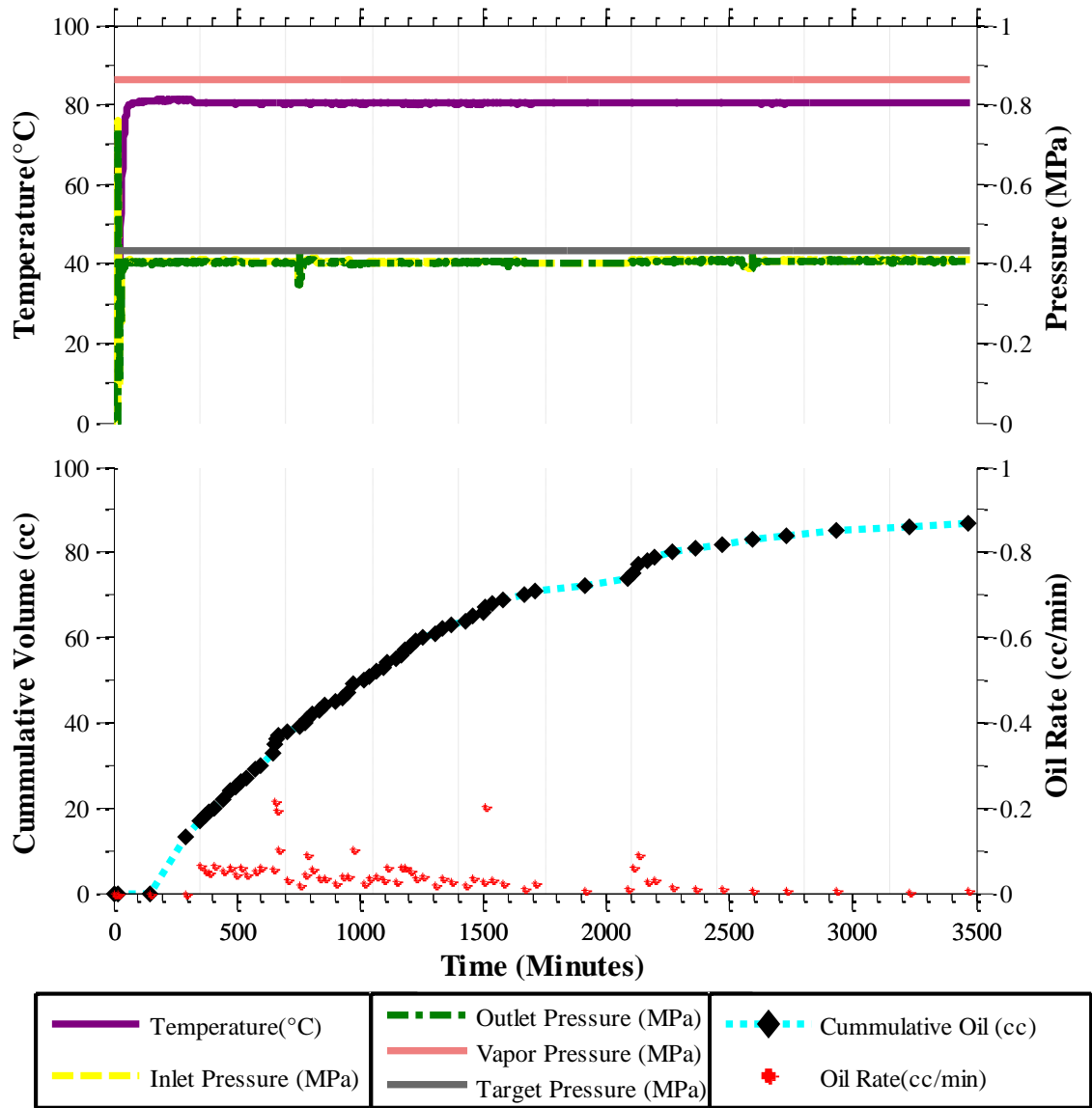


Figure 5.5: Results from experiment of n-Butane at 50% vapor pressure at 80 °C

5.3.5 Discussion

The recovery fraction of six experiments were plotted in Figure 5.6. The two experiments of DCM and n-Butane at 90% of the diluent vapor pressure at 80°C were borrowed from the chapter 5, and were displayed in gray dotted with yellow round marker and dotted red for DCM and n-butane, respectively. DCM was proven to be asphaltenes-

free from the study in chapter 3, and chapter 4. Decreasing the system pressure not only decreased the drainage rate but also reduced the ultimate recovery. Specifically, in the case of DCM as diluent, at 90% of the vapor pressure, the ultimate recovery was 74%; when that pressure dropped to 75%, the oil recovery dropped to 43%; and upon reducing pressure further to only 50%, recovery shrunk to only 27%. The same observations were found in the n- Butane cases. In our experiment, when the diluent vapor came into contact with the bitumen, the diluent diffused into the body of bitumen resulting in the reduction of surface tension. When the percentage of the vapor pressure decreased, solubility worsened causing higher IFT, hence creating lower capillary number which in turn, causing higher residual oil. Reduction of diluent oil ratio due to decreased solubility might impact the asphaltenes precipitation process.

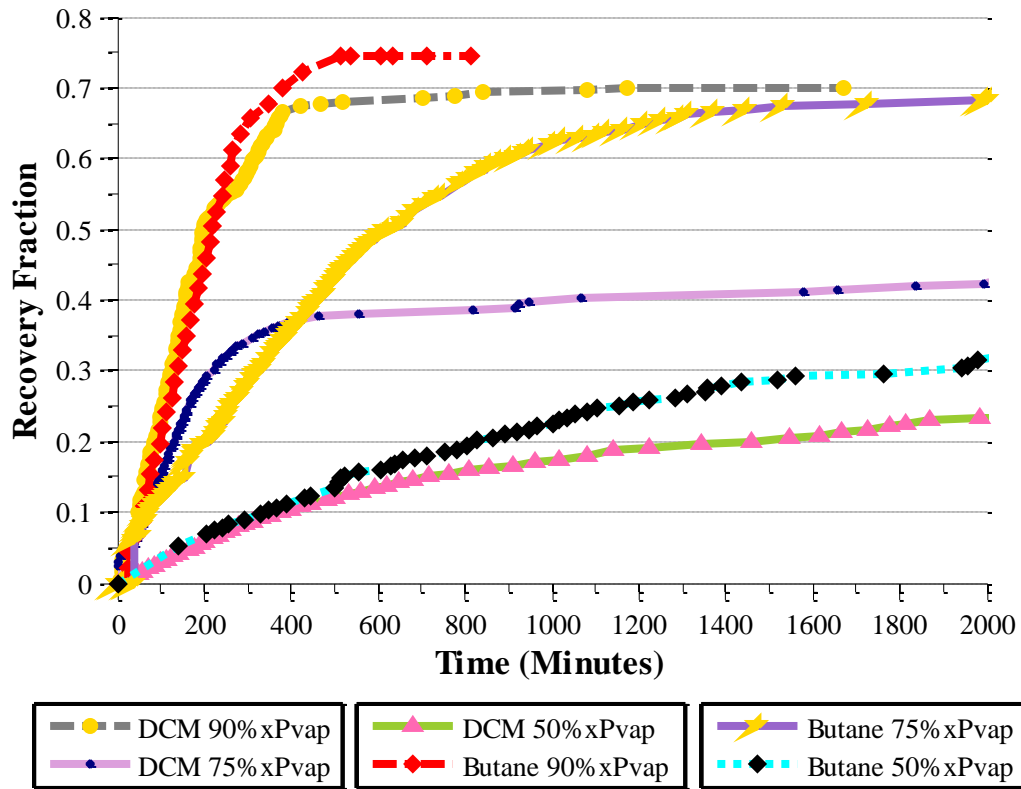


Figure 5.6: Summary of Chapter 5 experiments recovery fractions.

The effect of asphaltenes on the production mechanism of vapor diffusion drainage process was highlighted on each fraction of the vapor pressure. Because the comparison between DCM and n-Butane at their 90% vapor pressure was shown in the chapter 4, we only focus in the lower percent of their pure diluent vapor pressures cases for this section. At the same temperature and pressure, the oil production mechanism of the last four experiments were influenced by permeability, density difference, and diluent solubility which controlled the diluent content at the diluent-bitumen interface. Due to the fact that the permeability of the n-Butane cases was higher, its oil production rate was slightly higher than of DCM case at the same condition (0.075 cc/min compare to 0.069 cc/min). The performance of the DCM at the pure diluent vapor pressure was better than n-Butane

as the same condition per predicted using Henry's constant. However, we observed the abnormal behavior in the production trend, where the oil shifts the slope dramatically after 200 minutes of production.

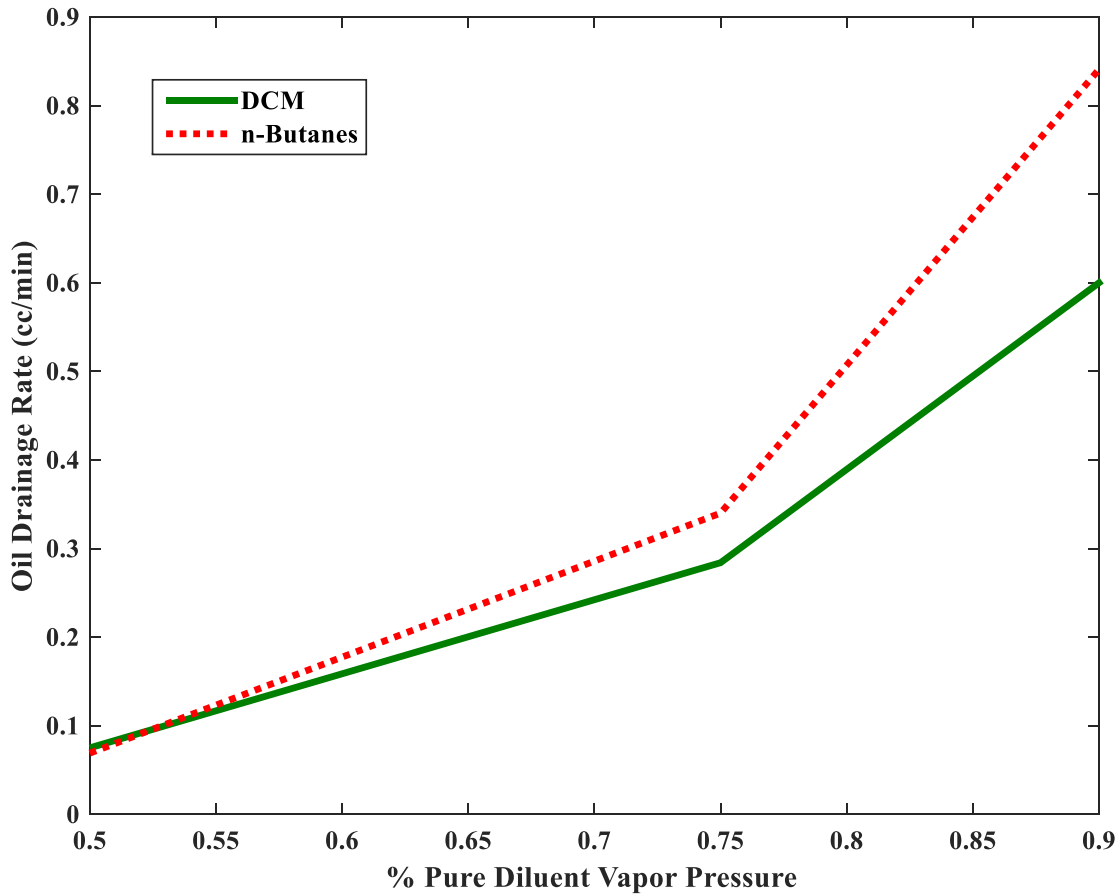


Figure 5.7: % Vapor Pressure plot vs. Oil Drainage Rate

The residual mass of was reported in Figure 5.8. Asphaltenes analysis of the residual mass for four cases shown the higher asphaltenes content on the top section where the retention time of the pure diluent was longest, but the amount of solid was negligible compare what we obtain from liquid diluent. The compositional content of the residual oil

was not much different from the original oil after vapor diluent injection. Therefore, we believed at lower partition pressure, asphaltenes impact on the process was insignificant.

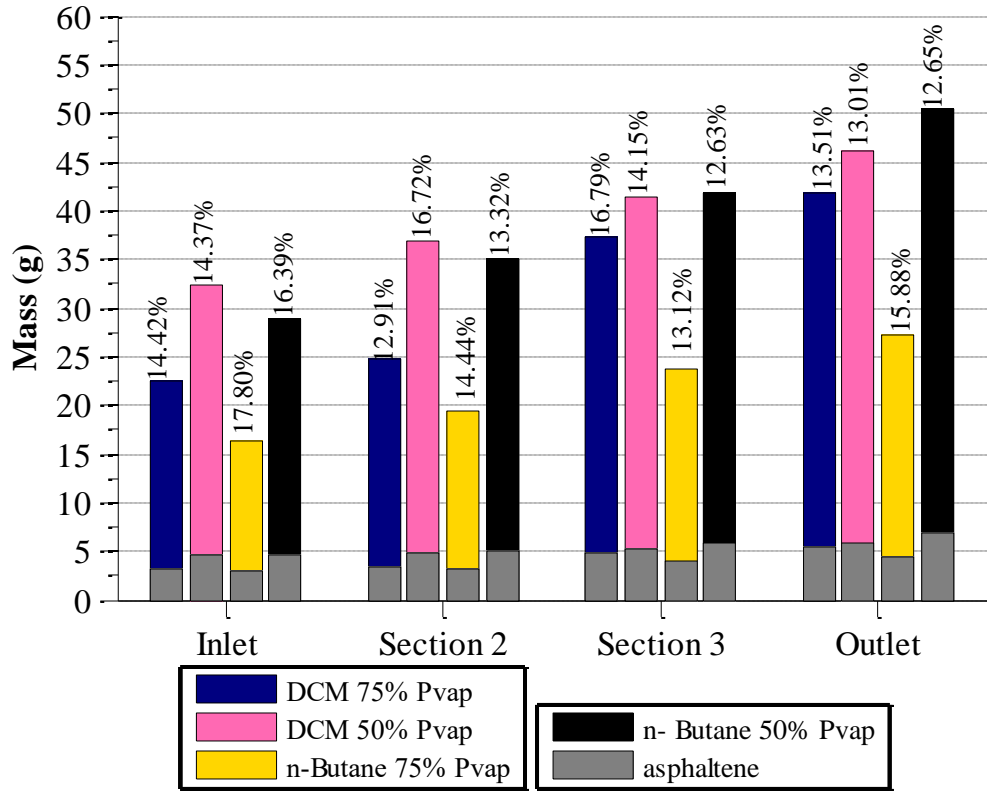


Figure 5.8: Mass balance analysis for pressure partition effect

The mass balance cross-check for the four experiments was shown in the Table 5.3. Sum of oil recovered in gram in the next to last column was the sum of the oil produced during the experiment, residual mass extracted from core after experiment, and mass of oil produced during bypassing flushed before experiment.

Case #	Mass oil original (cc≈g)	Mass Oil Produced (cc≈g)	Total Mass Oil Retrieve from Core (g)	Sum of oil recovered (g)	Rel. Error (%)
1	296.2	110.1	126.3	294.5	0.57
2	300.1	78.1	156.6	291.4	2.89
3	298.7	167	86.8	309.0	3.44
4	301.1	50.3	156.2	256.8	1.47

Table 5.3: Experiment grid for Chapter 5 experiments.

5.4 CHAPTER SUMMARY

Condensation of vaporized hydrocarbon when utilized to recover heavy oil can completely alter the oil production mechanism and cause unwanted asphaltene precipitation and deposition. Asphaltene precipitation by only vapor extraction is not as severe as that reported for liquid diluent in which the deposition of asphaltene could be potentially problematic to the reservoir especially fractured reservoir.

During field operations, controlling of the vapor chamber during vapor diffusion drainage process is a critical task. When the pressure of the system falls below the dew point, the drainage is significantly reduced and the ultimate recovery is also diminished. Lowering pressure of the vapor diffusion drainage process decreased the solubility of vapor diluent into the bitumen. Once the pressure fell below some pressure threshold, the main factor that controls the drainage rate was the rock relative permeability, and diluent type, as the asphaltene impact on the production mechanism is no longer significant.

Chapter 6: Conclusion and Future Works

. This work was composed of the study of two different production processes: (1) liquid diluent on bitumen recovery, and (2) vapor diffusion drainage process. We spliced the sandstone core vertically in the middle to mimic matrix- fracture interaction. Due to the permeability contrast, the diluent would flow only in the fracture initially.

Under the dilution process, if the injection rate was very fast, the diluent bleached only a light fraction of the bitumen, and acted as the carrier for those light fractions. A part of the diluent diffused into the bitumen creating a lower viscosity mixture, and drained sideways into the fracture under natural convection. Such process is governed by dispersive mixing. Dispersive mixing is comprised of molecular diffusion and mechanical dispersion. Far more complicated, bitumen and heavy oil contains a high concentration of asphaltenes. Mixing with solvent was one of the main factor contributing de-stabilize the asphaltenes, and causing flocculation and precipitation of solid particle inside porous media. During this study, almost all of the scenarios of dilution were investigated. i.e., different injection rates, temperatures, diluent types.

- We found the critical injection pump rate in Chapter 2 that for this particular set up, the critical pump rate for the maximum oil production is 4 cc/min.
- . In the same chapter, we also proved the existence of the critical injection rate at which the diluent bitumen ratio reached a threshold where asphaltene precipitation becomes a disaster that caused extreme blockage resulting in ending early of bitumen production.
- Compensating for the complication of controlling asphaltlenes, liquid diluent process yields a very high production rate with low diluent to bitumen ratio of 2.3. In term of water consumption, with injection pump

rate lower than the critical rate, dilution process is more efficient because it provides enough retention time for the diluent to dissolve into the bitumen body.

- Different diluent types result in different recovery rate and ultimate recovery.
- We also found that changing diluent type make a big impact on controlling asphaltene precipitation.
- The decrease of mixture viscosity and the increase of diffusivity of diluent into bitumen as temperature increases are the main factors for the increase in oil recovery.
- In the vapor diffusion drainage process, the bitumen drainage rate reduced as the pressure of the systems decreased below the vapor pressure.
- At 90% of the vapor pressure line, the oil production rate was still 50% lower than the higher extraction rate during the liquid diluent process. The behavior of vapor diffusion process deviated from the liquid diluent process as the pressure fell below the vapor pressure.
- We also observed no solid deposition of asphaltene on the surface of the rock as that in liquid extraction cases.
- Existence critical pump rate in vapor diffusion cases was proven.
- When the pressure falls below 75%, the bitumen extraction depends mostly on the reservoir properties such as: permeability, capillary pressure.
- In another word, the impact of diluent type observed on the last four experiments where the system pressure fall below 90% P_{vap} suggests that diluent type is no longer of significance contribution. Despite recovering oil

at a much lower rate, vapor diffusion process has the benefits of yielding a lower percentage of asphaltenes drop out.

From these studies, we propose a novel technology in which liquid diluent and vapor can be combined. i.e., injecting condensable vapor solvent into a cold reservoir: when condensing, the liquid diluent will bleach away the light component of the oil, leaving behind residual oil with larger concentration of asphaltenes. When the swept portion is heated to the target temperature, the vapor will diffuse into the residual oil and drain down under natural convection force.

The spectrum of diluent injection is broad. During the span of four years and the course of 25 experiments, we were still unable to cover all aspects of this study. To bring the technology closer to field application, more studies should be further carried out such as the impact of water saturation both on extraction mechanism and asphaltenes precipitation and transportation, the effect of different rock types, etc. Also, controlling asphaltenes precipitation plays important role in this technology. I suggest the use of diluent that inhibits asphaltenes precipitation when mixing with the main diluent to delay the onset of asphaltenes precipitation. I suggest the experimental sets shown in Table 6.1 for future works.

Furthermore, for study in depth of the vapor diffusion mechanism, I suggest conducting two more experiments of n- Butane with two different type of oil that have similar asphaltenes content but different viscosities. With that, one can determine the important of mixture viscosity on diluent solubility and diffusivity.

Goal	Rock Type	Diluent	Water Saturation	Reservoir Condition P(bar), T(°C)	Injection Condition P(bar), T(°C)
Hybrid	Sandstone	n-Butane	No	10, 25	10, 85
Water Saturation	Sandstone	n-Butane	Yes	10, 25	10, 85
Rock type	Carbonate	n-Butane	No	10, 25	10, 85
Mixture Diluent	Sandstone	n-Butane+ toluene	No	10, 25	10, 85
Rock type	Tighter sandstone	n-Butane	No	10,85	10, 85

Table 6.1: Experiment grid for future work.

Bibliography

- Farouq Ali, S.M. Heavy Oil-Ever More Mobile. *J. Pet. Sci. Technol.*, 37 (2003): 5-9, 2002
- Energy Information Administration. Annual Energy Outlook 2016.
<http://www.eia.gov/outlooks/aeo/>
- James, L.A. 2009. *Mass Transfer Mechanisms during the Solvent Recovery of Heavy Oil*. PhD dissertation, University of Waterloo, Waterloo, Ontario, Canada (June 2009)
- Panuganti S. R., Mohammad T., Vargas F. M., Gonzalez L., Chapman W., SAFT model for upstream asphaltene applications, *Fluid Phase Equilibria*, Volume 359, 15 December 2013, Pages 2-16, ISSN 0378-3812,
<http://dx.doi.org/10.1016/j.fluid.2013.05.010>
- McCain, W.D., Jr. *The Properties of Petroleum Fluids*. 2nd ed. Tulsa, OK: PennWell. (1990)
- Speight J. G., *The Desulfurization of Heavy oils and Residua*, second ed. Marcel Dekker Inc., New York
- Gross, J., Sadowski, G. Perturbed-Chain SAFT: An Equation of State Based on a Perturbation Theory for Chain Molecules. *Industrial & Engineering Chemistry Research* 2001 40 (4), 1244-1260. DOI: 10.1021/ie0003887
- Buckley JS, Wang J (2002). Standard Procedure for Separating Asphaltenes from Crude Oil. PRRC 02-02
- Gates, I. D., & Wang, J. Y. J. (2011, January 1). Evolution of In Situ Oil Sands Recovery Technology in the Field: What Happened and What's New? Society of Petroleum Engineers. Doi: 10.2118/150686-MS
- Pathak, V., Babadagli, T., & Edmunds, N. R. (2012, January 1). Experimental Investigation of Bitumen Recovery from Fractured Carbonates Using Hot-Solvents. Society of Petroleum Engineers. Doi: 10.2118/159439-MS
- Rankin, K. M., Nguyen, B., Dorp, J., Verlaan, M., Castellanos Diaz, O., and Nguyen, Q. Solvent Injection Strategy for Low-Temperature Production from Fractured Viscous Oil Reservoirs. 2014. *Energy & Fuels*

- Briggs, P. J., Baron, P. R., Fulleylove, R. J., & Wright, M. S. (1988, February 1). Development of Heavy-Oil Reservoirs. Society of Petroleum Engineers. doi:10.2118/15748-PA
- Lyman, T. J., Piper, E. M., & Riddell, A. W. (1984, January 1). Heavy Oil Mining Technical and Economic Analysis. Society of Petroleum Engineers. doi:10.2118/12788-MS
- Bellows, L. A., & Bohme, V. E. (1963, May 1). Athabasca Oil Sands. Society of Petroleum Engineers. doi:10.2118/517-PA
- BLM. Bureau of Land Management, U.S Department of Interior
- Ali, S. M. F., & Snyder, S. G. (1973, October 1). Miscible Thermal Methods Applied to a Two-Dimensional, Vertical Tar Sand Pack, With Restricted Fluid Entry. Petroleum Society of Canada. doi:10.2118/73-04-01
- Awang, M., & Ali, S. M. F. (1980, January 1). Hot-Solvent Miscible Displacement. Petroleum Society of Canada. doi:10.2118/80-31-29
- Abass, E., & Fahmi, A. (2013, April 15). Experimental Investigation of Low Salinity Hot Water Injection to Enhance the Recovery of Heavy Oil Reservoirs. Society of Petroleum Engineers. doi:10.2118/164768-MS
- Rivet, S., Lake, L. W., & Pope, G. A. (2010, January 1). A Core Flood Investigation of Low-Salinity Enhanced Oil Recovery. Society of Petroleum Engineers. doi:10.2118/134297-MS
- Boerrigter, P. M., Verlaan, M., & Yang, D. (2007, January 1). EOR Methods to Enhance Gas Oil Gravity Drainage. Society of Petroleum Engineers. doi:10.2118/111403-MS
- Hascakir, B., Babadagli, T., and Akin, S. 2008. Experimental and Numerical Simulation of Oil Recovery from Oil Shales by Electrical Heating. 2014. *Energy & Fuels*
- Das, S. K., Butler, R.M., Mechanism of the vapor extraction process for heavy oil and bitumen, *Journal of Petroleum Science and Engineering*, Volume 21, Issues 1–2, September 1998, Pages 43-59, ISSN 0920-4105,
- Mokrys, I. J., & Butler R. M. (1993). In Situ upgrading of heavy oils and bitumen by propane DE asphaltting: the Vapex process. SPE Productions Operations Symp. Oklahoma City, Oklahoma, U. S. A., March 21 -23, 1993.

- Das, S. K., Butler, R. M., 1995, Extraction of heavy oil and bitumen using solvents at reservoir pressure. Paper No. 95-118, Sixth Petroleum Conference of the South Saskatchewan Section. The petroleum Society of CIM, Regina, Canada, October 16- 18
- Farouq Ali, I. J., and Abad, B.P. Bitumen Recovery from Oil Sands, Using Solvents in Conjunction with Steam; *Journal of Canadian Petroleum Technology*, Vol. 15, No. 2, pp 80-90, July- September 1976
- Allen, J.C., Gaseous Solvent Heavy Oil Recovery Method; Canadian Patent No. 1027851, 14 March 1974
- Wang J., and Buckley J. Procedure for Measuring the Onset of Asphaltene Flocculation. PRRC 01- 18
- Nenniger, J.E. and Dunn, S.G. How Fast is Solvent Based Gravity Drainage? Proceedings: Canadian International Petroleum Conference, 17-19 June 2008, Calgary, Alberta, Canada, Paper 2008-139
- Burger, K.K. Mohanty, Mass transfer from bypassed zones during gas injection, SPERE 12 (May (2)) (1997) 124.
- Das, S.K. 2002. VAPEX- A Unique Canadian Technology. *Journal of Canadian Petroleum Technology* 41(8), 32-34
- DeMirjian, H. A. (1978, January 1). Heavy Oil Recovery by Conventional and Mining Methods. Society of Petroleum Engineers. doi:10.2118/6996-MS
- Zendehboudi, S., Mohammadzadeh, O., & Chatzis, I. (2009, January 1). Experimental Study of Controlled Gravity Drainage in Fractured Porous Media. Petroleum Society of Canada. doi:10.2118/2009-186
- Zendehboudi, S., & Chatzis, I. (2011, February 1). Experimental Study of Controlled Gravity Drainage in Fractured Porous Media. Society of Petroleum Engineers. doi:10.2118/145158-PA
- Arciniegas L. M., Babadagli T., Quantitative and visual characterization of asphaltenic components of heavy-oil after solvent interaction at different temperatures and pressures, *Fluid Phase Equilibria*, Volume 366, 25 March 2014, Pages 74-87, ISSN 0378-3812, <http://dx.doi.org/10.1016/j.fluid.2014.01.006>.

Hart A., Shad A., Leeke G., Greaves M., and Wood J. Optimization of the CAPRI Process for Heavy Oil Upgrading: Effect of Hydrogen and Guard Bed *Industrial & Engineering Chemistry Research* 2013 52 (44), 15394-15406

DOI: 10.1021/ie400661x

Behbahani T. J., Ghotbi C., Taghikhani V., Shahrabadi A., Experimental investigation and thermodynamic modeling of asphaltene precipitation, *Scientia Iranica*, Volume 18, Issue 6, December 2011, Pages 1384-1390, ISSN 1026-3098, <http://dx.doi.org/10.1016/j.scient.2011.11.006>.

Trivedi, J. and Babadagli, T. Greenhouse Gas Sequestration during Tertiary Oil Recovery: Optimal Injection Strategies. *Oil Gas European Magazine*, 33 (1), 22-26 (2007)

Branco, V.A.M., Mansoori, G.A., Xavier, L.C.D.A., Park, S.J., Manafi, H. Asphaltene flocculation and collapse from petroleum fluids. *J. Petrol. Sci. Eng.* 2001; 32:217–230.

Hoepfner M. P., Limsakaoune V., Chuenmeechao V., and Maqbool T., A Fundamental Study of Asphaltene Deposition. *Energy & Fuels* 2013 27 (2), 725-735. DOI: 10.1021/ef3017392

Maqbool T., Balgoa A. T., Fogler H. S., Revisiting Asphaltene Precipitation from Crude Oils: A Case of Neglected Kinetic Effects. *Energy & Fuels* 2009 23 (7), 3681-3686 DOI: 10.1021/ef9002236

Pereira J. C., Delgado-Linares J., Briones A., Guevara M., Scorzza C., and Salager J-L, The Effect of Solvent Nature and Dispersant Performance on Asphaltene Precipitation from Diluted Solutions of Instable Crude Oil. *Petroleum Science And Technology* Vol. 29, Iss. 23, 2011

Hirschberg, A., deJong, L. N. J., Schipper, B. A., and Meijer, J. G., *Soc. Pet. Eng. J.* 24, 283-293 (1984).

Huggins, M.L. (1941) *J. Chem. Phys.*, 9 (5): 440–440.

Nazmul H. G., Dabros T., and Masliyah J. H. ,†. Optical Monitoring of Asphaltene Aggregation. *Industrial & Engineering Chemistry Research* 2005 44 (1), 75-84

DOI: 10.1021/ie049689x

Heavy-Oil-Recovery Enhancement with Choline Chloride/Ethylene Glycol-Based Deep Eutectic Solvent

James, L.A. and Chatzis, I. 2004. Details of Gravity Drainage of Heavy Oil during Vapour Extraction. Proceedings: International Symposium of Society of Core Analysts, Abu Dhabi, UAE, 5-9 October, 2004.

Perkins, T.K. and Johnston, O.C.: "A Review of Diffusion and Dispersion in Porous Media", Soc. Pet. Eng. J., (March, 1963), 70-84.

Miadonye, A., Puttagunta, V. R., Srivastava, R., Huang, S. S., & Dafan, Y. (1997, January 1). Generalized Oil Viscosity Model For the Effects of Temperature, Pressure And Gas Composition. Petroleum Society of Canada. doi:10.2118/97-01-04

Einstein, A., Ann. Phys. 17, 549 (1905)

Wilke,C.R., ChangPin, A.I.Ch.E.J. 1, 264, (1955)

King, C. J., Hsueh, L., Mao, K.-W., J. Chem. Eng. Data, 10, 348 (1965).

Sitaraman, R., Ibrahim, H. S., Kubor, N. R., J. Chem. Eng. Data, 8, 198 (1963).

Hayduk, W., and B.S. Minhas, Can. J. Chem. Eng., 60, 295 (1982)

Ting D., Hirasaki P., and Chapman G. J., W.G. (2003) Pet. Sci. Technol., 21 (3–4): 647–661.

Wiehe I. A., Liang K. S. , Asphaltenes, resins, and other petroleum macromolecules, Fluid Phase Equilibria, Volume 117, Issue 1, 1996, Pages 201-210, ISSN 0378-3812, [http://dx.doi.org/10.1016/0378-3812\(95\)02954-0](http://dx.doi.org/10.1016/0378-3812(95)02954-0).

Pathak, V., Babadagli, T. and Edmunds, N.R. 2011. Mechanics of Heavy Oil and Bitumen Recovery by Hot Solvent Injection. Paper SPE 144546 presented at the SPE Western North American Regional Meeting, Anchorage, Alaska, U.S.A, 7-11 May. DOI: 10.2118/144546-MS

Smith F. L., Harvey A. H., Avoid Common Pitfalls When Using Henry's Law. Environment Management. September 2007